MASTER THESIS

Markers recognition in a camera-based calibration system for immersive applications

Author: Andrea Tresaco

Supervisor (Fraunhofer): Volker Hahn

Supervisor (UPC): Josep R. Casas

November 2009

This report is the result of my project (PFC) carried out at Fraunhofer IGD (Institut für Graphische und Datenverarbeitung) in the department of Imaging and Medical Recognition in Darmstadt (Germany).

The department of Imaging is working on applications dealing with immersive media and teleconferencing into the European project hArtes.

I would like to thank Ferrán Marqués for helping me to find a contact in Germany disposed to offer a project to a Spanish student. I would also thank the person who reply my petition and offered me the opportunity to make my project and supervise it in Germany, Volker Hahn, and also Josep R. Casas who offered to supervise it in UPC in Spain.

Specially, I would like to thank my parents, sister and Rubén for their unconditional support and love.

I would also thank Neri for being from the first day of university until now by my side.

And finally thanks to Michael for helping me with IPP troubles.

Table of Contents

1. Introduction

1.1. The hArtes Project

My project is part of a European project called hArtes (Holistic approach to real time configurable embedded systems) developed by the collaboration of different European enterprises, research institutions and universities from Germany, France, United Kingdom, Italy and The Netherlands.

The Cognitive Computing and Medical Imaging Department of the Fraunhofer Institute for Computer Graphics (Fraunhofer-Institut für Graphische Datenverarbeitung IGD) contributes to the project by using the hArtes platform for the development of a real-time system for immersive audio, which will be an integrative part of an HD video based telepresence system. The system will allow users to be virtually present at any place they like by using the capabilities of an HD omnidirectional video camera system which, in combination with a microphone array for 3D sound recording, will be used for real time capturing. The audiovisual data will be rendered by an immersive video projection system complemented by a 3D rendering based on wavefield synthesis.

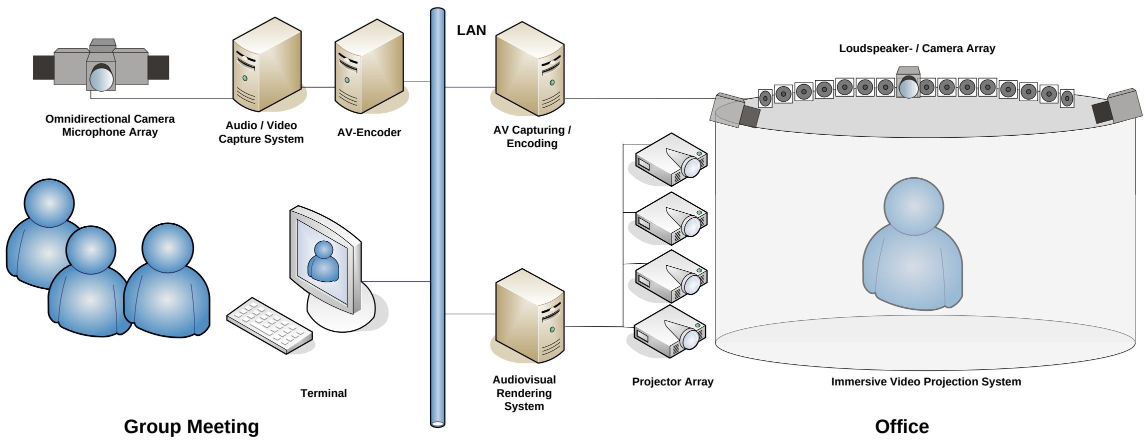
Omnidirectional Camera Microphone Array
Audio / Video Capture System
AV-Encoder
LAN
AV Capturing / Encoding
Loudspeaker- / Camera Array
Terminal
Audiovisual Rendering System
Projector Array
Immersive Video Projection System
Group Meeting
Office

Fig. 1.1 System Overview telepresence for group meeting. Audio system in the above branch and video system in branch below.

The telepresence approach reached by Fraunhofer is designed as an immersive platform combining high definition 360 degrees video recording and playback with 3D audio using the possibilities of parallel signal processing and audiovisual array technology as shown in Fig. 1.1. A microphone array records the sounds that will be reproduced inside the immersive environment (where the user is) thanks to loudspeakers and the visual rendering system provides images to projector array which projects image onto the cylindrical surface of the immersive platform. Its scalable camera system exploits the potential of common graphics hardware for real time stitching and transmission of ultra high definition video panoramas providing resolutions far beyond actual HD video technology. Its immersive video projection environment gives users the impression of being virtually present at any location at any time.

The system could be used for a range of applications including:

- High end video-conferencing
- Live broadcasting of sport events, theatre and music events.
- Interactive multimedia presentations
- 360 degrees cinema, theatres or concerts
- immersive gaming

My project is a contribution to the calibration of a projectors array and camera-based system by analyzing features of markers through image processing techniques.

1.2. hArtes Scenario and Objectives of IGD

In this point the elements forming the scenario of the immersive platform and the objectives of our project are described.

Scenario of the hArtes Project

Fig. 1.2 shows the scenario built by Fraunhofer institute in Darmstadt for the development of different projects and studies dealing with hArtes project.

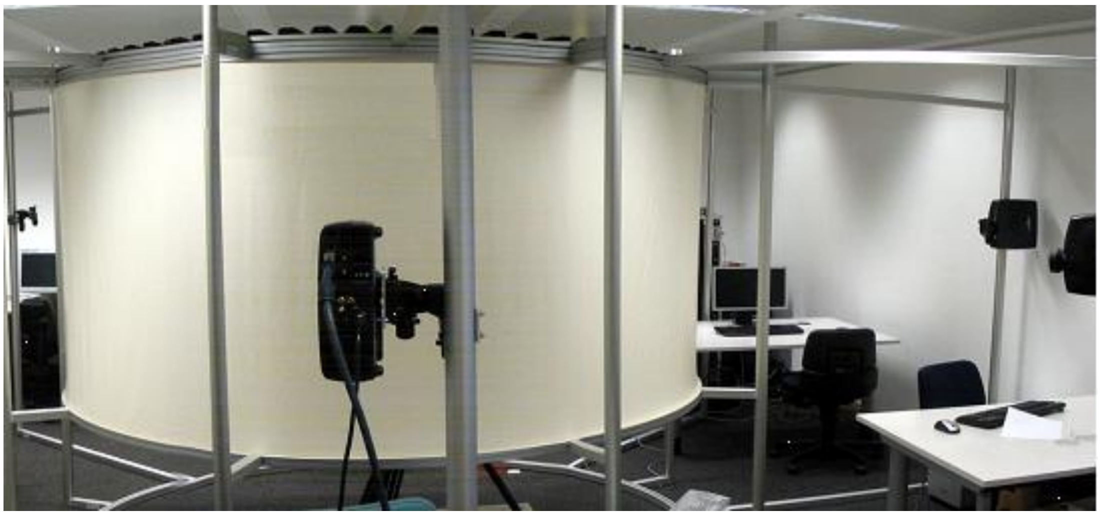

Fig. 1.2 Room of IGD where the immersive scenario is placed

In the room of our work we can find a central cylindrical surface surrounded by eight projectors and cameras fixed to this central structure and separated 45 degrees from each other. The cameras are fixed above the projectors (in the same vertical structure) to record what on the cylindrical structure is projected. There is also a group of loudspeakers and microphones covering the inside surface of the cylinder as can be seen in Fig. 1.3.

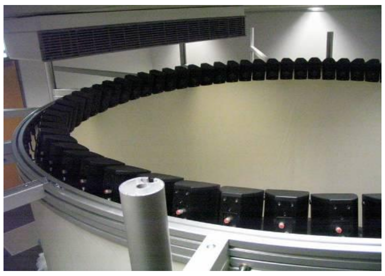

Fig. 1.3 Loudspeakers can be seen from above inside the cylindrical structure

With the description of the scenario the two differentiated parts of study can be easily seen; one is dealing with audio and the other one dealing with video. By combining these two systems, the immersive impression pursued by hArtes can be reached and all the applications described in Section 1.1 can be implemented.

In our particular case we are interested in video branch of the system described.

Objectives of IGD in hArtes

Once we know the scenario we are prepared to face the situation.

The projectors, fixed to the central cylindrical structure, project an image onto the cylindrical surface. This images projected are coming from a computer and can be single images or videos (already saved in the computer or real time recorded by a omnidirectional system of video cameras as shown in Fig. 1.4 below).

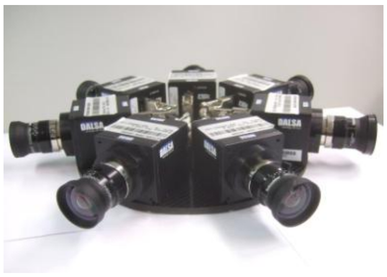

Fig. 1.4 Omnidirectional camera system

There are eight projectors surrounding the 360 degrees panorama covering each of them an angle of 45 degrees. The objective of hArtes project is that, if a user projects an image or video through the eight projectors onto the cylindrical surface and a user is inside the cylindrical structure he has the impression of being in the scene projected. That means that, as a user is inside the structure he sees a scenario, decided depending on the application (it can be a computer game, a concert, a museum….), in which he is evolved as it reality was (immersion).

In practice, this theoretical strategy presents some problems in the projection.

Human sight is very sensitive to continuity, colour and brightness changes in image. So if we project a video (real time or recorded) and someone, who is inside the structure, finds a change (continuity, colour and brightness) in the junction between projections coming from neighbouring projectors the immersive sensation is lost. (see Fig. 1.5)

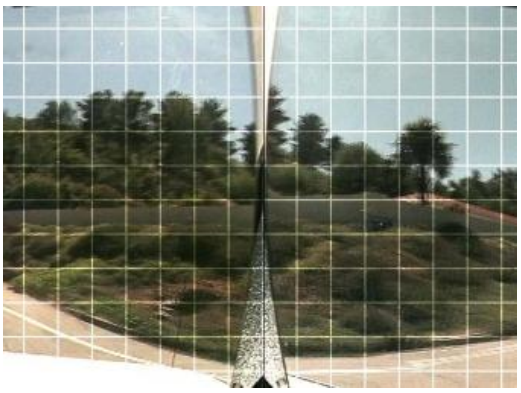

Fig. 1.5 Junction between two consecutive projections projected on a non planar surface

So one objective of IGD in the context of hArtes project is to correct those misalignments or overlapping in the junctions between projections so the changes are not noticeable for the person who is inside.

Proposal of a solution

Once we know which the problem is, we have to propose a solution.

We wanted to apply the necessary corrections in the calibration system in order to obtain unnoticeable variations between consecutive projections and that can be done at the same time image is projected or a priori, so at this point we came across a question which would determine the direction of our project.

What is better, to make a continuous calibration of the system as it works or a pre-calibration of the system and then running the application desired?

We analyse the possibility of working in real time or not. After some readings we decided that real time was not a necessary condition. The decision was taken considering the features of the system and the complexity of algorithm execution. On one hand, the system is designed to be in a fixed place (non-portable) so once calibrated it will maintain its features for a certain period of time and the process can be done once a week, a month, a year... what user decides to ensure the calibration of the system. On the other hand, if the algorithm has to be runned on real time, the number of parameters (extrinsic and intrinsic) to consider and operations required have to be as simple and fast as possible to allow real time execution. This fact increases the difficulty of the implementation of the algorithm. If we do not consider real time we can make all operations we consider necessary to provide an accurate system for markers extraction.

So the solution we chose was to make a pre-calibration of the system which can be reached by working directly with the projections recorded by the camera placed above the projectors and facing the problem as an image processing problem.

To reach the objective we have brought up the global solution described in Fig. 1.6.

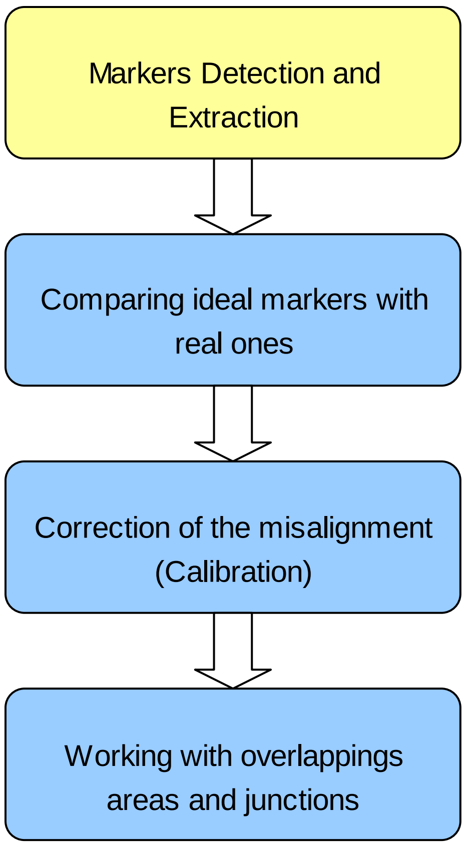
Markers Detection and Extraction
Comparing ideal markers with real ones
Correction of the misalignment (Calibration)
Working with overlappings areas and junctions

Fig. 1.6 Block diagram of our proposal of solution for avoiding misalignments and discontinuities between consecutive projections

First of all, the proposed strategy is to create a grid, an ideal grid, consisting on 9 black squares with a small white hole in the middle, which will be our reference for the whole process. From now on, in this report, these squares are called markers.

Secondly the image formed by all markers will be projected onto cylindrical surface see Fig. 1.7.

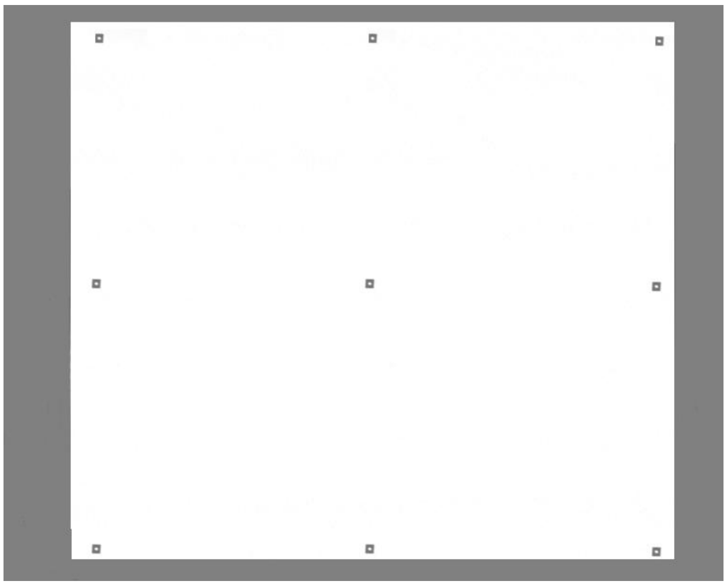

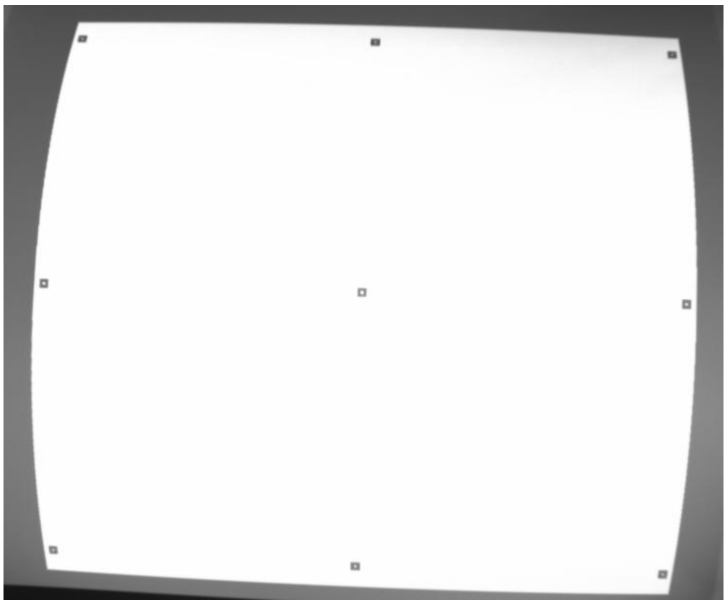

Fig. 1.7 Up: image created by us to become our reference image (grid) for calibration. Down: projection of our grid onto the cylindrical surface. As can be seen the contours and markers appeared deformed due to projection onto a non planar surface.

As the surface on which we are projecting is not planar, the ideal markers appeared in different positions and orientations in the projected image and with some of their form-features modified as described in Section 2.4. Depending on the distance and orientation of each projector (although all the system is metrical built there can be some errors) markers can appear in very different positions and deformed so it makes it necessary to identify where are the markers, comparing this position to the ideal and then correcting the misalignment between them. In order to determine which is the correct position we have some external markers forming part of the structure. These markers are different from internal ones described above; they are four circles fixed in a specific distance to the structure and they are also affected by projective and affine features as well as in internal case. Once detected those external markers we will have four fixed points perfectly identified and which should be always in the same well-known place so they are a very good reference to correct the position of projector by adjusting the distances between ideal external and internal markers.

Once calibrated the problems remaining in the overlapping areas and junctions should be corrected to give a total immersive appreciation.

1.3. The Objective of my Project

My objective inside hArtes, and as a result my project, is the first point in the global solution shown in Fig. 1.6, markers detection and extraction (see Fig. 1.8)

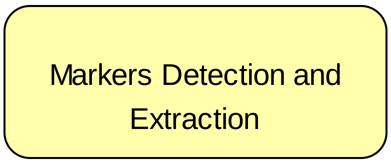

Fig. 1.8 Our objective in hArtes project

My project consists in the development of an application (GUI) in C++ language capable of determine univocally which of the parts in the image are the markers desired and reject the areas undesired in the image. By applying image processing functions and transformations we come across markers detection and extraction.

The objective of my project is to develop an application in C++ language to univocally determine which regions in the image captured from the camera (image projected by projectors onto the cylindrical surface) are markers and which ones not through techniques of image processing.

In our project we come across different problems.

- Light conditions: The image captured by the camera is not uniformly illuminated. The light is not equally applied in each part of the scene and can vary depending on the room or space where the system is placed or the focus light used. Depending on the focus light we will find shadows which can difficult and also cause wrong detections in the univocal determination of the markers in the image

- Markers form: As introduced in Proposal of solution (Section 1.2) our markers detector should be able to detect between two forms of markers; internal markers, which are black squares with a hole in the middle; and external markers which are orange circles with a black hole in the middle. The techniques of image processing used to determine squares and circles are different. So the application has to be able to detect both of them.

- Perspective and affine problems: When we project internal and external markers in the borders they become rectangles and ellipses, due to the surface's form. These two features are important, so we are not only looking for squares and circles but also rectangles and ellipses.

Taking all these points into account we have implemented a GUI in C++ language to work with images through image processing techniques.

In what follows, in Sections 2.2, 2.3 and 2.4, segmentation, shape classification and object recognition techniques are explained. As pre-processing techniques preceding the classification process can greatly enhance recognition accuracy, we have included in our system a first pre-processing step explained in Section 2.1. Thereafter, once we know the techniques available, in Section 3 we discuss the suitable methods and techniques which will give better solutions for our application.

In Section 4, are described the tools needed for the implementation and the details of the application developed. Finally, the results of our GUI application are shown in Section 5.

2. State of the Art

The structure of this state of the Art follows the scheme shown below.

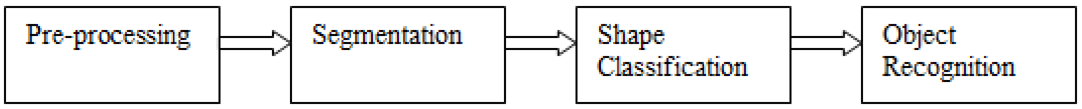

Fig. 2.1 Image processing chain used in our project

The starting point is an image obtained by camera; we apply pre-processing, segmentation, shape classification and object recognition techniques as image processing chain for recognizing markers. We obtain an image containing the markers we want to extract.

The methods and techniques of each step are exposed as follows and the selection of the better solution in our case is discussed in further Sections.

2.1. Image pre-processing

The use of pre-processing techniques preceding image processing chain can greatly enhance recognition accuracy.

The best processing is no processing at all. If image acquisition has high quality this step is not necessary except if what is searched is to suppress information of no relevant areas in order to make easier the image processing or analysis. If image acquisition has low or middle quality this step becomes useful in order to suppress undesired distortions.

There are different pre-processing techniques that can be applied to an image to improve it before processing. In this memory are explained only explained those applied in our project which are pixel brightness transformation and local pre-processing.

Pixel brightness transformation: Gray-scale transformation

The aim of brightness transformation is to modify pixel brightness depending on the characteristics of each pixel.

The process of gray-scale transformation consists in taking the image brightness and, through a look-up-table (LUT), change it into a new image brightness in real time for displaying. The result of the transformation is a gray-scale digital image in which the value of each pixel is a single sample carrying all the information of brightness. The gray-scale images intended for visual display (screen and printed) are commonly stored with 8 bits per sampled pixel, which allows 256 different intensities to be recorded, going from black to white and having different gray intensities (shades of gray).

Local pre-processing

The aim of the local pre-processing is filtering for enhancement details (the high spatial frequency components), so this technique will provide a more detailed image than the original, obtaining an improved image to our purpose. The trick with “local” contrast enhancement is that it increases local contrast in smaller regions, while at the same time preventing an increase in “global” contrast, thereby protecting large-scale shadow/highlight detail.

As a spatial filtering it works with the direct manipulation of the pixels using a small neighbourhood of the pixel in the gray-scale image to produce a new brightness value in the output image. This contrast enhancement can be achieved by a sharpening operator, based on derivatives of the image function.

First order operators (using first derivative measurements) are particularly good at finding edges in images as for example Sobel and Roberts edge enhancement operators. Laplacian is a second derivative method of enhancement. It is particularly good at finding detail in images.

The strength of the response of a derivative operator is proportional to the degree of discontinuity of the image at the point at which the operator is applied. Thus, image differentiation enhances edges and other discontinuities (such as noise) and deemphasizes areas with slowly varying gray-level values.

Sharpening operator has the objective of making edges steeper. We can obtain sharpened output image $sh(i,j)$ as:

$$sh(i,j) = f(i,j) - k \cdot L(i,j)$$

where $f(i,j)$ corresponds to original image and the constant *k* gives the strength of sharpening where $L(i,j)$ is a measure of the image function sheerness, calculated using Laplacian.

Another way of writing the sharpening expression should be in terms of matrix:

Sharpened image = $\begin{pmatrix} 0 & 0 & 0 \\ 0 & 1 & 0 \\ 0 & 0 & 0 \end{pmatrix} - \frac{1}{\alpha+1}\begin{pmatrix} \alpha & 1-\alpha & \alpha \\ 1-\alpha & -4 & 1-\alpha \\ \alpha & 1-\alpha & \alpha \end{pmatrix} = \frac{1}{\alpha+1}\begin{pmatrix} -\alpha & \alpha-1 & -\alpha \\ \alpha-1 & \alpha+5 & \alpha-1 \\ -\alpha & \alpha-1 & -\alpha \end{pmatrix}$

where α is a value between 0 and 1 and controls the shape of the Laplacian.

A graphical sharpening example is shown in *Fig. 2.2*.

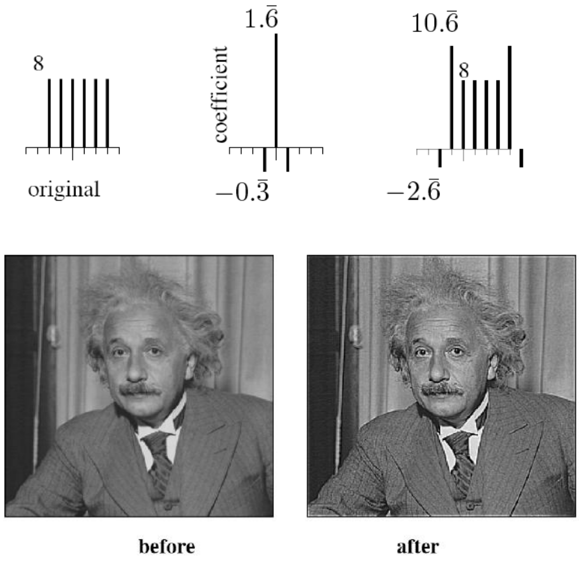

Fig. 2.2 Up: original image, sharpening filter and result. Down: application to the filter to an image where details are enhanced and the rest smoothed. (slides by Bernt Schiele from TU-Darmstadt)

Differences are accentuated and constant areas are left unchanged. Also noise is accentuated.

2.2. Segmentation

Segmentation is the process of dividing a digital image into different regions. Each region is formed by a set of pixels with similar characteristics such colour, intensity or pattern. The whole image is covered by regions and adjacent regions have different features.

The goal of segmentation is to simplify the information or change the representation into something meaningful and easier to analyze.

In image processing there are many algorithms and techniques developed for image segmentation: clustering, histogram based, edge detection, region growing, level set, graph partitioning, model based, multi-scale and watershed transformation.

The simplest method of image segmentation is Thresholding. Sezgin and Sankur in [6] classified thresholding methods into groups depending on the information the algorithm manipulates:

- Histogram shape based methods: it analyzes peaks, valleys and curvatures of a smoothed histogram
- Clustering based methods: gray-level samples are clustered in two parts to separate background from foreground (object of interest). In other cases they are modelled as a mixture of two Gaussians
- Entropy based methods: uses entropy of foreground and background regions, the cross-entropy between the original and binarized image...
- Object attribute based methods: searches similarity between the gray-level image and the binarized one (shape similarity, edge coincidence…)
- Spatial methods: uses probability distribution or correlation between pixels
- Local methods: adapt the threshold value on each pixel to local image characteristics.

The goal of all these techniques is to determine a value called threshold and comparing each pixel on the image with this value. If the value of the pixel is greater than the threshold, its value becomes 1 (white), otherwise it becomes 0 (black). That method assumes that the objects are brighter than the background. For that reason white or bright pixels are supposed to be an object and black or dark ones background.

The aim of this thresholding is to change the pre-filtered greyscale image into a binary image, so the process is used as binarization as explained in [7] and shown in Fig. 2.3.

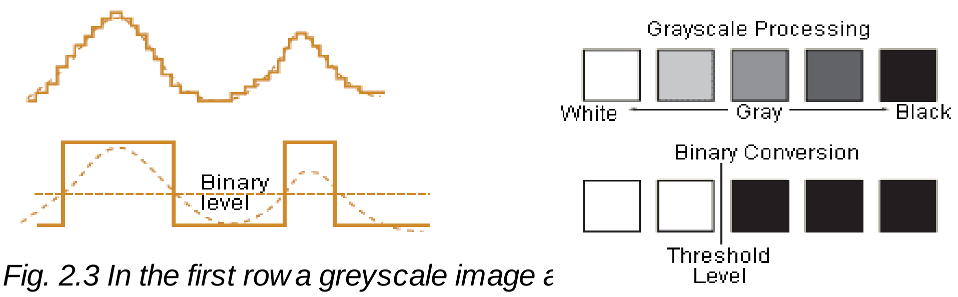

Fig. 2.3 In the first row a greyscale image a te, gray, black) are shown. In the second raw there is the binarized image of first row. Given a threshold level, all the pixels above become white and all below black.

In a greyscale image, brightness graduation can be differentiated and it is divided into 256 different levels. When the transformation to binary image is made, the brightness graduation can not be differentiated and we can only find two levels 0 or 1 determined by threshold value.

The obtained threshold can be applied to the image using global techniques which set a global threshold for the entire image or local techniques that apply different threshold values in each part of the image. In this second technique the value depends on the neighbour pixel values.

2.3. Shape Classification

In the previous sub-sections we were searching techniques and methods to improve images for a better display.

At this point of the image processing chain the objective is to analyze the content of the image. So the first step is to select the segmentation algorithm to divide the image into regions of interest. Then each region will be analyzed to determine if a region is accepted or discarded. In this memory are only explained those techniques which allow determining rectangularity.

Region identification: Labelling

A region is a set of pixels where all the pixels are adjacent or touching. The formal definition of connectedness is as follows [3]: Between any two pixels in a connected set, there exists a connected path wholly within the set, where a connected path is a path that always moves between neighbouring pixels. Thus, in a connected set, you can trace a connected path between any two pixels without ever leaving the set.

There are 2 kind of connectivity, 4 and 8 connectivity, depending on how many neighbours are used to calculate it. They can be seen in Fig. 2.4 where actual pixel corresponds to blue one.

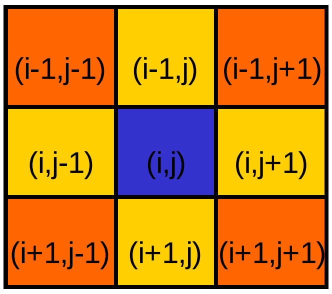

Fig. 2.4 4-connectivity corresponds to yellow pixels; 8-connectivity to yellow and orange pixels

In computing, as we run the image normally from the left-up corner (first pixel) to the right-down (last one), we consider connectivity in terms shown in Fig. 2.5 because the rest of pixels are not read when we are computing actual pixel (in blue).

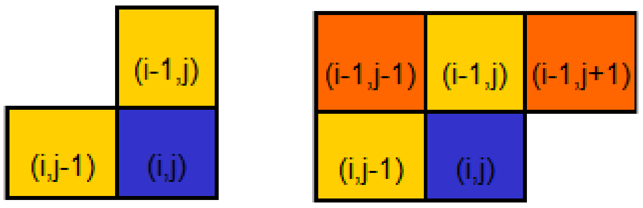

Fig. 2.5 Left: In computing 4-connectivity;Right: in computing 8-connectivity

Region based- shape representation and description

The use of descriptors becomes very useful in shape description. In general, descriptors are some set of numbers which describe a given shape. The shape may not be entirely reconstructable from the descriptors but the descriptors for different shapes could be different enough so the shapes can be discriminated.

A good descriptor is that with the greater the difference in significantly different shapes and the lesser the difference for similar shapes. Descriptors work in a qualitative way so they attempt to quantify shape so the human intuition does not perceive the difference between real and descript.

Simple scalar region descriptors

A large group of shape description techniques are represented by heuristic approaches which yield acceptable results in description of simple shapes. Some heuristic region descriptors are: area, perimeter, (non)compactness, (non)circularity, eccentricity, elongatedness, rectangularity, orientation (direction)...

These descriptors cannot be used for region reconstruction and do not work for more complex shapes.

Moments

Moments describe numeric quantities at some distance from a reference point or axis. They are commonly used in statistics to characterize the distribution of random variables. The use of moments for image analysis is straightforward if we consider a binary image as a two dimensional density distribution function. In this way, moments may be used to characterize an image segment and extract properties that have analogies in statistics.

Considering image size MxN and *i* and *j* image coordinates, different order moments and parameters related with them can be defined.

- First order moments:

$$m_{pq} = \sum_{i=0}^{M-1} \sum_{j=0}^{N-1} i^p j^q f(i,j)$$

$$m_{pq} = \sum_{i=0}^{M-1} \sum_{j=0}^{N-1} i^p j^q f(i,j)$$

- Centroids:

$$x_c = \frac{m_{10}}{m_{00}}$$

$$y_c = \frac{m_{01}}{m_{00}}$$

- Central moments: translation invariance

$$\mu_{pq} = \sum_{i=0}^{M-1} \sum_{j=0}^{N-1} (i - x_c)^p (j - y_c)^q f(i,j)$$

Reeves and Rostampour [14][15] used standard moments for global generic shape analysis. They selected four “ideal” symmetric generic shapes: rectangle, ellipse, diamond and concave object. They evaluated a parameter called Kurtosis parameter to determine those shapes. It can be calculated as:

$$Kx = \frac{\mu_{40}}{{\mu_{20}}^2} - 3$$

Kurtosis parameter is a measure of the peakedness of the probability distribution of a real-valued random variable. Higher kurtosis means more of the invariance is due to infrequent extreme deviations, as opposed to frequent modestly-sized deviations.

The “minus 3” of the equation is a correction to make the Kurtosis of the normal distribution equal to zero.

2.4. Object Recognition

One of the primary functions of the human visual system is object recognition, an ability that allows us to relate the visual stimuli falling on our retinas to our knowledge of the world.

Humans recognize a multitude of objects in images with little effort, despite the fact that appearance of an object can have a large range of variation due to photometric effects, scene clutter, changes in shape (non-rigid objects) and viewpoint.

The requirements of an object recognition system are:

- Invariant viewpoint: translation, rotation, scale
- Robust: to noise, to local errors in early processing modules, to illumination (shadows), to partial occlusion and to intrinsic shape distortions.

From a given input image an appropriate set of features are extracted. The aim of this process is to take a large amount for image data and retain only that information necessary to identify or distinguish the object. The knowledge from the shape of the object may be used to govern the extraction of features.

A matching algorithm (SIFT) will compare the ideal object with the object in the image and with the help of the extracted features it will determine if the object of the image corresponds to one of the searched objects or not.

Invariance: Local features

Invariants are properties which remain unchanged under an appropriate class of transforms [20]. To accomplish the requirement of invariance of our object recognition system we have to study all the invariant transformations that we can apply to our image to obtain an invariant viewpoint. That means that the object can be identified either it is smaller/bigger than the model, or it is rotated, or translated…

Following 5 effects of different transformations applied to a rectangle using Geometric transformation invariants can be seen:

1. **Translation**

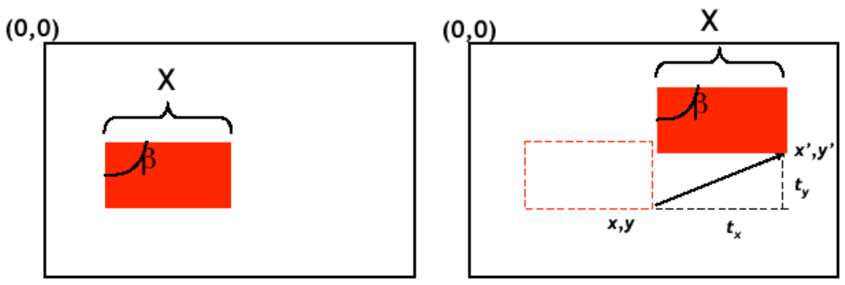

Fig. 2.6 Rectangle is moved to another position (translated) remaining invariant: length, angle, length ratio and parallel lines.

If we have the original image coordinates (x,y) the general equations to a translation in 2D coordinates are:

$$x' = x + t_x = 1 \cdot x + 0 \cdot y + t_x \cdot 1$$

$$y' = y + t_y = 0 \cdot x + 1 \cdot y + t_y \cdot 1$$

Equations can be easily determined if we take a look to Fig. 2.6. The homogeneous coordinates can be expressed in matricial notation: *X=X'+t*

$$\begin{pmatrix} x' \\ y' \\ 1 \end{pmatrix} = \begin{pmatrix} 1 & 0 & t_x \\ 0 & 1 & t_y \\ 0 & 0 & 1 \end{pmatrix} x \begin{pmatrix} x \\ y \\ 1 \end{pmatrix}$$

The invariants are length, angle, length ratio and parallel lines.

2. Rotation

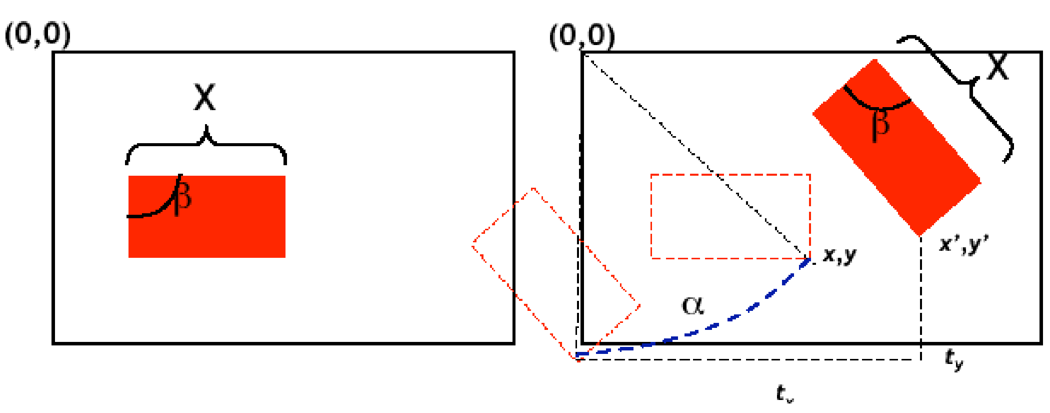

Fig. 2.7 Rectangle is rotated respect a point remaining invariant: length, angle, length ratio and parallel lines

The equations which describe the rotation feature in 2D that can be seen in Fig. 2.7.

$$x' = \cos(\alpha) \cdot x + \sin(\alpha) \cdot y + t_x$$

$$y' = -\sin(\alpha) \cdot x + \cos(\alpha) \cdot y + t_y$$

These equations can be expressed in homogeneous coordinates as:

$$\begin{pmatrix} x' \\ y' \\ 1 \end{pmatrix} = \begin{pmatrix} \cos(\alpha) & \sin(\alpha) & t_x \\ -\sin(\alpha) & \cos(\alpha) & t_y \\ 0 & 0 & 1 \end{pmatrix} x \begin{pmatrix} x \\ y \\ 1 \end{pmatrix}$$

The invariants here are length, angle, length ratio and parallel lines.

3. Similarity

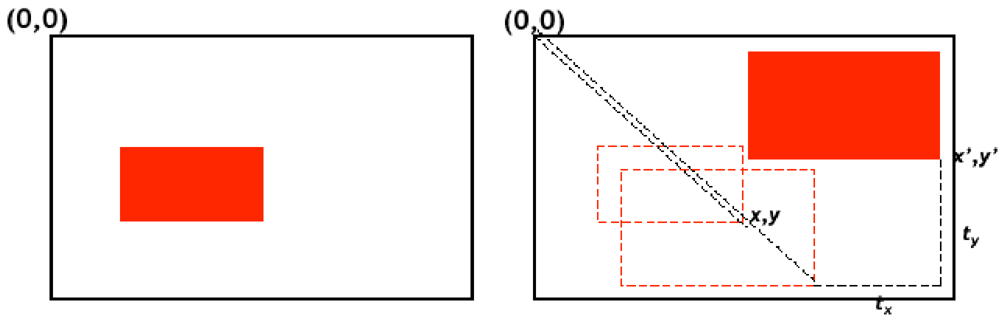

Fig. 2.8 Rectangle is smaller or bigger but relation between sides remain invariable

The equations to describe this movement are:

$$x'=s\cdot x + 0\cdot y + t_x \cdot 1$$

$$y'=0\cdot x + s\cdot y + t_y \cdot 1$$

In matrix notation x'=S·x+t

$$\begin{pmatrix} x' \\ y' \\ 1 \end{pmatrix} = \begin{pmatrix} s & 0 & t_x \\ 0 & s & t_y \\ 0 & 0 & 1 \end{pmatrix} x \begin{pmatrix} x \\ y \\ 1 \end{pmatrix}$$

4. Affine

The movement of the rectangle is shown in Fig. 2.9

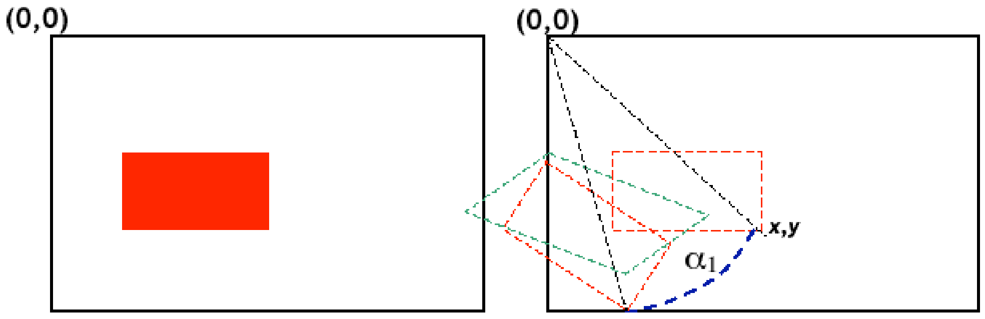

Fig. 2.9 Red rectangles are invariant to length, angle, length ratio and parallelism. Our interest rectangle (green one) is only invariant to parallelism

The equations to express this movement are:

$$x' = \cos(\alpha_1)\cdot s_x\cdot x + \sin(\alpha_1)\cdot s_y\cdot y + t_x$$

$$y' = -\sin(\alpha_1)\cdot s_x\cdot x + \cos(\alpha_1)\cdot s_y\cdot y + t_x$$

In matricial $x' = S\cdot R(\alpha_1)\cdot x$

When we apply the movement described in Fig. 2.9 to green rectangle no length, no angle and no length ratio are invariant, only parallelism.

Fig. 2.10 helps us to define relationships between original rectangle and the one moved.

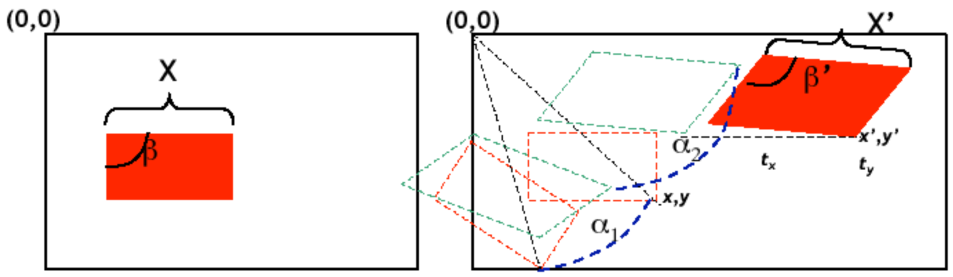

Fig. 2.10 Expression of variables involved in this movement

$$R(\alpha_2)\cdot S\cdot R(\alpha_1) = \begin{pmatrix} \cos(\alpha_2) & \sin(\alpha_2) \\ -\sin(\alpha_2) & \cos(\alpha_2) \end{pmatrix}\cdot\begin{pmatrix} sx & 0 \\ 0 & sy \end{pmatrix}\cdot\begin{pmatrix} \cos(\alpha_1) & \sin(\alpha_1) \\ -\sin(\alpha_1) & \cos(\alpha_1) \end{pmatrix}$$

The general expression in matrix notation:

$$x' = R_2\cdot S\cdot R_1\cdot x + t$$

$$\begin{pmatrix} x' \\ y' \\ 1 \end{pmatrix} = \begin{pmatrix} \multicolumn{2}{c}{R(\alpha_2)\cdot S\cdot R(\alpha_1)} & t_x \\ & & t_y \\ 0 & 0 & 1 \end{pmatrix} \cdot \begin{pmatrix} x \\ y \\ 1 \end{pmatrix}$$

5. Projective

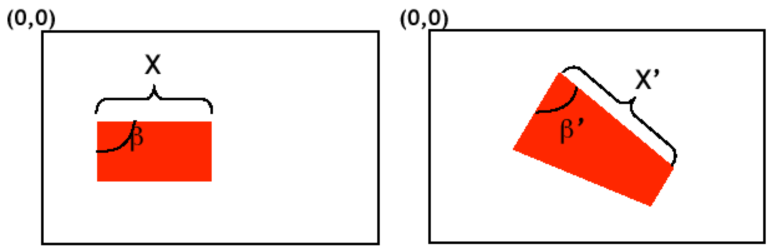

Fig. 2.11 Rectangle is not invariant to length, angle, length ratio and parallelism

With the transformation of Fig. 2.11 length, angle, length ratio and parallelism are not invariant.

That can be expressed in homogeneous coordinates as:

$$\begin{pmatrix} x' \\ y' \\ z' \end{pmatrix} = \begin{pmatrix} h_{11} & h_{12} & h_{13} \\ h_{21} & h_{22} & h_{23} \\ h_{31} & h_{32} & 1 \end{pmatrix} \cdot \begin{pmatrix} x \\ y \\ 1 \end{pmatrix}$$

and in image coordinates:

$$\begin{pmatrix} x'' \\ y'' \\ 1 \end{pmatrix} = \frac{1}{z'} \cdot \begin{pmatrix} x' \\ y' \\ z' \end{pmatrix}$$

All these features described above can be local or global features. We are looking for local features because global fail in image transformations (scale change), in occlusions and background clutter (segmentation-hard), in colour (light changes) and in geometric (contour based fail if no shape).

The key properties of a good local feature are:

- Must be highly distinctive, a good feature should allow for correct object identification with low probability of mismatch
- Should be easy to extract
- Invariance, a good local feature should be tolerant to: image noise, changes in illumination, uniform scaling, rotation and minor changes in viewing direction.
- Should be easy to match against a database of local features.

Detector + Descriptor: SIFT

The local features become the interesting points on the object (marker) and they can be extracted to provide a feature description of the object. These interesting points can be used to identify the object when there is an image containing the object we are looking for and many other objects. That is the reason why it is important that the set of features extracted is robust to changes in image scale, noise, illumination and local geometric distortion, for performing reliable recognition.

The ideal interest points/regions are those which are numerous repeatable, representative in orientation/scale and fast to extract and match (as shown in Fig. 2.12).

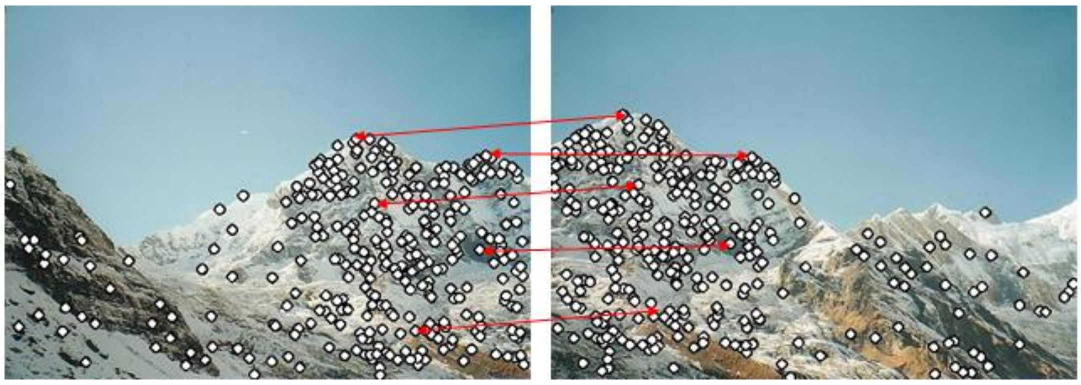

Fig. 2.12 Interest points in the image on the left are matched with the same points on the right although they are not in the same image position (M. Brown and D. G. Lowe. Recognising Panoramas. In Proceedings of the International Conference on Computer Vision (ICCV2003)

There is a patented algorithm developed by Lowe [16] [18] that can robustly identify objects even among clutter and under partial occlusion called SIFT. The name comes from Scale Invariance Feature Transform and is a good approach for detecting and extracting local feature descriptors that are reasonably invariant to changes in illumination, image noise, rotation, scaling and small changes in viewpoint.

There are other newer feature detectors as SURF (Speeded Up Robust Features)[23]. As shown in the study [24] SURF descriptor is better than SIFT at matching computing time but worse at match ratio and total number of correct matches as well as the quality and total number of the created keypoints.

There are also works in which the behaviour of SURF to affine transformations is not as good as SIFT [26].

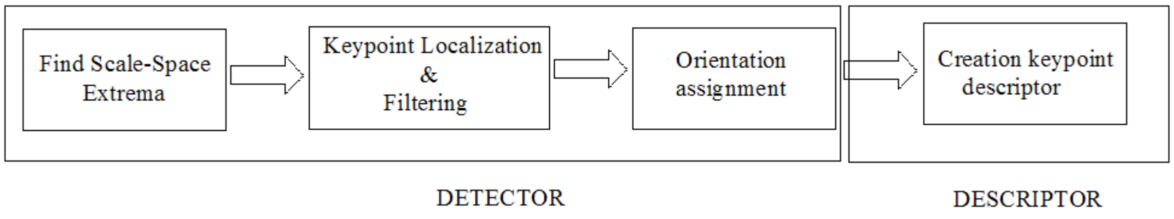

Fig. 2.13 Four Stages of SIFT algorithm divided in two blocks, detector and descriptor

SIFT can be divided into 2 blocks: Detection and Description. Altogether has 4 stages shown in Fig. 2.13

1st Step: Find Scale-Space Extrema: it searches over all scales and image locations. It is implemented by using a difference-of Gaussian function to identify potential interest points that are invariant to scale and orientation.

2nd Step: Keypoint Localization and Filtering: at each candidate location a detailed model is fit it determine location and scale. Keypoints are selected based on measures of their stability and this way improve keypoints and throw out bad ones.

3rd Step: Orientation assignment: removing effects of rotation and scale: On each point 1 or more orientation based on local image gradient directions are assigned.

4th Step: Create keypoint descriptor: (using histograms of orientation) The local image gradients are measured at the selected scale in the region around each keypoint. These are transformed into a representation that allows for significant levels of local shape distortion and change in illumination.

As follows each step for the understanding of SIFT algorithm is widely explained.

1st Step: Detection of scale-space Extrema

Koenderink (1984) and Lindeberg (1994) show that under a variety of reasonable assumptions the only scale-space kernel is the Gaussian function.

The scale-space is described as a continuous function of scale σ: L(x, y, σ), the result of the convolution between a variable-scale Gaussian G(x, y, σ) and the input image (resulting image from segmentation) where:

$$G(x, y, \sigma) = \frac{1}{2\pi\sigma^2} e^{-(x^2+y^2)/2\sigma^2}$$

Experimentally, Maxima and minima of Laplacian-of-Gaussian gives best notion of scale ([21]) producing the most stable image features compared to another image functions such as the gradient, Hessian or Harris corner function. Thus using Laplacian-of-Gaussian (LoG) operator:

$$\sigma^2 \nabla^2 G$$

LoG is expensive to calculate so with the help of heat diffusion equation, the definition of Difference-of-Gaussians (DoG) and parameterized in terms of σ rather than the more usual $t=\sigma^2$:

$$\frac{\partial G}{\partial \sigma} = \sigma \nabla^2 G$$

$\nabla^2 G$ can be computed from the finite difference approximation to $\partial G/\partial\sigma$ using the difference of nearby scales at *kσ* and *σ*:

$$\sigma \nabla^2 G = \frac{\partial G}{\partial \sigma} \approx \frac{G(x, y, k\sigma) - G(x, y, \sigma)}{k\sigma - \sigma}$$

The efficiency of DoG is based in a simple operation, subtraction of two images.

Therefore, isolating difference of Gaussian:

$$G(x, y, k\sigma) - G(x, y, \sigma) \approx (k-1)\sigma^2 \nabla^2 G$$

That shows that when difference of Gaussians (DoG) function has scales differing by a constant factor it already incorporates the σ^2 scale normalization required for the scale-invariant Laplacian. The factor *(k-1)* in the equation is a constant over all scales and therefore does not influence in extrema location. The approximation of the error will go to 0 as *k* goes to 1, but in practice Lowe study has almost no impact on the stability of extrema detection of localization for even significant differences in scale such as $k=\sqrt{2}$.

So in conclusion what is done is to construct a scale-space like shown in Fig. 2.14

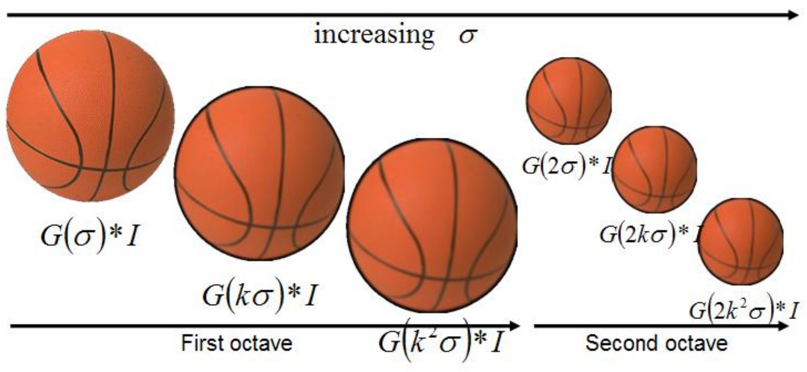

Fig. 2.14 Scale Space of DoG

For each octave of scale space the initial image is repeatedly convolved with Gaussians to produce the set of scale space images separated by a constant *k*. Each octave is then divided into intervals *s* so $k=2^{1/s}$. We must procedure *s+3* images in the stack of blurred images for each octave so that final extrema detection covers a complete octave.

Adjacent Gaussians images are subtracted to produce the difference of Gaussian images. Fig. 2.15 shows the computing of DoG.

After each octave the Gaussian image is down sampled by a factor of 2 and the process is repeated.

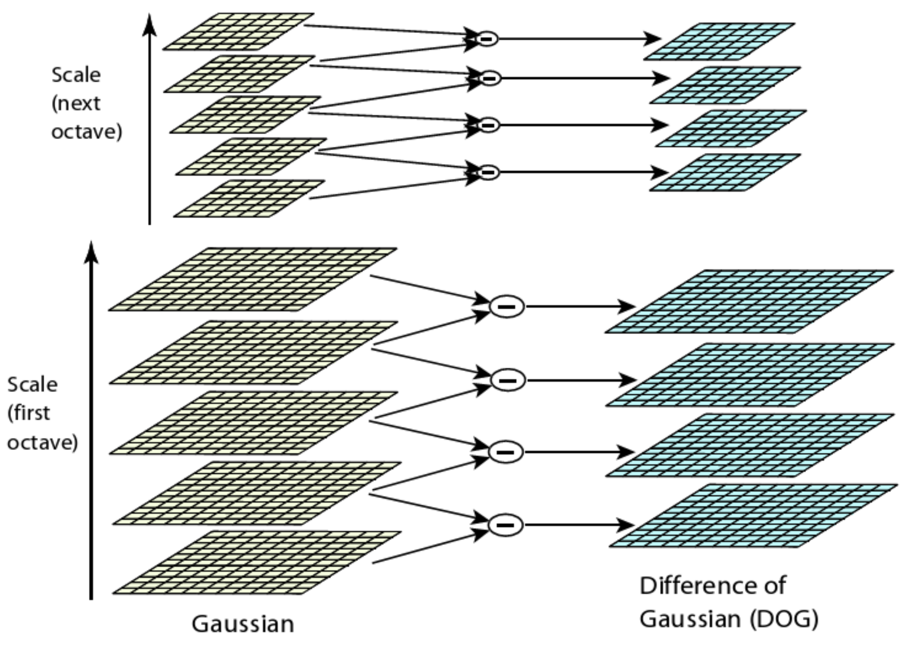

Fig. 2.15 Difference of Gaussians are computed. For each octave there are s intervals so $k=2^{1/s}$, s+3 Gaussian must be processed. σ doubles for the next octave.

All extrema (maxima and minima of the DoG) within 3x3 neighbourhood are chosen so that the pixel marked with X is compared to its 26 neighbours at the current and adjacent scales (see Fig. 2.16)

It is selected as maxima only if it is larger than all of the neighbours or minima if it is smaller than all of them.

The cost of this check is reasonably low due to the fact that most sample points will be eliminated following the first few checks.

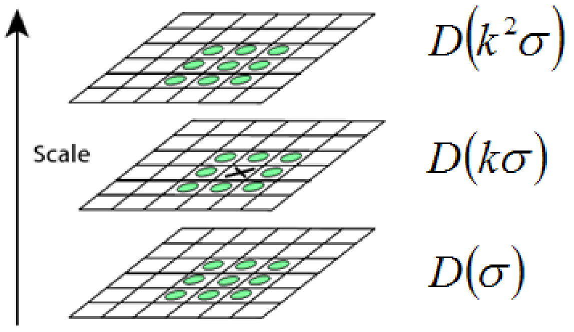

Fig. 2.16 Maxima and minima of DoG images are detected by comparing the pixel marked as X to its 26 neighbours in 3x3 regions at the current and adjacent scales (marked with circles)

2nd Step: Keypoint Localization & Filtering

In this section for each candidate keypoint is needed:

- Interpolation of nearby data is use to accurately determine its position
- Keypoints with low contrast are remove
- Responses along edges are eliminated
- The keypoint is assigned an orientation

After scale space extrema (keypoint candidates) are detected by comparing a pixel to its neighbour, the next step is to perform a detail fit to the nearby data for location, scale and ratio of principal curvatures. This information allows that points, with low contrast (and therefore sensitive to noise) and poorly localized along the edge, are rejected.

The initial approach of Lowe [16] searched to locate each keypoint at he location and scale of the central sample point. With the new approach [19] the interpolated location of the maximum is calculated. This fact improves matching and stability.

The interpolation is done using Taylor expansion series (up to the quadratic terms) of the Difference-of-Gaussian scale space function D(x,y,σ). It is shifted so that the origin is at the sample point:

$$D(x) = D + \frac{\partial D^T}{\partial x} x + \frac{1}{2} x^T \frac{\partial^2 D}{\partial x^2} x$$

D and derivatives are evaluated at the sample point and the offset from this point $x=(x,y,\sigma)^T$.

The location of extrema, x_M, is determined by taking the derivative of this function with respect to x and setting it to zero, giving:

$$x_M = -\frac{\partial^2 D^{-1}}{\partial x^2}\frac{\partial D}{\partial x}$$

If the offset x_M is larger than 0,5 in any dimension , indicates that the extrema lies closer to another candidate keypoint. In this case, the candidate keypoint is changed and the interpolation performed instead about that point. Otherwise the offset is added to its candidate keypoint to get the interpolated estimate for the location of the extrema.

To reject unstable extrema with low contrast the value of the second order Taylor expansion is computed at the offset x_M.

$$D(x_M) = D + \frac{1}{2}\frac{\partial D^T}{\partial x}x_M$$

If this value is less than 0.03 (assuming image pixel values in the range [0, 1]), the candidate keypoint is discarded. Otherwise is kept, with final location $y + x_M$ and scale σ, where y is the original location of the keypoint at the scale σ.

For stability is not sufficient to reject keypoints with low contrast. The DoG function will have strong response along edges, even if the candidate keypoint is poorly determined and therefore unstable to small amounts of noise. A poorly defined peak in DoG will have a large principal curvature across the edge but a small one in the perpendicular direction, that means that we want to reject points with strong edge response in one direction only.

The principal curvatures can be computed from 2x2 Hessian matrix at the location and scale of the keypoint:

$$H = \begin{pmatrix} Dxx & Dxy \\ Dxy & Dyy \end{pmatrix}$$

The eigenvalues of H are proportional to the principal curvatures of D. Borrowing from the approach used by Harris and Stephens (1988)[25] we can avoid explicitly computing the eigenvalues, as we are only concerned with their ratios. It turns out that the ratio $r=\alpha/\beta$ of the two eigenvalues, where α is the larger one and β the smaller one is sufficient for SIFT purposes.

$$Tr(H) = D_{xx} + D_{yy} = \alpha + \beta$$

$$Det(H) = D_{xx}D_{yy} - D_{xy}^2 = \alpha\beta$$

In the unlikely event that the determinant is negative the curvatures have different signs so the point is discarded as not being an extrema.

Then,

$$R = \frac{Tr(H)^2}{Det(H)} = \frac{(\alpha+\beta)^2}{\alpha\beta} = \frac{(r\beta+\beta)^2}{r\beta^2} = \frac{(r+1)^2}{r}$$

which depends only on the ratio of the eigenvalues rather than the individual values. R is minimum when the eigenvalues are equal to each other. Therefore the higher the absolute difference between the two eigenvalues, which is equivalent to a higher absolute difference between the two principal curvatures of *D*, the higher the value of *R*.

For some threshold eigenvalues ratio r_{th}, if *R* for a candidate keypoint is larger than $R < \frac{(r+1)^2}{r}$ that keypoint is poorly localized and hence rejected. In Lowe 2004 this value r_{th}=10 and it is efficient to compute with less than 20 floating point operations to test each keypoint.

3rd Step: Orientation assignment: removing effects of rotation and scale

The last step done by detector is to determine the keypoint orientation based on local image gradient directions and this way achieving invariance to rotation. A gradient orientation histogram is computed in the neighbourhood of the keypoint, using Gaussian smoothed image at the closest scale to the keypoint's scale, *L(x, y, σ)*, so all computations are performed in a scale-invariant manner. Gradient magnitude and orientation are pre-computed using pixel finite differences:

$$m(x,y) = \sqrt{(L(x+1,y) - L(x-1,y))^2 + (L(x,y+1) - L(x,y-1))^2}$$

$$\theta(x,y) = \tan^{-1}\left(\frac{L(x,y+1) - L(x,y-1)}{L(x+1,y) - L(x-1,y)}\right)$$

The magnitude and direction calculations for the gradient are done fore every pixel in a neighbouring region around the keypoint in the Gaussian smoothed image L. An orientation histogram is formed with 36 bins covering each of them 10 degrees. Each sample in the neighbouring window added to the histogram bin is weighted by its gradient magnitude an by a Gaussian-weighted circular window with a σ that is 1,5 times the scale of the keypoint, that shows Fig. 2.17.

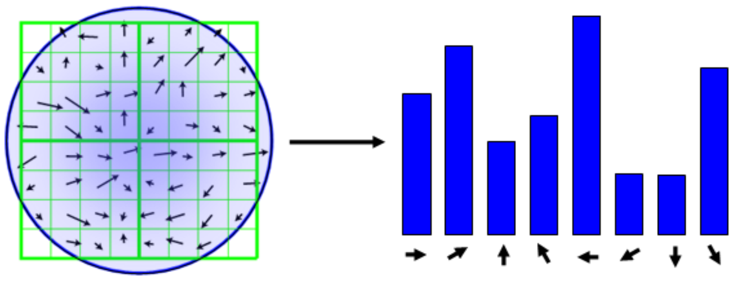

Fig. 2.17 Creation of gradient histogram (36 bins). Weighted by magnitude and Gaussian window (overlaid circle) with σ 1,5 times the scale of the keypoint

Peaks in the histogram correspond to dominant directions of local gradients. The highest peak in the histogram is detected, and then any other local peak is within 80% of the highest peak is used to also create a keypoint with that orientation. Therefore, for locations with multiple peaks of similar magnitude, there will be multiple keypoints created at the same location and scale but different orientations.

Only about 15% of points are assigned multiple orientations, but these contribute significantly to the stability of matching. Finally, a parabola is fit the 3 histogram values closest to each peak to interpolate the peak position for better accuracy.

As all the properties of the keypoints are measured relative to the keypoint orientation, we ensure it provides invariance to rotation.

4th Step: Descriptor

Previous steps found keypoint locations at particular scales and assigned orientations to them. This ensured invariance to image location, scale and rotation. Now we want to compute descriptor vectors for these keypoints such that the descriptors are highly distinctive and partially invariant to the remaining variations, like illumination, 3D viewpoint, etc. This step is pretty similar to the 3rd Step: Orientation Assignment.

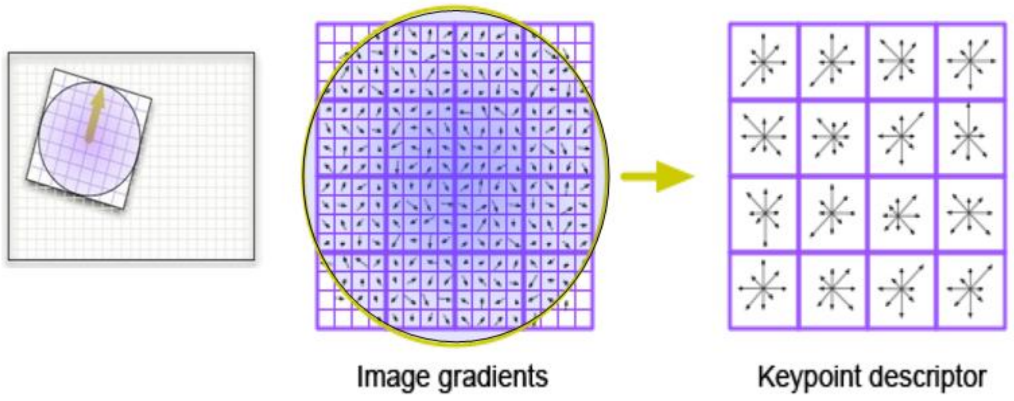

Fig. 2.18 Histogram of 4x4 samples per window in 8 directions with Gaussian weighted around centre. So we have a dimensional feature vector of 128 for each point (4x4x8)

The keypoint descriptor is created by fist computing the gradient magnitude and orientation at each image sample point in a region around the keypoint location using the scale of the keypoint to select the level of Gaussian blur for the image. In order to achieve orientation invariance, the coordinates of the descriptor and the gradient orientations are rotated relative to the keypoint orientation. Gradients are illustrated with small arrows at each sample location. The region is formed by a 16x16 set of samples. These are weighted by a Gaussian window (with σ equal to 0,5 times the width of the descriptor window) indicated by the overlaid circle. The purpose of this Gaussian window is to avoid sudden changes in the descriptor with small changes in the position of the window, and to give less emphasis to gradients that are far from the centre of the descriptor, as these are most affected by misregistration errors. These samples are then accumulated into orientation histograms summarizing the contents over 4x4 sub-regions with the length of each arrow corresponding to the sum of the gradient magnitudes near that direction within the region. So histograms contain 8 bins each, and each descriptor contains a 4x4 array of 16 histograms around the keypoint. This leads to a SIFT feature vector with 4 x 4 x 8 = 128 elements.

It is also important to avoid all boundary effects in which the descriptor abruptly changes as a sample shifts smoothly from being within one histogram to another of one orientation to another. Therefore, trilinear interpolation is used to distribute the value of each gradient sample into adjacent histogram bins, that means that each entry into a bin is multiplied by a weight of d-1 for each dimension, where d is the sample from the central value of the bin as measured in units of the histogram bin spacing.

Finally the feature vector is modified to reduce effects of illumination changes. First, the vector is normalized to unit length. A change in image contrast in which each pixel value is multiplied by a constant will multiply gradients by the same constant, so this contrast change will be cancelled by vector normalization. A brightness change in with a constant is added to each image pixel will not affect the gain of the gradient values. Therefore the descriptor is invariant to affine changes in illumination.

Although the dimension of the descriptor (128) seems high, descriptors with lower dimension than this do not perform as well across the range of matching tasks, [18].

The performance of SIFT descriptor is the best descriptor (together with GLOH, an extension of the SIFT descriptor designed to increase its robustness and distinctiveness)) as it explains the extensive survey of Mikolajczyk & Schmid [21].

The typical usage of SIFT for a set of database images is firstly to compute SIFT features and then save descriptors to database; for a query image firstly compute SIFT features, then for each descriptor find the closest descriptors (Euclidean distance) in database and finally verify matches (geometry and Hough transform).

Given SIFT's ability to find distinctive keypoints that are invariant to location, scale and rotation, and robust to affine transformations (changes in scale, rotation, shear, and position) and changes in illumination, they are usable for object recognition

3. Our contribution

Our goal is to recognize objects (where objects are our markers) in image. To identify them there are necessary some previous steps to prepare digital image to apply shape and object recognition techniques and, this way, distinguish desired areas from not desired ones (described in Sections 2.3 and 2.4) and extract those of our interest.

During all this section we explain which of the terms and methods described in Section 2 will be applied in our project in order to reach the objective raised of extracting markers from image. All the techniques described are thought to be implemented in a C++ application which will be explained more widely in Section 4.

First of all, what we are looking for is a photo (image) in which we can differentiate bright from dark regions to distinguish our markers from the parts of the cylindrical structure. Colour in image is not as important as the distinctiveness of the markers (internal and external part) from the rest of picture taken, and, as we want to work with images along the whole image processing chain, size of image (in terms of bytes) is also very important. The biggest the image is, the more complicated the operations are.

At this point it is also remarkable the fact that we have a video camera but we are going to use it as a photocamera as explained in Proposal of solution (Section 1) where the question of calibration in real time is discussed.

So altogether, a good solution in our case is to take a gray-scale image. That is the result of a gray-scale transformation in which pixel brightness of each pixel is changed without regarding to its position in the image. It is described in Section 2.1 as pre-processing step and it is done by the software provided by the camera provider (uEye Setup Version 3.1, www.ids-imaging.com) which allows us choosing the pixel colour depth that we desire in our capture from camera recording in real time.

This high quality gray-scale image taken by the camera as described in Appendix C is our testimage (testimage.bmp), the starting point of our study and analysis. It is shown in Fig. 3.1., its original size is 2048x 1536 and the format is bmp (bitmap).

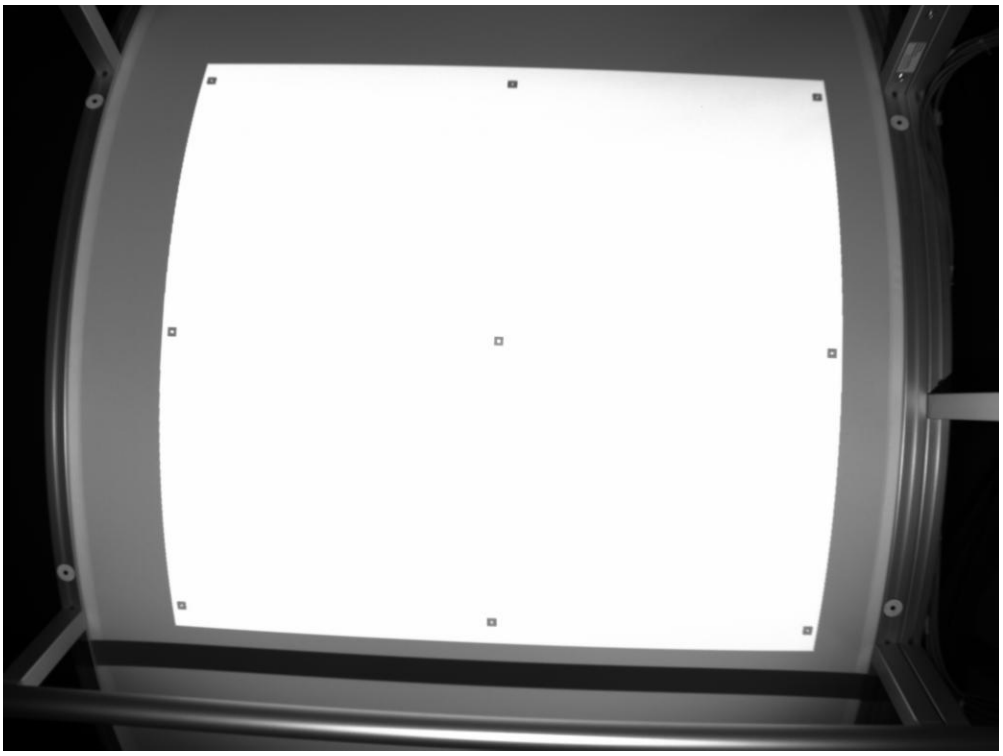

Fig. 3.1 Testimage taken by camera of the image projected by projector

In testimage we can see parts from the cylindrical structure where 4 round markers (external markers) are located and an image corresponding to image projected by projector onto the cylindrical surface where internal markers (squares) are shown.

From now on to easily identify and name the markers in the image we are going to consider the following notation. The notation will be a capital letter followed by a number. The capital letter will be I or E depending on which marker we are referring to, Internal or External; and the number corresponds to the position on the image considering the first one that up-left marker (1) and the last one down-right (visually perception if we read image horizontally).

Image pre-processing

Our markers present an abrupt variation of the brightness between the internal and external part. The internal markers are black squares with a white square hole in the middle, and the external markers are orange circles with a black circle hole in the middle as shown in Fig. *3.2*

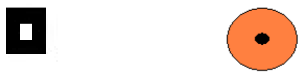

Fig. 3.2 These are the markers used in our project: internal and external, left and right respectively

There is not only an abrupt variation between internal and external part of markers but also appear a considerable variation between markers and the areas next to them (cylindrical structure, shadows...), so they are easily distinguishable when light conditions are appropriate (see Fig. 3.3)

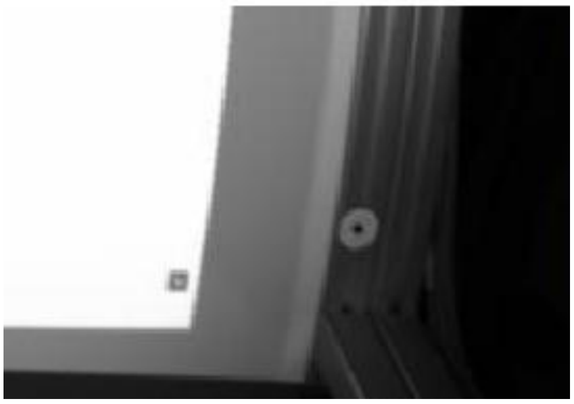

Fig. 3.3 The picture shows both markers (internal and external)

At this point we have consider that due to projection on the cylindrical structure markers do not look like ideal markers shown in Fig. 3.2 because they are affected mostly by affine and projective features described in Section 2.4 especially in the corners where the effects are more noticeable (see Fig. 3.4).

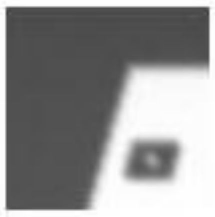

Fig. 3.4 Internal marker I1: left-up. The shape of square is affected by affine and projective features

Moreover, it is important to completely identify the internal part of a marker (holes as a distinctiveness feature of our markers) in order to, in further steps of the image processing chain, determine correctly if a region is or not a desired marker.

The aim of the local pre-processing is filtering for improving images. In our case with the sharpening filter, described in Section 2.1, fine details of image are enhanced, giving an improved image to our purpose and with a simpler implementation than first-derivative as described in [1].

This step was added before the image processing chain after seeing some results described in Section 5 (Results) in which the inside regions of our internal markers almost disappear. So without this step the results obtained at detecting markers are not good enough.

With this filter differences are accentuated and constant areas are left unchanged. Also noise is accentuated but as our image has high quality, the effect is barely noticeable. This effect of the filter to the image can be seen in Fig. 5.13 and Fig. 5.14 from Results.

Until now what we have is a sharpened image from original one and what we want is to label different regions in image and apply some criteria to discard not desired regions.

Segmentation

Region identification (labelling) expects a binary image to determine the different regions so the pre-filtered gray-scale image has to be converted to a binary image (binarization).

Our case of study has a strong dependency of light conditions. This point makes important to find a robust threshold technique in order to avoid problems if the structure is moved to a brighter or darker place or the light in the salon varies. According to that we can come across a situation in which a part of an image is more illuminated than other one and in the darker one is the object we are looking for. So when there are changes in illumination across the image, an inconstant illumination, it is better to use local instead of global threshold. This way the threshold can vary smoothly across the image. Different thresholds can be chosen depending on the part of the image to distinguish desirable from undesirable objects in the image.

Now we need to find a method for dividing the image into different parts so that each part can have a different threshold, local threshold, and thus we can solve the problem of different lightning conditions.

How these parts should look is taken from Wall's algorithm [8]. The strategy is to divide geometrically the image, not depending on pixel characteristics or values.

The image can be divided into blocks of different sizes *m_m* and *n_n* decided by programmer/user, width and height of blocks can have equal or different sizes. Once decided the height (m_m) and width (n_n) the blocks remain constant (m_m*n_n pixels) in the whole image for that calibration except the ones in the boundaries (down or/and right), which are as small/big as image size allows.

Our image has a height of 1536, if each Wall's block has 256 of height size we will have 6 blocks of size Xx256, but if each block has a height size of 200, we will have 7 blocks of size Xx200 and the last row (the one down) of size Xx136 (1536-(7x200)). For a visually understanding see Fig. 5.7.

Once we know how to divide image to minor effects of changes in illumination, now the decision is how to choose the threshold value. As the regions can vary depending on user's desire the threshold should be such as it varies depending on the pixels of the block. That's why an adaptive threshold is needed [7]. This way and according to Wall's algorithm we will find so many thresholds as blocks in image.

The threshold value can be selected by user (random, mean, median...) or also computer can generate one automatically (automatic thresholding) and there are many different methods (Otsu, K-means… [6]). All this information is explained in Section 2.2.

Our decision is a clustering based method that works with an iterative technique robust against image noise and described in [9](Ridley and Calvard) .

The algorithm described by Ridley and Calvard's and implemented in our project consists in six steps. In Appendix A, Ridley and Calvard's deduction and mathematics involved are explained for the understanding of the algorithm used. The steps are:

1. To calculate histogram of the region of the image and set the mean intensity of the image, set T=mean (I)
2. To divide the histogram into two parts separated by T
3. To calculate an above mean T_{abv} and a below mean T_{bel}, one for each part of the histogram
4. To calculate the average between T_{abv} and T_{bel} resulting a new value of mean $T'=(T_{abv} + T_{bel})/2$
5. To repeat calculation of T_{abv} and T_{bel} but now with the new mean T'

6. To repeat the process until threshold does not change any more

Thanks to this algorithm we are able to find a suitable threshold for each part and they are also well adapted to changes in light conditions because it takes into account the pixel and the characteristics of their neighbours.

The different results obtained if we apply a global or local threshold to image and different threshold algorithm results are shown in Section 5.

As we have introduced before we were thresholding the image in order to apply labelling. After that we will decide which properties of the objects are the best to distinguish markers.

Region identification: Labelling

From binarized image we find the different regions present in image. A region, as described in Section 2.3, is a set of pixels where all the pixels are adjacent or touching. In our case we have chosen an 8-connectivity, see Fig. 2.4 and Fig. 2.5. The region identification method consists on labelling each region with a unique number where the largest number gives the total number of regions in the image.

The algorithm for approaching the labelling assumes that zero pixels represent background and non-zero pixels are objects. In a first iteration our algorithm searches pixel per pixel through the entire image (row by row) a non-zero pixel. The criterion are (see Fig. 2.5):

- If all the neighbours of the actual pixel *(i,j)* have zero value (background pixels) a new, and as yet unused, label is given to the pixel.
- If there is just one neighbouring pixel with a value different from zero, it assumes that *(i,j)* has the same value as this pixel.
- If there is more than one pixel with different value, the algorithm considers a label collision and it stores the pair of pixels in another data structure as equivalent.

In a second iteration the whole image is scanned again and the algorithm decides if the label collisions become one or another value analyzing the neighbouring pixels and the label they have adopted.

After this second iteration all pixels in image different from zero (possible markers) are labelled by a number which identifies them as part of a specific region.

Region based-shape representation

Now that all regions are identified we are going to analyze the content of the image. The objective is to find some features of our markers (size, shape) in order to univocal identify them from the rest of the objects in the image as for example parts of the cylindrical structure. That means that we have to analyse for each region if those features, also called region descriptors, are accomplished or not and depending the results discard or maintain region as a candidate for marker.

In this project we focus our attention in three region descriptors: area (size), rectangularity based on bounding box and rectangularity based on moments (the definition of terms has been made in Section 2.3).

With the help of the first region descriptor mentioned we will discard regions in both cases, internal and external markers. The other two region descriptors will be valid only in the case of internal markers because the strategy adopted to identify external markers is based in contours developed by Steffen Terörde in his Mater Thesis for IGD and TU-Darmstadt. Steffen is a student who developed an algorithm for detecting ellipses in image. We have integrated some of his programming codes into our GUI. In Section 3.1 IGD Contribution a short resume of the procedure is explained.

We have applied the following descriptor for both markers extraction:

1. Area (Size): corresponds to the number of pixels conforming the shape. It can be calculated with zero order moment m_{00}.

It is obvious that our markers are small and there are other regions in image really big if we compare them. So the first criterion to discard regions will be area (size). Differences between big and small objects are so great that it is not so important determining a frontier upper number once we know the size of internal markers (around 300 pixels) and external markers (around 900). In Section 5 (Results) will be shown the necessity of having a below value for the range in order to minor the effect of noisy regions. Attending to that we have considered for each case a range equal to ± (mean size of markers /2).

$$\text{Internal markers} \in (150, 350)$$

$$\text{External markers} \in (450, 1350)$$

It is in those known ranges where mostly problems are found and where another criterion is needed to discard markers from other small objects. As can be seen in Results (Section 5)

From now on we are only interested in determining features for internal markers. To ensure rectangularity of the regions we have chosen two descriptors:

2. Rectangularity based on Bounding Box: ratio which determines how rectangular a shape is. Attending to the conclusions of [11] and [12] and the complexity in terms of programming of other methods (like Rotating Callipers described in [12] and [13]), one method chosen to determine rectangularity in our project is based on minimum bounding box.

A box is a rectangular region whose edges are parallel to the coordinate axes. Its limits can be found as the minimum and maximum of each coordinate axes (x and y) determining 4 extreme points satisfying the inequalities:

$$x_{min} \leq x \leq x_{max}$$

$$y_{min} \leq y \leq y_{max}$$

So a minimal bounding box of a finite geometric object is the box with minimal area that contains the object. An illustrative example is shown in Fig. 3.5.

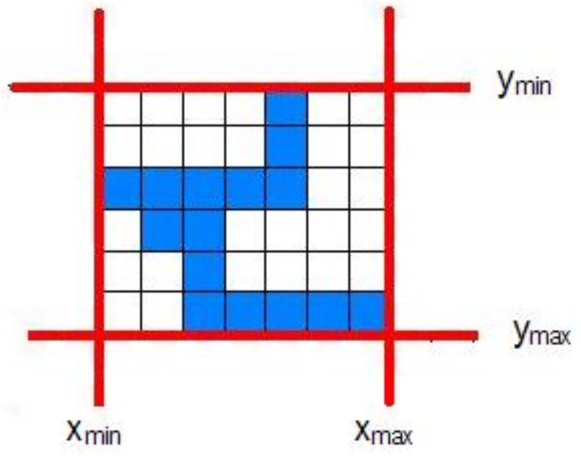

Fig. 3.5 Minimal Bounding Box determined by x_{min}, x_{max}, y_{min},y_{max}

This method is computationally the simplest of all linear bounding containers, and the one most frequently used in many applications. At runtime, the inequalities do not involve any arithmetic and it only compares raw coordinates with pre-computed *min* and *max* constants.

Rectangularity ratio (*R*) is the result of the proportion between the area of the object or region (*OA*) and the area of the bounding box (*BB*) or region's area against the area of the minimum bounding rectangle:

$$R = \frac{OA}{BB}$$

When both rectangles, containing and contained, have the same features this ratio is ideally 1. In our case this ratio is not ideally 1 because our markers have a hole in the middle and they are affected by projective and affine features. The hole of the internal marker has a size of approximately 1/9 of rectangle's region. (see Fig. 3.6):

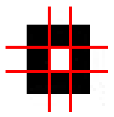

Fig. 3.6 Internal Marker divided into 9 equal parts to calculate the percentage of area occupied by marker and not by the hole inside the Bounding Box

Attending to projective and affine properties we have considered that all the objects (regions) with a ratio of at least a 75% are suspected to be desired markers.

3. Rectangularity based on Moments (Kurtosis parameter): Another way to describe shape uses statistical properties called moments.

Our interest is focused in:

- zero order moment m_{00} =Area (for calculating first descriptor described above)
- first order moment m_{10}. Thanks to it we can calculate the centroid in the x-axis: x_c (Central moments corresponding to translation invariance) necessary to determine second order moments.
- second order moments: μ_{20} and μ_{40}. With them we are able to determine Kurtosis parameter.

We use the results of the study developed by Reeves and Rostampour [14][15] to determine, using standard moments, if the shape of our interest region is a rectangle or not .

The rectangle should have a Kurtosis parameter Kx =-1.2 using:

$$Kx = \frac{\mu_{40}}{\mu_{20}^{2}} - 3$$

At this point we have also considered a little margin around -1.2 (from -1.05 to -1.35) for not being so strict because most of markers are affected by affine and projective features. This criterion appeared to be in Section 5 a good solution at identifying markers.

We have tested different possibilities of ratios and its combination. As can be seen in Section 5 the best solution is to combine both rectangularity descriptors and decide that a region is rectangular when accomplish the equation:

```
ratio>0.75 and ((kx<-1.05 )and(kx>-1.35))
```

To ensure that objects extracted after feature description correspond to our internal markers and to give robustness to the markers extraction chain we apply SIFT detector and descriptor explained in Section 2.4

Object recognition: SIFT

From image an appropriate set of features are extracted. The aim of object recognition is to take a large amount for image data and retain only that information necessary to identify or distinguish the object. The knowledge we have from the shape of the object we are looking for may be used to govern the extraction of features.

A matching algorithm will compare the ideal marker with the marker in the image and with the help of the extracted features it will determine if the object of the image corresponds to one of our searched markers or not.

As our application has not to run at real time (the process is done once a week, month… what user decides) and has to attend to affine property what we are looking for is accuracy at determining keypoints and correct matches in the whole process and is not so important how long it takes in calculate them.

We have various possible algorithms to make this matching, the most known are SIFT and SURF. Attending that our markers are subjected to affine features and according to [26] we have decided that the better performance will be done by SIFT as described in Section 2.4. The results are shown in Section 5.

In our case the SIFT implementation used is that described in [10] which is compatible to Lowe's version. For applying the algorithm we need the image of study (marker) and a template (See Fig. 3.2). The algorithm will do the matching between both images to determine if they correspond to the same object or not.

The sift function returns a 4xK matrix frames containing the SIFT frames and a 128xK matrix descriptors containing their descriptors. Each frame is characterized by four numbers which are:

- (x1; x2): for the centre of the frame
- σ: The scale σ is the smoothing level at which the frame has been detected
- Ɵ: frame's orientation

The coordinates (x1; x2) are relative to the upper-left corner of the image, which is assigned coordinates (0; 0), and may be fractional numbers (sub-pixel precision).

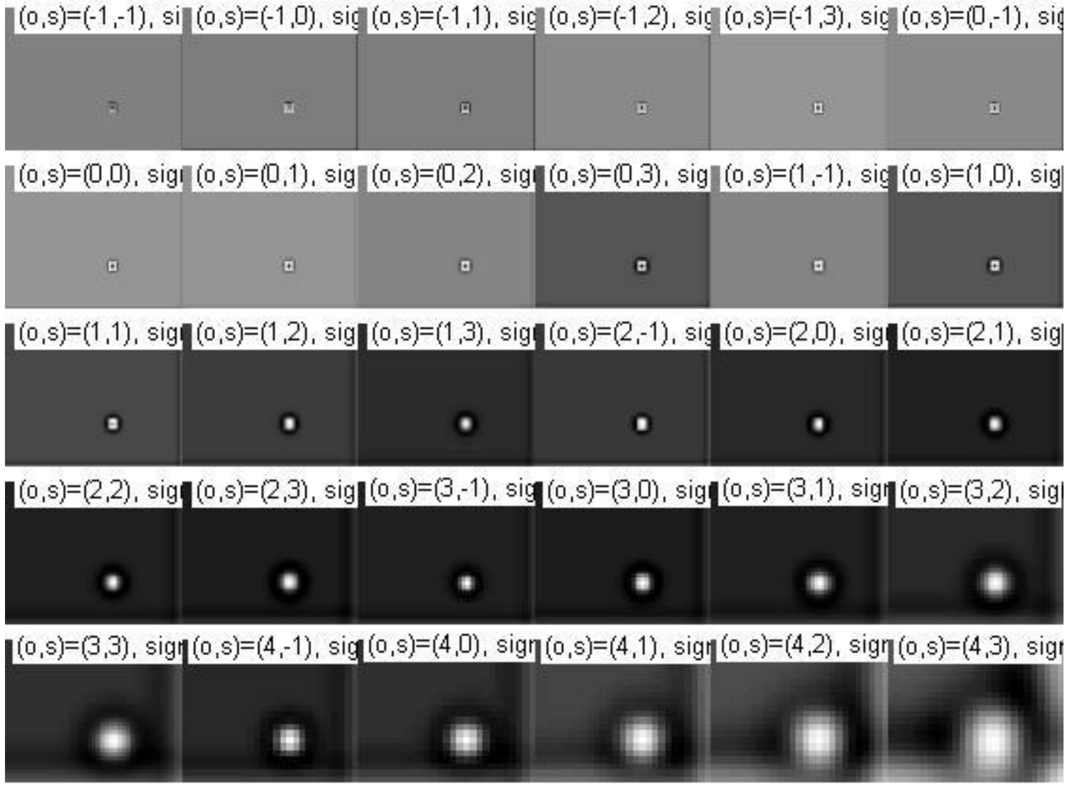

Fig. 3.7 Difference of Gaussian scale space of template image

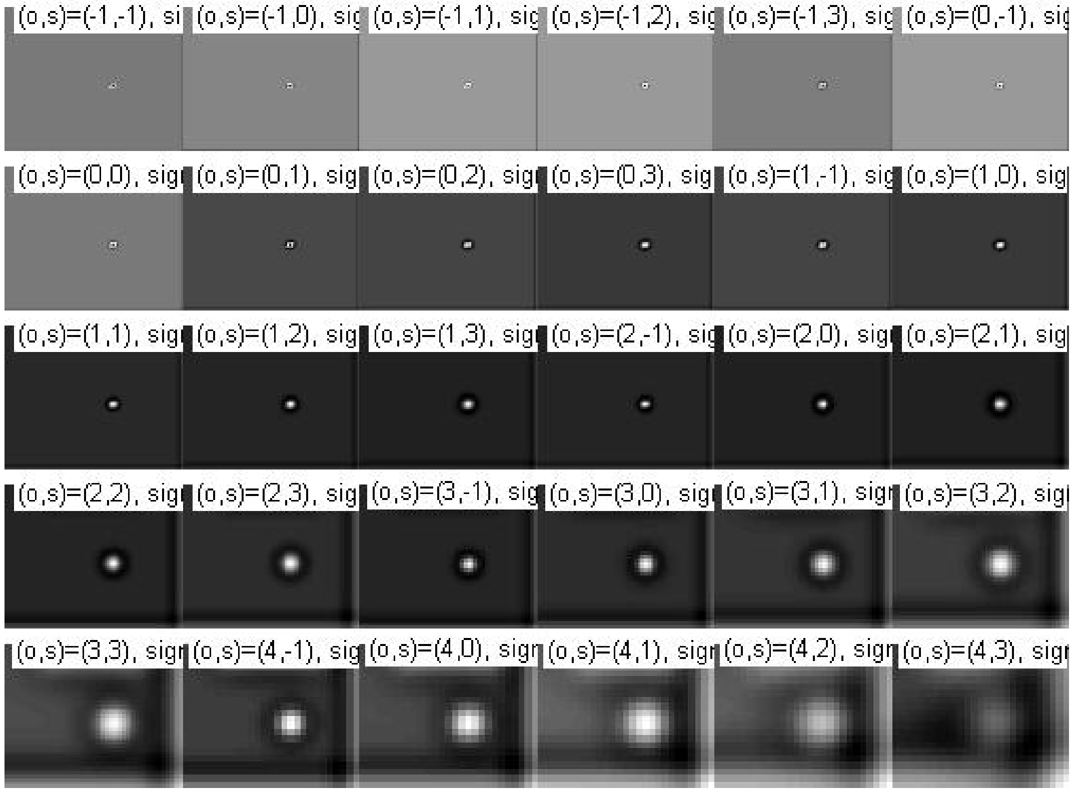

Fig. 3.8 Difference of Gaussian scale space of marker of study

In this implementation, a SIFT frame is also denoted by a circle, representing its support, and one of its radii, representing its orientation. The support is a disk with radius equal to six times the scale σ of the frame. If the standard parameters are used for the detector, this corresponds to four times the standard deviation of the Gaussian window that has been used to estimate the orientation, which is in fact equal to 1.5 times the scale σ. This number can also be interpreted as size of the frame, which is usually visualized as a disk of radius 6σ.

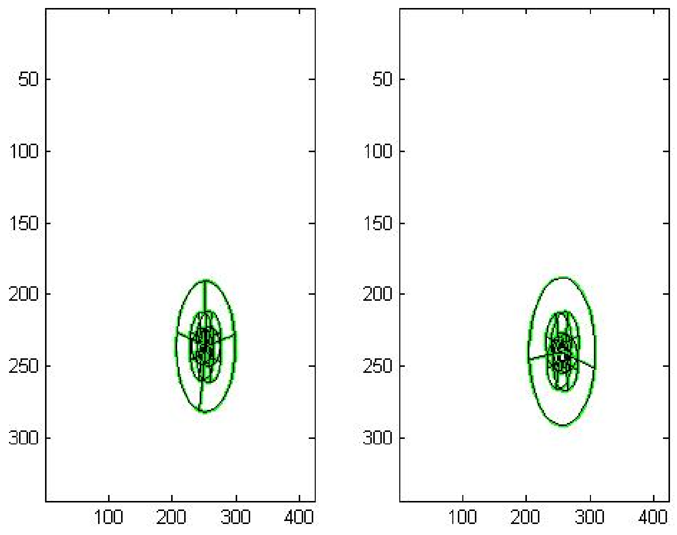

Fig. 3.9 On the left the marker of our study, in this case I6. On the right the template marker

Once frames and descriptors of two images have been computed, the algorithm can be used to estimate the pairs of matching features. This function uses Lowe's method to discard ambiguous matches [16].

At the end what we obtain is an image in which we can see the representations of both images and lines connecting the frames or keypoints. The lines show the correspondence between markers and template and allow us to confirm that the marker extracted is a real marker. If no lines are represented that means that the algorithm was not able to ensure the matching.

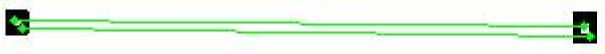

Fig. 3.10 Matching done by SIFT between marker I6 and template

In Appendix I can be seen an example of the report provided by the algorithm during the execution where all parameters calculated are shown

3.1. Usage of existing code property of IGD

As mentioned in previous section we want to univocal identify internal and external markers. In this second case, in IGD Fraunhofer, they already had an application developed by Steffen Terörde, a student who had developed his Master Thesis in IGD for his university, TU-Darmstadt, before I arrived. We are interested in the part of the strategy referring to identify ellipses in image basing in contours.

The procedure used in our project is described as follows. After labelling the image and discarding big regions we go through image pixels determining if a pixel belongs or not to the contour we are looking for and we save this maximum and minimum coordinates in a contour points array.

The directions used to determine contour points are visually described in Fig. 3.11. Our interest pixel is coloured in black, and all its neighbours have a number. Some of these pixels (0, 1, 2 and 3) are also coloured to easily identify directions described between interest pixel and them. At the end, considering all neighbour pixels, we have covered all possible directions and this way we are able to determine a contour.

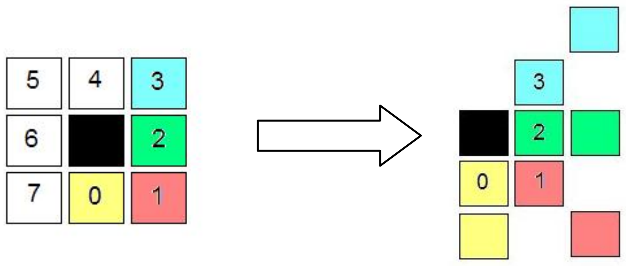

Fig. 3.11 Left: all neighbour pixels are labelled with a number and some are coloured. Right: show direction (colour) taken by each numbered pixel

The maximum and minimum points (same concept as Minimum Bounding Box) determine the edges of the contour. We erase the pixels between them and we draw the line corresponding to the contour.

With the new contour we determine where theoretically the centre of the ellipse should be and with a tolerance determined by programming we draw a point in the middle of the ellipse. If a point appears at the end of the execution means that the application has found an object in the image with shape of ellipse. If not, region is not considered a ellipse and for that reason it is discarded as external marker.

4. Tools and Implementation

4.1. Requirements

The requirement of the project was to program a Win 32 console application implemented in C++ programming language. This way, the application will be compatible with some other applications and functions already developed by IGD and the different parts and modules can be reusable for different projects in the future.

The application should recognize markers at image, internal and external (squares and circles) as described in previous sections.

Our application should have an interactive interface where user can select and see which markers wants to detect. So a requirement of our GUI is having a screen where user visually could identify the markers presents in image and also verify if the results obtained by the code are effective at recognizing internal and external markers.

4.2. Tools

As a first approximation we have implemented our code in Matlab to see if results were successful to our purpose. Once we have tested or rejected the different techniques/methods for each step in the image processing chain, the final solution has been implemented in C++ thanks to IPP and Ttmath libraries. An open source library called OpenCV has been also tested.

The programming languages and environments shortly introduced above are explained as follows:

MATLAB: The name stands for MATrix LABoratory. MATLAB is a high-performance language for technical computing. It integrates computation, visualization, and programming in an easy-to-use environment where problems and solutions are expressed in familiar mathematical notation where the basic data element is an array that does not require dimensioning. Some Typical uses of the application include: Math and computation, algorithm development, modelling, simulation, prototyping, data analysis, exploration and visualization.

Visual C++: is one of the most widespread and important languages available today for developing applications for the Windows operating system C++, an object oriented programming language. It implements data abstraction using a concept called classes, along with other features to allow object-oriented programming. Parts of the C++ program are easily reusable and extensible; existing code is easily modifiable without actually having to change the code. C++ maintains aspects of the C programming language and some of its features allow low-level access to memory but also contain high level features.

OpenCV: is a computer vision library originally developed by Intel. It is free for commercial and research use under a BSD license (open source software). The library is cross-platform, and runs on Windows, Mac OS X, Linux, VCRT (Real-Time OS on Smart camera) and other embedded operating systems. In fact it is 4 libraries in one: computer vision algorithms (CV), experimental/beta (cvaux), linear algebra (cxcore) and media/window handling (highgui). It focuses mainly on *real-time* image processing, as such, if it finds Intel's Integrated Performance Primitives (IPP) on the system, it will use these commercial optimized routines to accelerate itself.

IPP: Intel® Integrated Performance Primitives (Intel® IPP) is an extensive library of multicore-ready, highly optimized software functions for digital media and data-processing applications. Intel IPP offers thousands of optimized functions covering frequently-used fundamental algorithms. The library supports only Intel (AMD not supported) processors and is available for Windows, Linux and Mac OS X operating systems. Intel IPP is divided into three major processing groups: Signal (with linear array or vector data), Image (with 2D arrays for typical colour spaces) and Matrix (with nxm arrays for matrix operations).

TTMath: is a small library which allows one to perform arithmetic operations with big unsigned integer, big signed integer and big floating point numbers. It provides standard mathematical operations like adding, subtracting, multiplying, dividing etc. TTMath is developed under the BSD license which means that it is free for both personal and commercial use. The main goal of the library is to allow one to use big values in the same way as the standard types like int, float, etc.

4.3. OpenCV

As a first option we have tried to find a open source application already programmed which could help to recognize our markers.

In the OpenCV library there are many examples in image processing area and one of the demos included is called squares.cpp. Its functionality is to find squares in the image. To do that, the code tries different threshold levels using Canny instead of zero threshold level o helping to catch squares with gradient shading. Then applies threshold and find contours and 4 points (vertices). Once contours are determined it looks for minimum angle between joint edges and if all angles are near to 90 degrees it concludes that this contour belongs to a square. Then it draws lines to show to user where are the squares found.

We have tested it with our reference image but it does not work properly despite adjusting the different parameters as shown in Section 5 (Results). Our markers are not detected.

So the strategy of finding an open source application already developed is discarded and we have to develop our own application.

4.4. Implementation

Before implementing the GUI, we have implemented a first approximation program with MATLAB to ensure that the concepts were right and reachable before programming a GUI with Visual Studio in C++ language.

The strategy is to work with the original image, scene of real world captured by the camera, as a matrix, where the elements of each raw and column are pixels of the image. Through the knowledge of image processing theory and the different instances and functions of MATLAB we have implemented each step of the image processing chain that represents the better solution at extracting our searched markers.

As the results in MATLAB are successful (See Section 5), the image results are respectable with markers features and location and operations are computationally not complicated so the time of execution is not too much (although we are not searching a real time application) the solution implemented in C++ is a “copy” from MATLAB. It uses algorithms and functions implemented and tested in MATLAB and potentiated by tools as Intel Primitives.

C++ project structure

The goal of this project is to implement a GUI with Visual Studio in C++ compatible with other projects already developed by Fraunhofer IGD and knowing the possibilities that C++ language brings. Then using the capabilities of the C++ language combined with IPP and TTMath Mathematical Library we have searched the optimal methods to uniquely identify our markers.

We have implemented a console Win32 Application in a Microsoft Visual C++ 8.00 programming environment. The result is a GUI that makes easy the use of the code to the final user.

The title of the GUI is Markers Detection and the design consists in 3 parts. The different boxes corresponding to different blocks in the image processing chain are shown on the left and inside them we can find different options (buttons) that can be chose by user; a big screen for showing pictures is on the right side and a small information visor at the bottom. All these details can be seen in the Fig. 4.1 below.

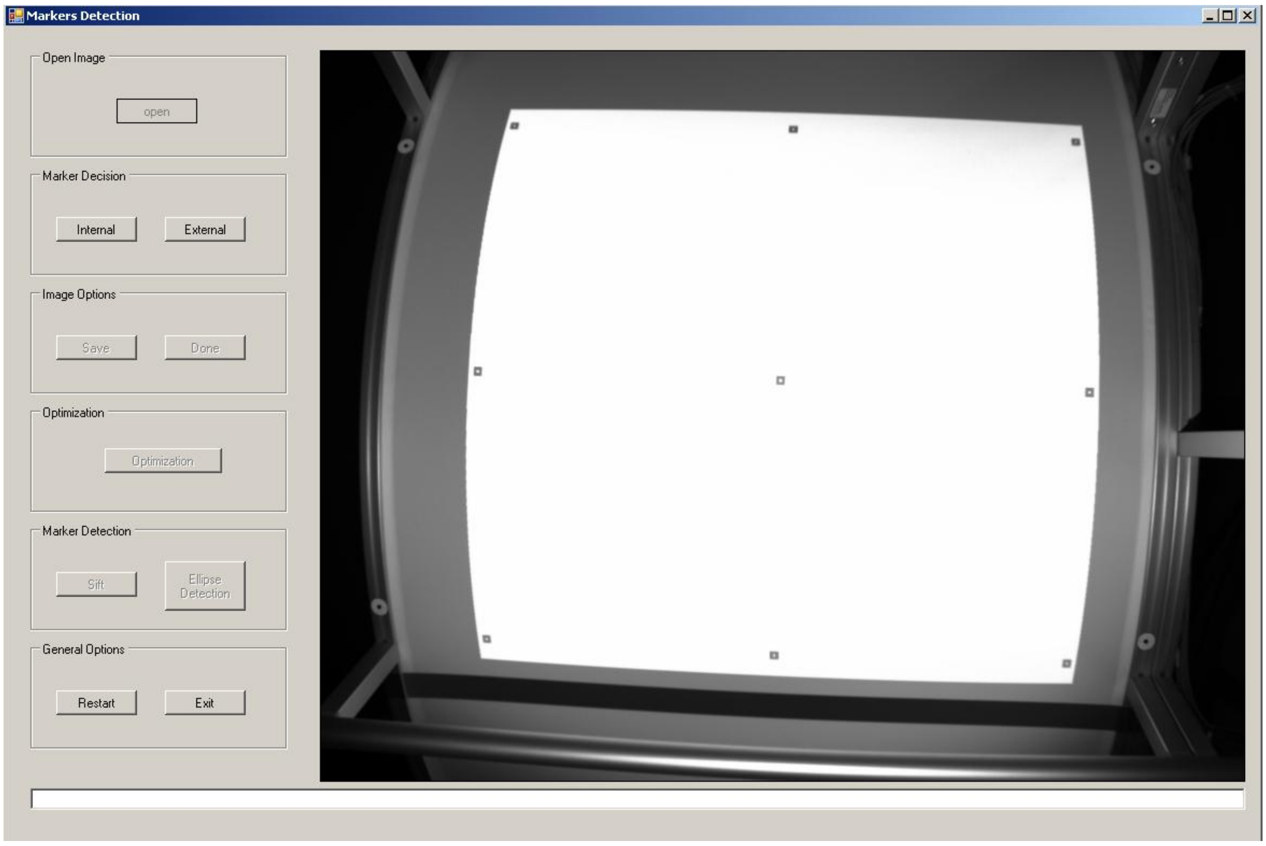

Fig. 4.1 Main window of our GUI Application where options, buttons and pictures are.

The structure of the programming code developed is as follows:

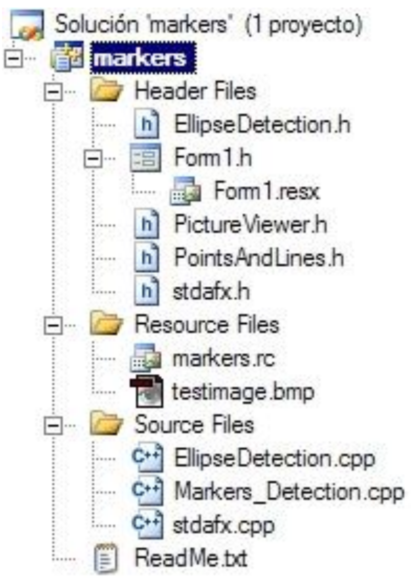

```
Solución 'markers' (1 proyecto)
markers
  Header Files
    EllipseDetection.h
    Form1.h
      Form1.resx
    PictureViewer.h
    PointsAndLines.h
    stdafx.h
  Resource Files
    markers.rc
    testimage.bmp
  Source Files
    EllipseDetection.cpp
    Markers_Detection.cpp
    stdafx.cpp
  ReadMe.txt
```

Fig. 4.2 Shows the structure of the project Markers and its different header and source files. Initial image (testimage) is included in our resource files.

The project has a main function Markers_Detection.cpp in which Form1 is runned (Form1.h).

```
Application::Run(gcnew Form1());
```

Design of GUI and functionality of Options

In this section the design of the GUI and the structure of the code are explained. After an overview, each group of options and buttons implemented are described giving detailed information about C++, IPP and TTMath functions needed and implemented in each case.

All includes and defines necessary to run the application properly are at the beginning of the code followed by the initialization of global variables.

The design chose for GUI is shown in Fig. 4.3 below:

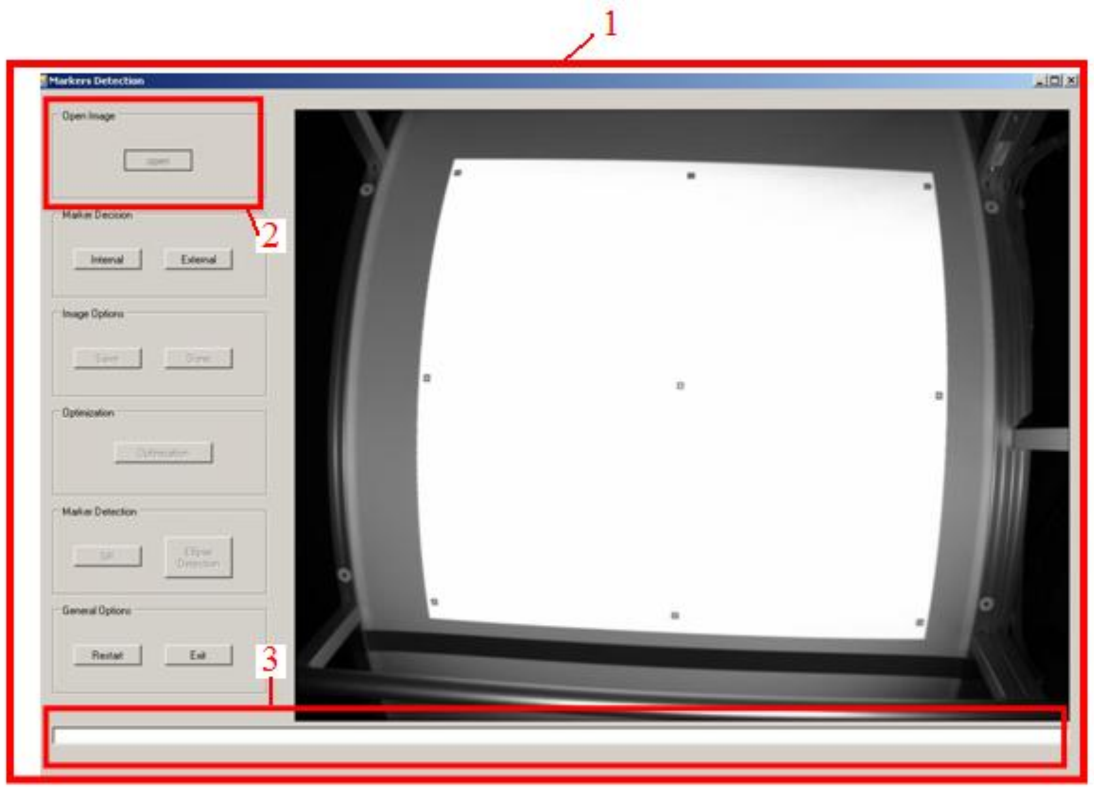

Fig. 4.3 Main window of our GUI Application where options, buttons and pictures are. The red rectangles enhance some details explained in the memory (Main window, GroupBox and Information Box)

In this screenshot of our application (Fig. 4.3) we can see 3 big boxes enhanced in red colour.

1: main window of the programme where are included all the sections, buttons, screens and information displays.

```
private: System::Windows::Forms::PictureBox^ pictureBoxBigView;
```

2: Each step of the image processing chain needs to have its own GroupBox where all the buttons are grouped. For example the code for Step 0 is:

```
private: System::Windows::Forms::GroupBox^ groupBoxOpenImage;
```

3: Corresponds to information box where all the comments about the process in course are shown:

```
private: System::Windows::Forms::TextBox^ textBoxOutput;
```

In this particular case of GroupBox (Open Image) we also need to create a File Dialog (Fig. 4.4) so we are able to open the desired image searching it in folders of our computer. In our case testimage.bmp:

```
private: System::Windows::Forms::OpenFileDialog^ openFileDialog;
```

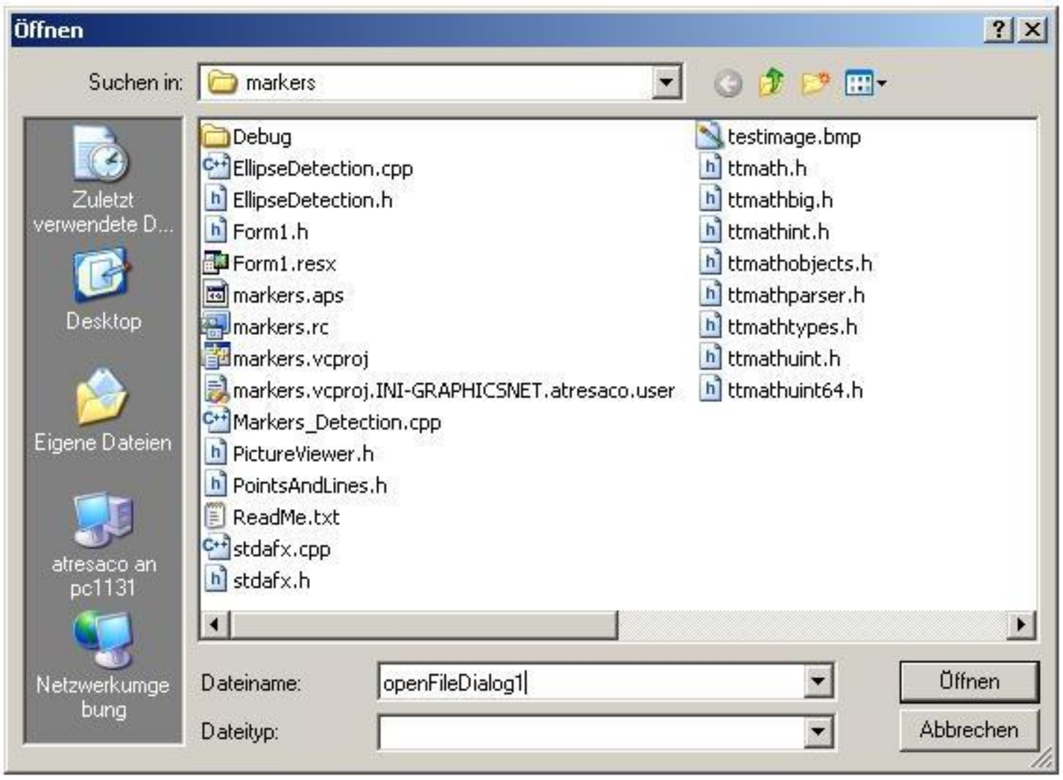

Debug
EllipseDetection.cpp
EllipseDetection.h
Form1.h
Form1.resx
markers.aps
markers.rc
markers.vcproj
markers.vcproj.INI-GRAPHICSNET.atresaco.user
Markers_Detection.cpp
PictureViewer.h
PointsAndLines.h
ReadMe.txt
stdafx.cpp
stdafx.h
testimage.bmp
ttmath.h
ttmathbig.h
ttmathint.h
ttmathobjects.h
ttmathparser.h
ttmathtypes.h
ttmathuint.h
ttmathuint64.h

Dateiname: openFileDialog1
Dateityp:

Fig. 4.4 File Dialog to open the desired image(testimage.bmp) searching it in folders of our computer

For each GroupBox there also 2 more items which have to be programmed. For example in case of Open Image they are shown in Fig. 4.5 below.

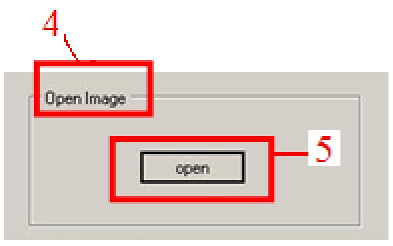

Fig. 4.5 GroupBox Open Image and its button

4: The label where the name of each GroupBox will be shown. It is not necessary that this name of the label (in this step of programming) agrees with the name shown in the console application. That is something editable after.

```
      private: System::Windows::Forms::Label^ labelBoxStep0_OpenImage;
```

5: For each Button inside the GroupBox we have to implement the instruction (the only difference is the name in each case):

```
      private: System::Windows::Forms::Button^ buttonStep0_OpenImage;
```

All this windows, boxes and options need to be created and initialized. The programming of the examples shown above is:

```
this->pictureBoxBigView= (gcnew System::Windows::Forms::PictureBox());

this->groupBoxOpenImage = (gcnew System::Windows::Forms::GroupBox());

this->buttonStep0_OpenImage= (gcnew System::Windows::Forms::Button());

this->labelBoxStep0_OpenImage=(gcnew System::Windows::Forms::Label());

this->openFileDialog=(gcnew System::Windows::Forms::OpenFileDialog());

this->textBoxOutput = (gcnew System::Windows::Forms::TextBox());
```

Once we have all boxes created we have to indicate the components of the PictureBox and for that reason we have to run the beginning action:

```
cli::safe_cast<System::ComponentModel::ISupportInitialize^

>(this->pictureBoxBigView))->BeginInit();
```

For each element forming part of our application we have to describe the features they will have. These features are exposed in Table 4.1.

	Features
PictureBox	BackColor, BorderStyle, Location (Point), Name, Size, SizeMode, TabIndex and TabStop
GroupBox	Controls, Location (Point), Name, Size, TabIndex, TabStop and

	Text
Button	Enabled, Location (Point), Name, Size, TabIndex, Text, UseVisualStyleBackColor
Label	Location (Point), Name, Size and TabIndex
FileDialog	FileName

Table 4.1 Features of each statement in our Win32 Console application

In the case of Buttons we have programmed Events that will have effect when the mouse is clicked:

```
this->buttonStep0_OpenImage->Click  +=  gcnew  System::EventHandler(this,
&Form1::buttonStep0_OpenImage_Click);
```

We configure the controls of each GroupBox and we give a name to the main window. This way the configuration of Console Win32 is ended `(EndInit)`.

```
this->Controls->Add(this->pictureBoxBigView);

this->Controls->Add(this->groupBoxOpenImage);

this->Controls->Add(this->textBoxOutput);

this->Text = L"Markers Detection";

(cli::safe_cast<System::ComponentModel::ISupportInitialize^       >(this-
>pictureBoxBigView))->EndInit();
```

We declare our own variables (self-defined) and we start with the programming of each function that a click of the mouse activates.

At the end of each execution the following buttons are enabled and actual are disabled except in GroupBox called General Options that can be selected at any time during the execution of the programme.

Button Open in Open Image Box

When we first run the application the only options available are Open Image and Exit. That can be seen because they are the only buttons enabled; the others can not be selected (see Fig. 4.6).

In the viewer on the right the image selected will be shown.

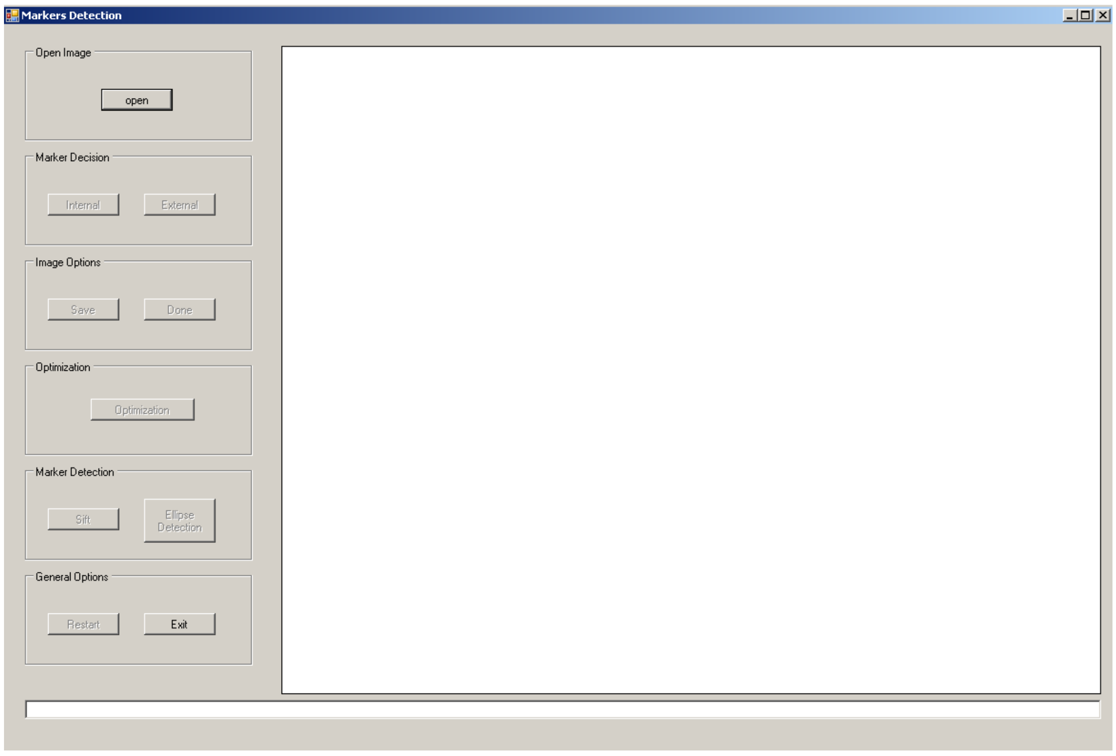

Fig. 4.6 Initial appearance of our GUI. Only Button Open from Open Image and Exit can be selected

The selection of this button opens a FileDialogBox in which we can chose the image within we want to work. See Fig. 4.7 below.

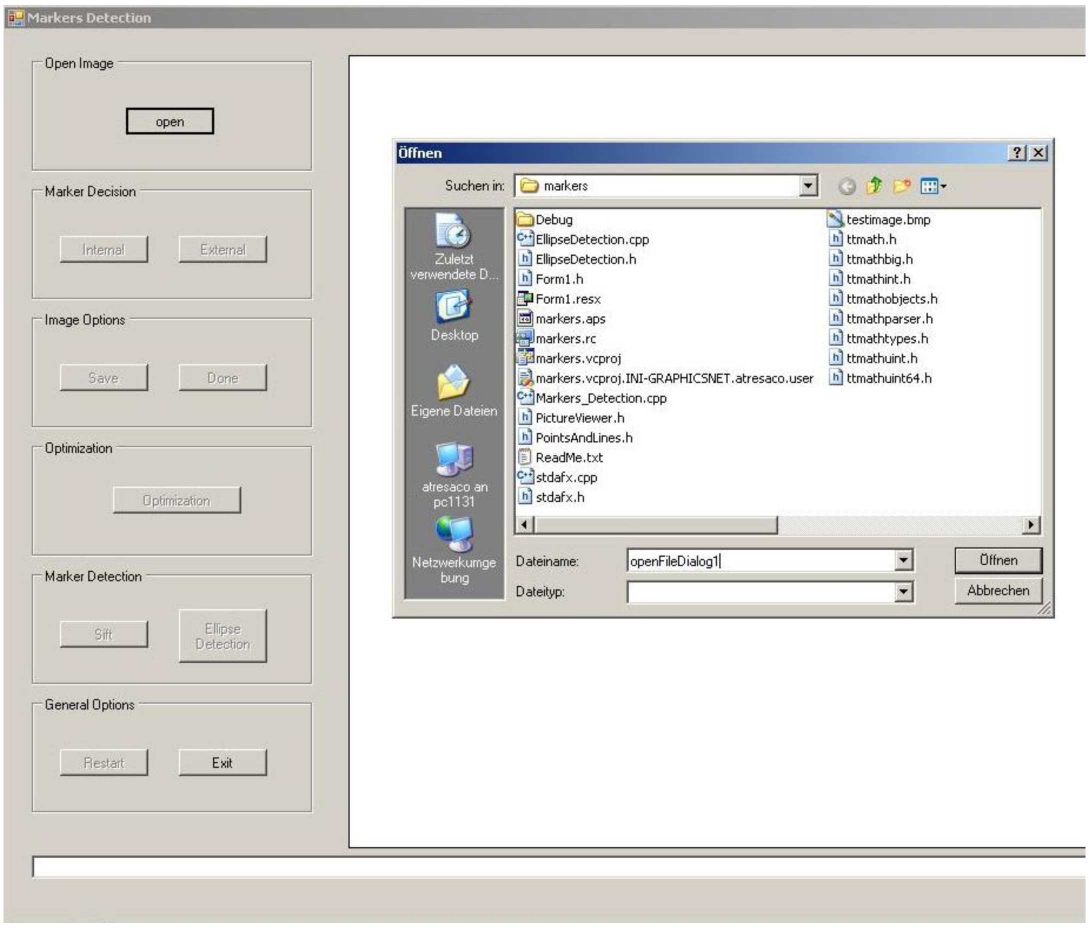

Dateiname: openFileDialog1
Dateityp:

Fig. 4.7 File Dialog to open the desired image(testimage.bmp) searching it in folders of our computer

The result is the visualization of the image on the right side screen (see Fig. 4.8).

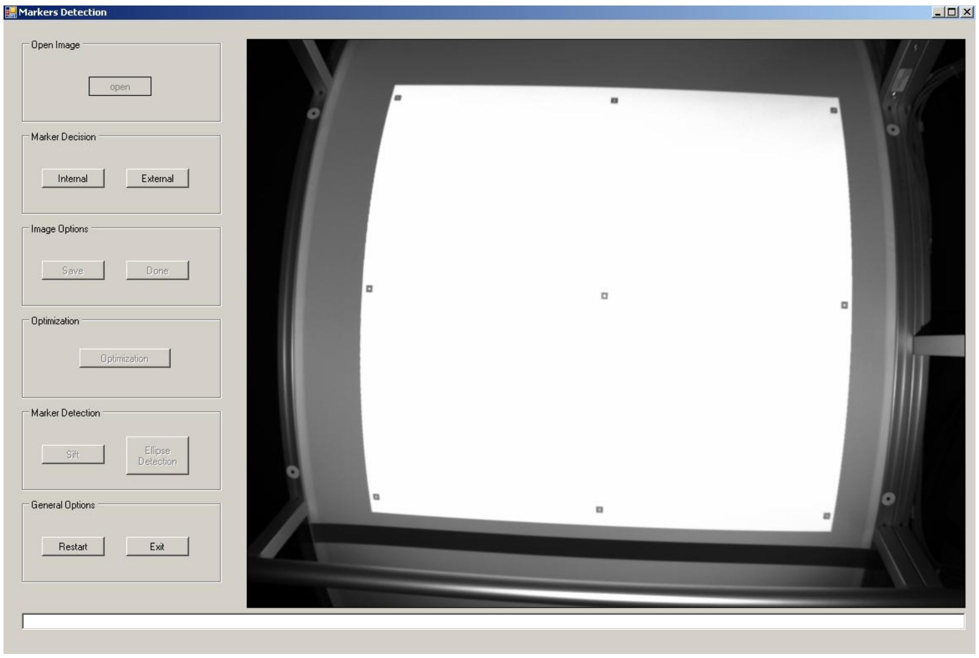

Fig. 4.8 Resulting appearance of GUI alter opening our testimage

Once we have opened the image, the button becomes disabled and next options available correspond to next step of the image processing chain.

From now on, we can find two possibilities of analysis. We can search for internal markers otherwise external markers.

Option 1: Button Internal in Marker Decision Box

In this point the goal is to obtain Internal Markers and that will be done following the steps described in Section 3 (Our contribution). First of all we will apply a pre-processing filter, following by a local threshold, a labelling of the resulting image and finally discarding big regions and not rectangular objects in image.

In our GUI when Internal Button is selected it is in a flat style and External Button appears disable, it can not be selected.

The image opened in step before can be seen on the right side. After applying all functions in this step the result will be shown instead and it will be a good approximation image to our final goal. All the process and results can be seen in Section 5.

Before explaining the functions involved in this step it is important to explain some conversions made to image formats in order to execute some functions faster or easier by using IPP.

All the images, original images and showing ones have bitmap format and during the process they are converted into IPP image format and reconverted again into bitmap for representation

The functions used to do that are:

`pin_ptr<Ipp8u> binSrc = (Ipp8u*) binData->Scan0.ToPointer();`

`Ipp<datatype>* ippiMalloc_<`*`mod`*`>(int `*`widthPixels`*`, int `*`heightPixels`*`, int* `*`pStepBytes`*`); (mod 8u_C1)`→This function allocates a memory block aligned to a 32-byte boundary for elements of different data types. Every line of the image is aligned by padding with zeros in accordance with the *pStepBytes* parameter, which is calculated by the function ippiMalloc and returned for further use.

`IppStatus ippiCopy_<`*`mod`*`>(const Ipp<datatype>* `*`pSrc`*`, int `*`srcStep`*`, Ipp<datatype>* `*`pDst`*`, int `*`dstStep`*`, IppiSize `*`roiSize`*`);`→ `(mod 8u_C4C1R and 8u_C1C4R)`→ copies pixel values between two images.

`ippiSet_8u_C4CR`

`IppStatus ippiSet_<`*`mod`*`>(Ipp<datatype> `*`value`*`, Ipp<datatype>* `*`pDst`*`, int `*`dstStep`*`, IppiSize `*`roiSize`*`); (mod 8u_C4CR)`→ Sets an array of pixels to a value. Setting channel of multi-channel data to a value

`void ippiFree(void* `*`ptr`*`);`→Frees memory allocated by the function ippiMalloc.

Once we know all formats of image we can start with the functions programmed in this step.

First of all we apply a pre-processing filter, this way, noise coming from camera and the fact of taking the photo is reduced and the contrast between objects and background is incremented so they are easier detectable.

The function used for filtering is:

`IppStatus ippiFilterSharpen_<`*`mod`*`>(const Ipp<datatype>* `*`pSrc`*`, int `*`srcStep`*`, Ipp<datatype>* `*`pDst`*`, int `*`dstStep`*`, IppiSize `*`dstRoiSize`*`);(mod 8u_C1R)`→ Filters an image using a sharpening filter.

The appearance of filter image is similar to original image but the matrix of values show they are different although to human sight there are not noticeable changes. This fact will be discuss and shown in Section 5.

Then the process of preparing image for local thresholding starts. The size desired for the blocks in Wall's algorithm *m_m* and *n_n* is introduced by programming. (*m_m* and *n_n* can be different). As the image is going to be separated in parts depending on height and width of Wall's blocks, we have to ensure that all regions in the image are considered. That is the reason why we construct some blocks with a different size at the end-right and end-button with one or both sides of size tmp1 and tmp2.

```
for(int i=0;i<height;i=i+m_m)

{

      for(int j=0;j<width;j=j+n_n)

{

            if(width-j<n_n)

            {

                  tmp1=width-j;

            }

            else

            {

                  tmp1=n_n;

            }

            if(height-i<m_m)

            {

                  tmp2=height-i;

            }

            else

            {

                  tmp2=m_m;

            }
```

We calculate histogram from Wall's block as an array that accumulates all the pixel values (colour) contained in region *m_m x n_n*, *m_m x tmp1* or *tmp2 x n_n*, depending on the region. (regionArray)

Then the threshold of each region is calculated with Ridley and Calvard's algorithm as explained in Section 2.2 and the result is applied to each region. So at the end what we have is our pre-processed image in so many parts and within so many thresholds as blocks with Wall's method were calculated. It is time to reconstruct the size of pre-processed image from small blocks. All this programming is made with vectors:

- regionArray[temps] where temps is the size of the Wall's block, is the array where pixel colour property is saved
- histoArray[SIZE_HIST] that is the array where the histogram of block is calculated
- mean [k]: array where all values calculated are saved. The iteration in searching the mean ends `while(mean[k-1]!=mean[k]);`

and the reconstruction is done by:

```
unsigned int f=0;

unsigned int g=0;

for(unsigned int q=0;q<temps;q++)

{

        if(g==tmp1)

        {

                f=f+1;

                g=0;

        }

        if(regionArray[q]<Threshold)

        {

        resbinImageInt->SetPixel(g+j,f+i,System::Drawing::Color::Black);

        }

        else

        {
```

```
      resbinImageInt->SetPixel(g+j,f+i,System::Drawing::Color::White);

      }

g=g+1;

}
```

After that process we obtain binary image (See Results) and after that we apply a closing for cleaning all those small black regions and isolated pixels (noise) resulting from binarization.

The closing is made with a structuring element of 3x3 called Mask by IPP.

The IPP functions used:

```
Ipp8u pMask[3*3]= {1,1,1,

                1,1,1,

                1,1,1};

IppiSize maskSize={3,3};

ippiMorphAdvInitAlloc_8u_C1R()

IppStatus ippiMorphCloseBorder_<mod>(const Ipp<datatype>* pSrc, int srcStep, Ipp<datatype>* pDst, int dstStep, IppiSize roiSize, IppiBorderType borderType, IppiMorphAdvState* pState);(mod 8u_C1R)
```
→performs closing of an image

```
ippiMorphAdvFree(pState);
```

Then the negative image is calculated. The black pixels become white and the white ones become black. This contrast transformation in image is a pre-step for labelling and it is really important. As we see in the image the desired markers are black. Labelling function considers that a non-zero value forms part of a concrete region. That means that in our situation, if we do not change the pixel values on the image our markers will be consider as part of the background and that is exactly the opposite we are searching. So with this contrast transformation the image (negative image) is prepared to apply labelling process described in Section 2.3.

The connectivity used to calculate labelling is 8-connectivity (computing) (See Fig. 2.5) and the functions used are mentioned below:

```
ippiLabelMarkersGetBufferSize_8u_C1R()
```

`ippiLabelMarkers_8u_C1IR()`

`IppStatus ippiLabelMarkers_8u_C1IR(Ipp8u* *pMarker*, int *markerStep*, IppiSize *roiSize*, int *minLabel*, int *maxLabel*, IppiNorm *norm*, int* *pNumber*, Ipp8u* *pBuffer*);`→ Labels markers in image with different values.

The resulting labelled image is shown in Section 5. (Results)

Once we have applied labelling the next step in our image chain is region based-shape classification. In this step we will solve the problem of having not only desired regions by analyzing the features of the objects in the picture.

Attending to descriptors described in Section 3 and with the criteria also there described for internal markers we discard by size those regions out of range and those not rectangular:

```
ratio>0.75 and ((kx<-1.05 )and(kx>-1.35))
```

The numbers involved in the calculation of the Kurtosis parameter are really big and C++ was not able to calculate them without errors so at this point we have to introduce an external mathematical library called *ttmath* which has helped us to solve this big operations.

The definitions of a big number using ttmath library are:

```
typedef ttmath::Big<1,2> MyBig;
```

and some variables declarations and initializations used:

```
MyBig Xc;

MyBig u20=0;

MyBig u40=0;
```

where *Xc* is the coordinate *x* of centroid (centre of gravity) and μ_{20} and μ_{40} are central moments (translation invariance) all of them described in Sections 2.3 and 3.

At the end of the execution of this button we obtain an image containing small rectangular regions as similar as possible to our ideal marker. We also obtain some other regions that are not desired and which will be rejected after cleaning image from isolated pixels and after applying matching algorithm SIFT.

Button Optimization in Optimization

This button is only available in case of Internal Marker and the aim is to clear image from noise, deleting isolated pixels. It can be reached thanks to IPP function

```
IppStatus ippiDilate_<mod>(const Ipp<datatype>* pSrc, int srcStep,
Ipp<datatype>* pDst, int dstStep, IppiSize roiSize,
const char* pMask, IppiSize maskSize, IppiPoint anchor);(mod 8u_C1R, not
in place operation)
```
→ Performs dilation of an image using a specified mask (structuring element of 3x3)

Button SIFT in Marker Decision

This button was thought to start running the C++ SIFT code as described in Section 2.4. But we were not able to insert the code in our current project so SIFT algorithm was applied via Matlab to the image obtained by GUI. Results are shown in Section 5.

Option 2: Button External in Marker Decision Box

The procedure of this option is the first step described in Option 1. To the digital image taken by the camera we apply pre-processing filtering to clean image and then we prepare image for thresholding. In Fig. 4.9 we can see binarization obtained with a *m_m* and *n_n* block size different from the one used before (in internal markers).

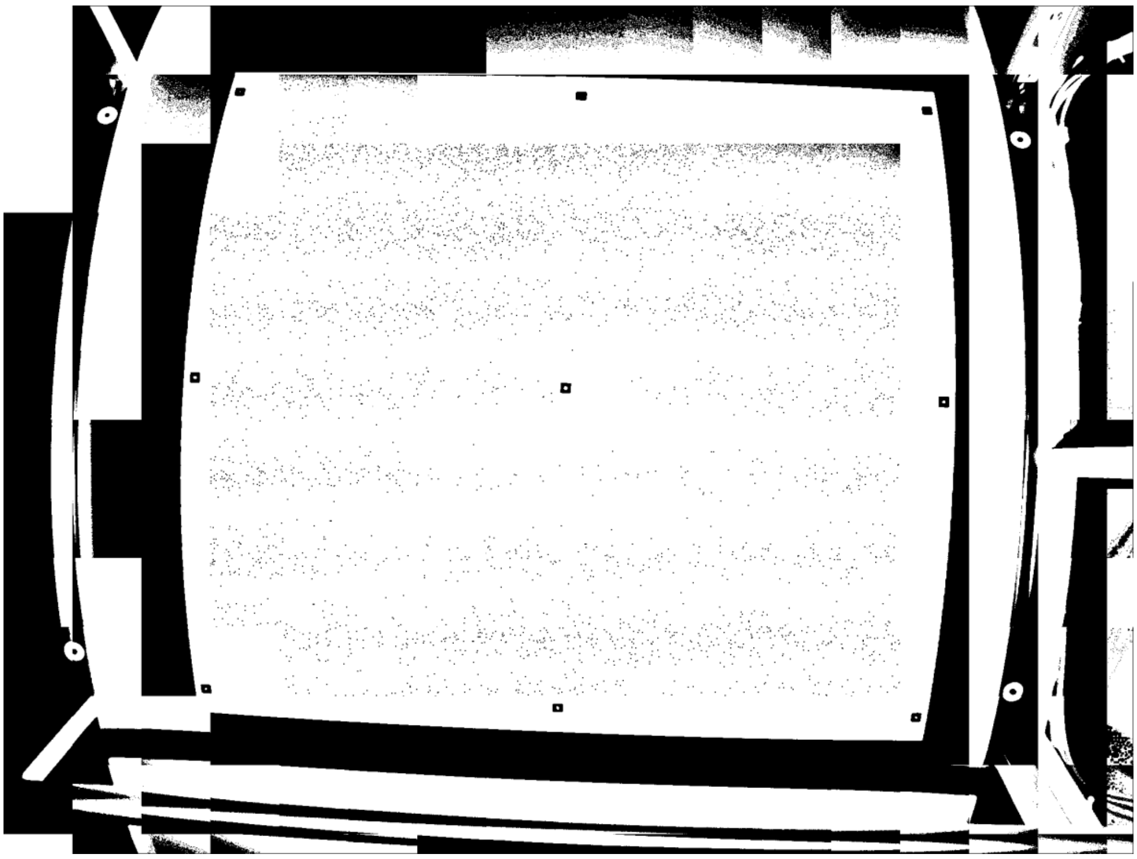

Fig. 4.9 Binary image with 128x128 Wall's blocks

In this case the appearance of external marker is an orange circle with a smaller black circled hole. Due to projective and affine features the original circles appear not as perfect circles but more as ellipses.

As far as we obtain the binarized image the process of binarization is the same as described in Option 1. Before applying labelling appear the first differences in the process between internal and external markers information extraction. Labelling function determines that a non-zero pixel value is part of a region. Our interest external pixels have contrary features as in Option 1, that means that now our interest pixels are those in white (orange in fact converted to lowest level intensity in binarization) so the cleaning of the binarized image for optimal labelling must be done directly to binary image without any previous contrast transformation. This way our markers are directly considered as desired regions. For that reason, now cleaning the image from noise before labelling means applying the mathematical operator opening with a 3x3 structuring element.

```
Ipp8u pMask[3*3]={1,1,1,

                  1,1,1,
                    1,1,1};//structuring element

IppiSize maskSize={3,3};

IppiPoint anchor={1,1};

IppiMorphAdvState* pState;

IppiBorderType borderType=ippBorderRepl;

ippiMorphAdvInitAlloc_8u_C1R()

IppStatus ippiMorphOpenBorder_<mod>(const Ipp<datatype>* pSrc, int
srcStep, Ipp<datatype>* pDst, int dstStep, IppiSize roiSize,
IppiBorderType borderType, IppiMorphAdvState* pState); (mod
8u_C1R)→performs opening of an image

ippiMorphAdvFree(pState);
```

Once we have all regions in image identified here we go a step after. As we know that external markers are not considered big regions and they are bigger than internal ones we can also apply the criterion of discarding regions by size but now not also applying a higher threshold but also a lower one. The range chose is that going from 800 to 1300 pixels. The results are shown in Section 5.

Then to extract useful information from image it is necessary to apply next step with next button.

Button Ellipse Detection

After labelling the image and discarding big regions, dilation is applied to clean image from isolated black undesirable pixels.

After that all the process described in Contribution of Section 3.1 is applied. This way we determine if a region is or not an external marker. The results of this extraction are shown in Section 5.

Other buttons

During the entire process of the application there are some buttons or options that can be selected in Image Options they are *Save* and *Done* and in General Options we can find *Restart* and *Exit*.

Save option is the function of saving an image in the current path of the project; *Done* indicates that the action is finished and activates the next step of the application; *Restart* gives us the opportunity of giving up all that was made and re-start over; and finally *Exit*, it stops the current action and ends the running of the application.

5. Results

As a starting point of our image processing chain we have the photo taken by camera placed above the projector. This photo is our testimage (testimage.bmp) shown in Fig. 3.1. In this section we will see the results of how, from this testimage, the markers we are looking for are extracted and recognized by applying methods and techniques described in Section 3.

The section has been divided into two experiments. In the first one, an open source code provided by Open CV with the aim of detecting squares is evaluated. After discarding it, the second experiment explained corresponds to the results obtained by our designed and implemented GUI. The results given in this second case are a combination of Matlab and C++ experiments.

As we have only one testimage a rotated image from original has been also used to test the application. The results are shown in Second Experiment.

First Experiment

We have included in a C++ project the code given in squares.cpp. The demo is provided by OpenCV and we have included all libraries (cvaux) in the right path in our project in order to run the demo.

The results of the demo with the one of the images given by default are shown in green in Fig. 5.1. We can see different shape objects and how the demo determines which of them are squares (overlaid green rectangle) and which ones are not (without selecting them).

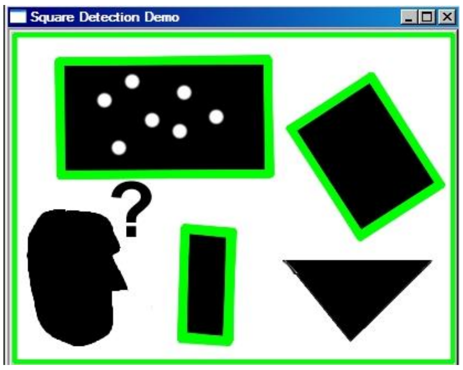

Fig. 5.1 Result of squares detection with a default image provided by OpenCV

We are going to see the behaviour of the program with our testimage. When we prove how works the demo with our image (testimage) configured with the default parameters the results are as follows (See Fig. 5.2)

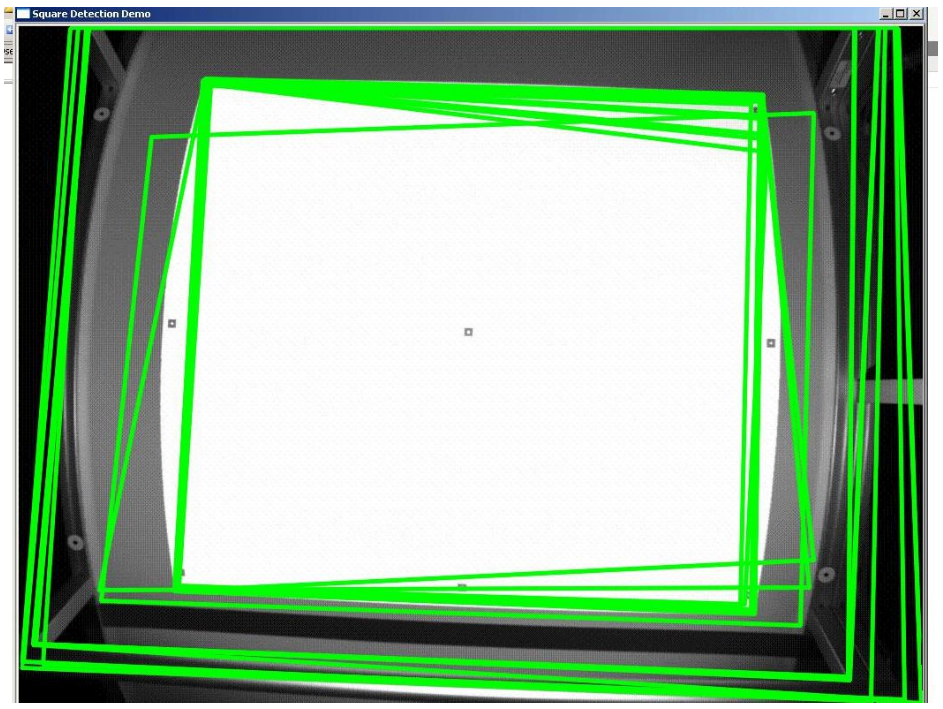

Fig. 5.2 Squares detected by squares.cpp with default values

As we can see it detects only big squares (obtained by joining contours with 4 vertices with angle similar to 90 degrees as described in Section 4.3) but it also has a lot of wrong detections. It determines many combinations that are no squares. In fact to our purpose all of them are wrong detections because any marker is detected.

To improve results we adjust parameters this way we could see if the demo is able to identify our internal markers or at least reduce the number of wrong squares detection. The results obtained after the evaluation of different parameters of the application were unsuccessful to our purpose although the application seems to consider affine features of squares (See Fig. 5.3)

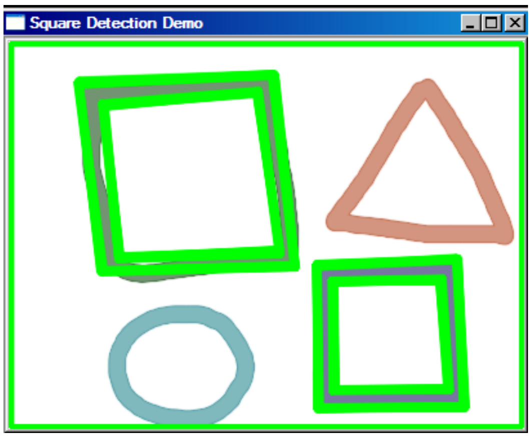

Fig. 5.3 Result of applying squares.cpp to a square under affine features

So altogether, the code is not good to our purpose because it does not univocal determines internal markers and adds a lot of wrong detections making results instable.

Second Experiment

The first step is to convert testimage (in greyscale) to binary image (see Section 2.2).

Segmentation

Several thresholding methods have been tested and results are shown in Fig. 5.4, Fig. 5.5 and Fig. 5.6 below:

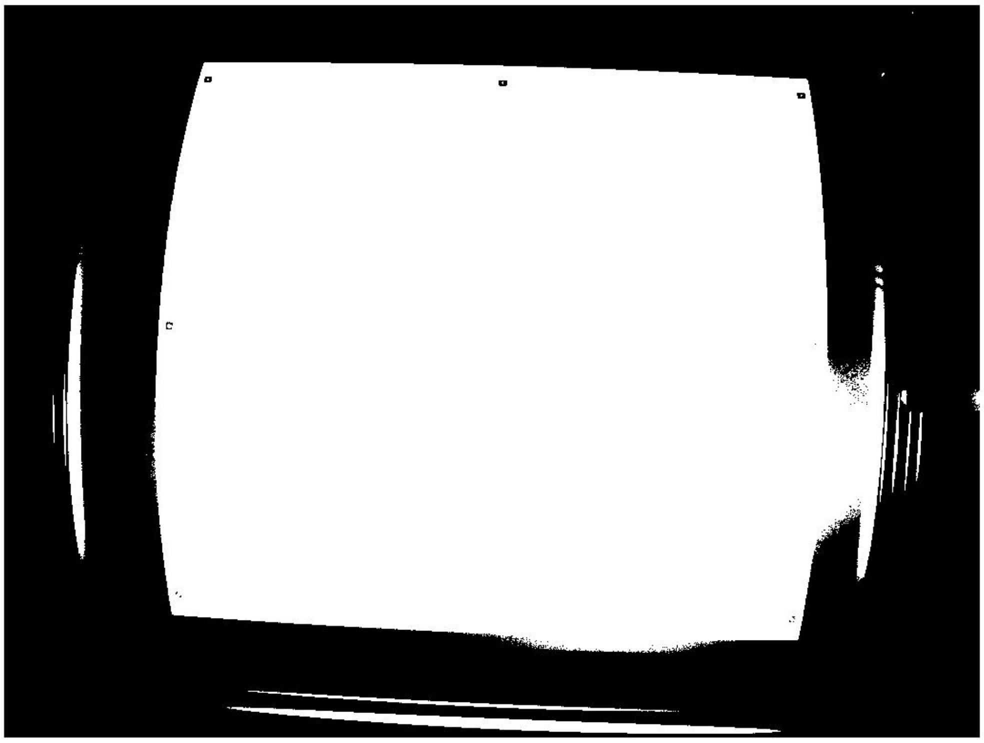

Fig. 5.4 Directly applying threshold to testimage with a level threshold of 0,5

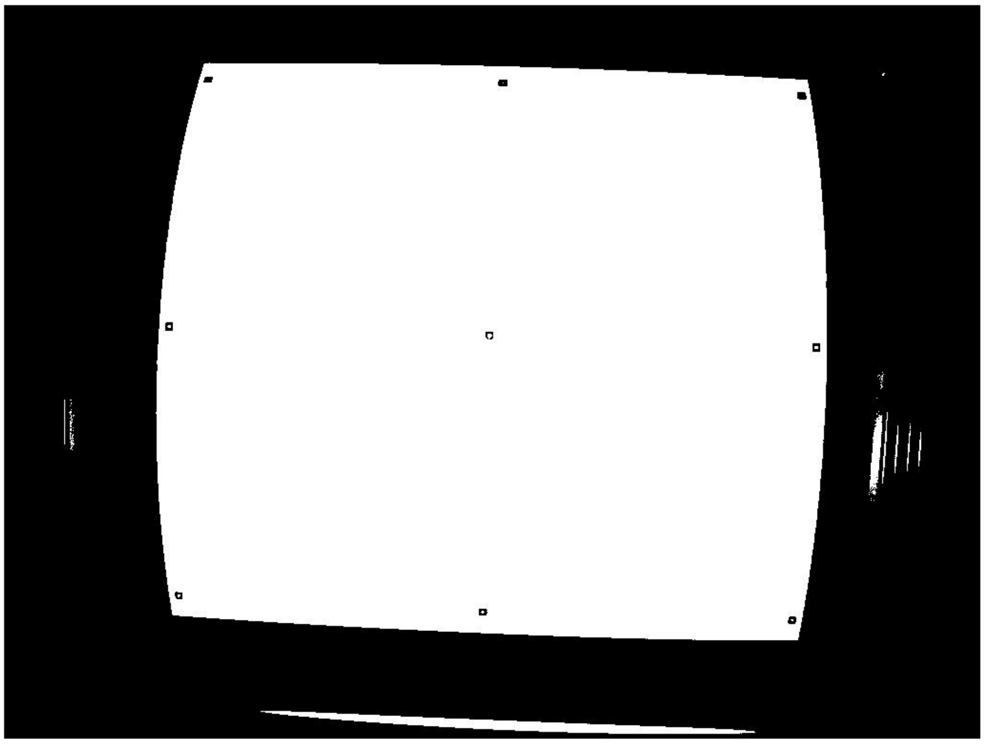

Fig. 5.5 Binary image calculated by Otsu's algorithm which determines the threshold level of image in 0.6157

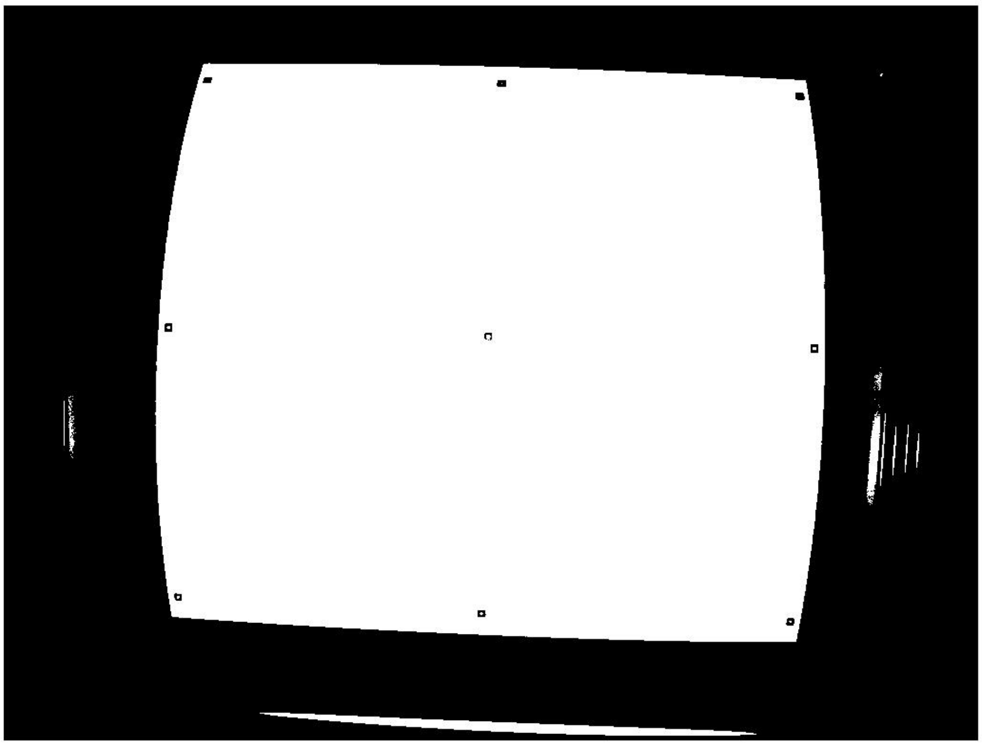

Fig. 5.6 Binary image calculated by Ridley and Calvard's algorithm which determines the threshold level of image in 0.6142

From images obtained we can see that applying a level threshold to the whole image does not detect external markers.

In case of internal markers, if we apply a level of 0.5 some of them are lost (I5, I6, I7, I8 and I9) so it is necessary the running of an algorithm to adjust this threshold value in order to adapt it to the features of our image.

The results of the threshold level calculated by Otsu's and Ridley and Calvard's algorithms are really nearby 0.6157 and 0.6142 respectively. It is remarkable that the marker in the middle, I5, appear in both binarizations as a non connected region. This fact is due to different illumination in scene where central marker receives more directly the light coming from the lightning source making it appear brighter than the rest of the markers.

Also pixels in the upper row I1, I2 and I3 lose their inside hole, so their shape do not remain unchanged.

As the light arriving at each point of the image is not the same, it is not uniformly illuminated, the whole image can not be analyse with the same threshold because the behaviour in each region will respond different ways. That makes necessary, as described in Section 2.2, dividing image in smaller blocks and applying a threshold according to the neighbours, so the image has so many local thresholds as regions in which it is divided.

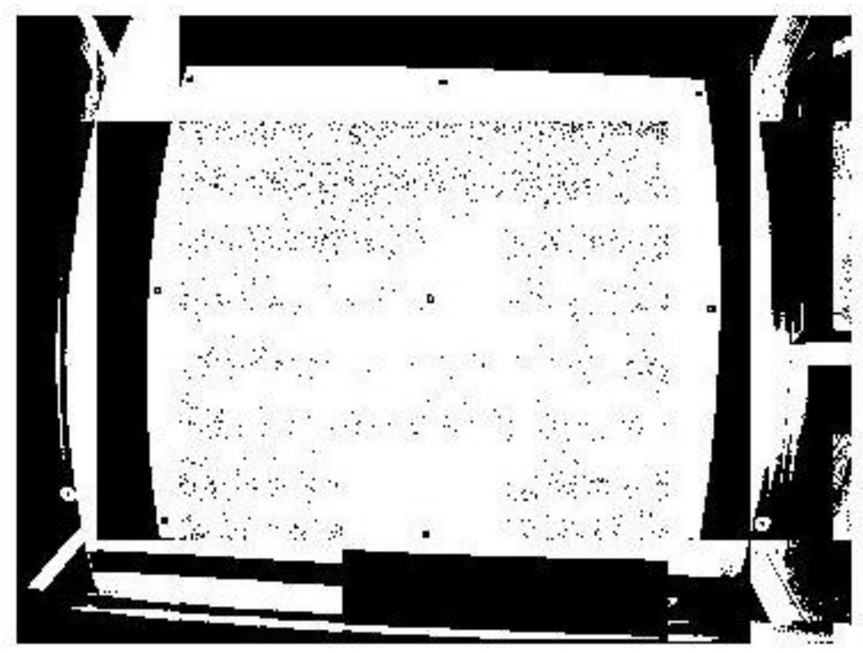

Fig. 5.7 Binary Image with 256x200 Wall's block size.

If we compare Fig. 5.7 and Fig. 5.11 we see that the size of the blocks in Wall's algorithm is really important because depending on the size of blocks we obtain different results of binarized image. This fact is determinant for next steps in image processing steps as describe further in this report and especially in external markers extraction.

In Fig. 5.8, Fig. 5.9, Fig. 5.10 and Fig. 5.11 below can be seen the resulting images of applying Wall's algorithm with both threshold methods.

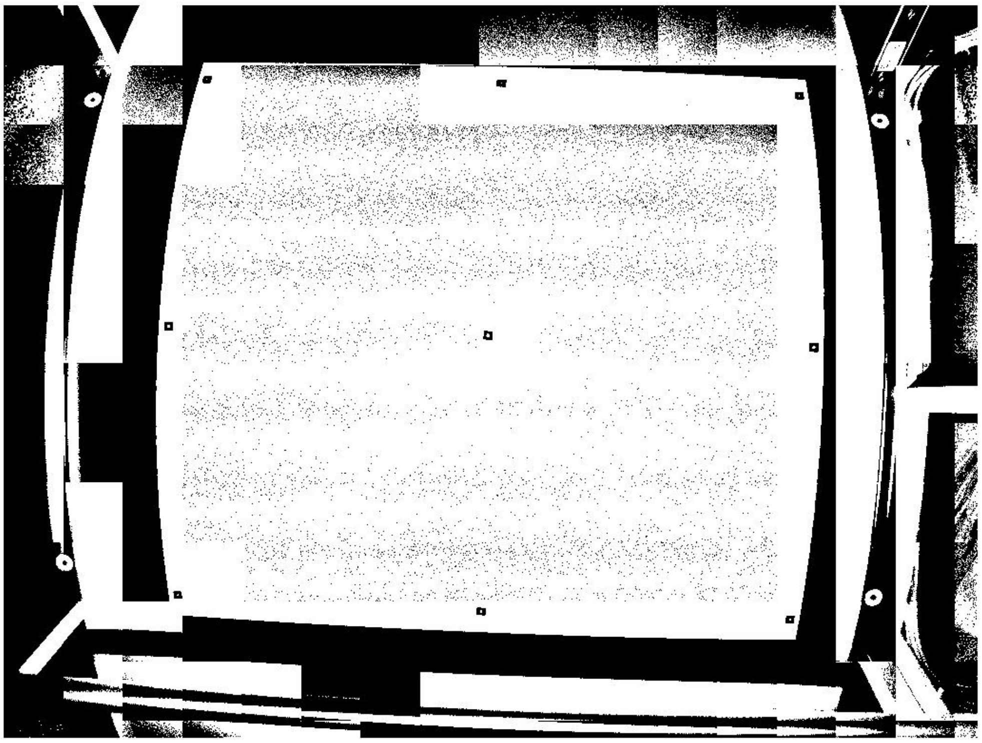

Fig. 5.8 Binarized image using Otsu's method with Wall blocks of 128x128

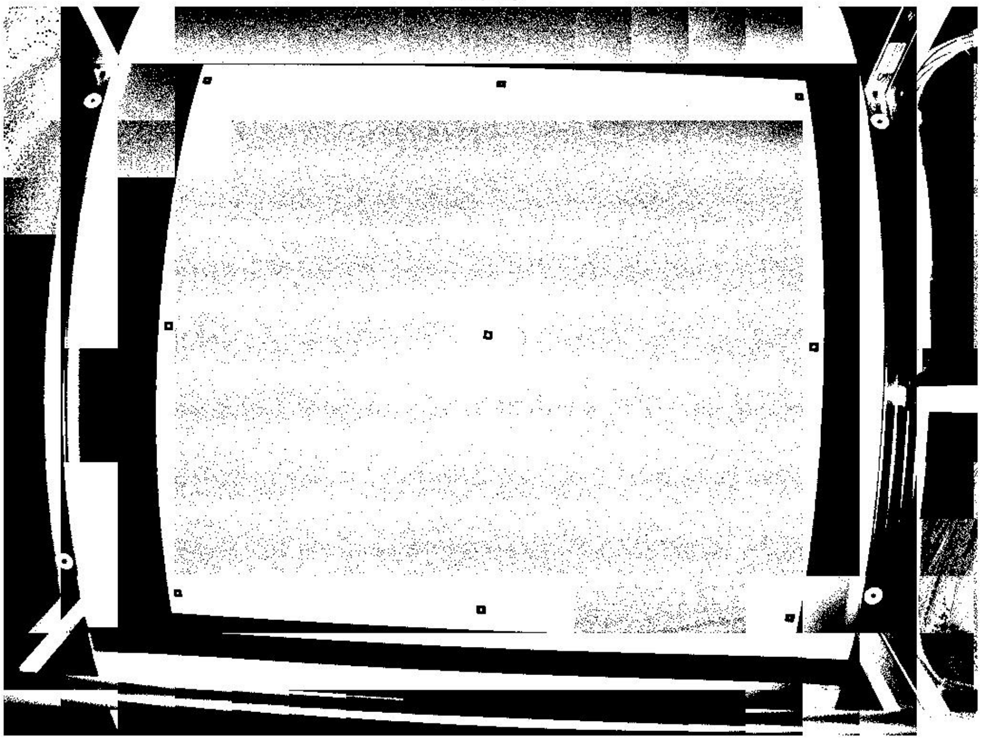

Fig. 5.9 Binarized image using Ridley and Calvard's method with Wall blocks of 128x128

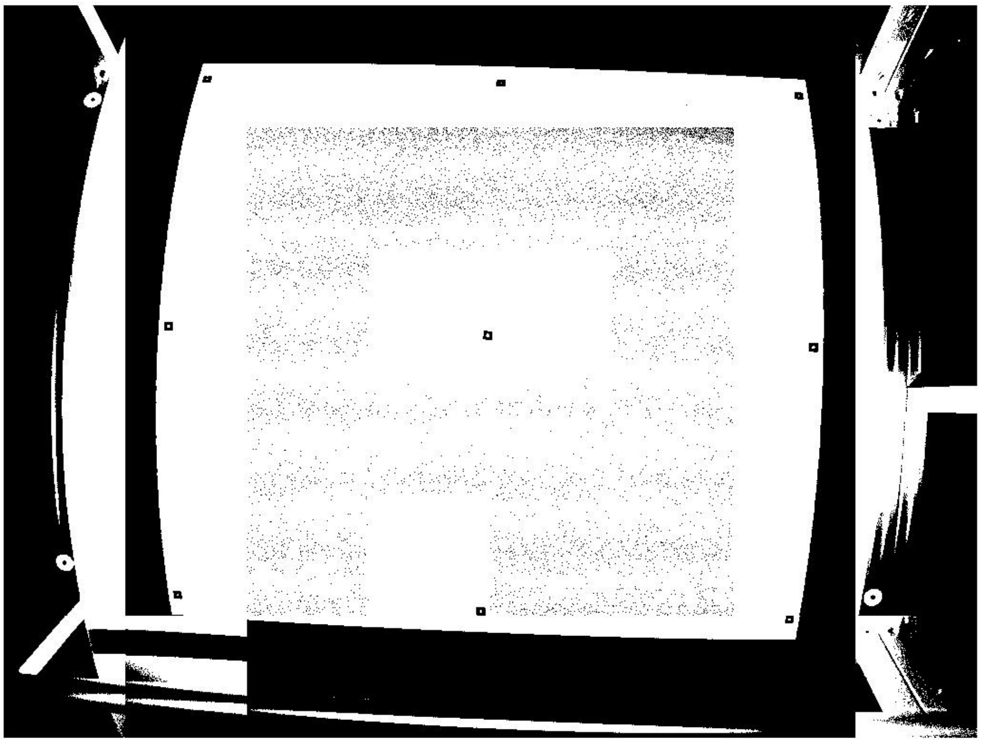

Fig. 5.10 Binarized image using Otsu's method with Wall blocks of 256x256

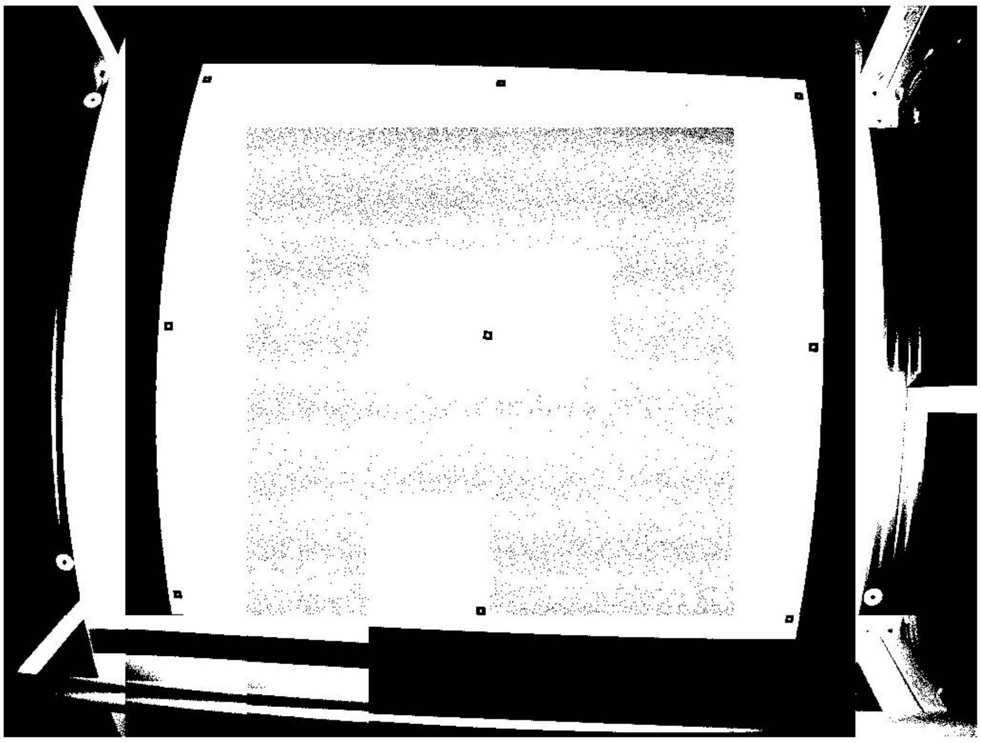

Fig. 5.11 Binarized image using Ridley and Calvard's method with Wall blocks of 256x256

As can be seen from figures above applying a local-thresholding method, indepently of the thresholding algorithm used, changes notably the appearance of the resulting binarized image. In image are noticeable the starting and ending of Wall's blocks.

If we analyse the results we see that marker E2 is not identified when blocks are of 256x256 although it appear clearly with a 128x128 region. That demonstrate that it is very important the adjustment of this blocks in order to have more definition in markers we are interested in. In our application the default blocks used are 256x256 for internal markers and 128x128 for external. If this block does not binarize objects desired properly it will be impossible to detect them in next steps.

Another point of study is the decision of which thresholding algorithm to use. The decision taken is Ridey and Calvard's algorithm as described in Section 3 and Appendix A. In the images above can be seen that this algorithm respects better (very little difference) white pixels because the threshold is a little slower. It is important for us when we are determining internal part of the markers, especially I1, I2 and I3, where light conditions are worst. All that combined with the easier development of the programming code are the definitive reason of the final decision.

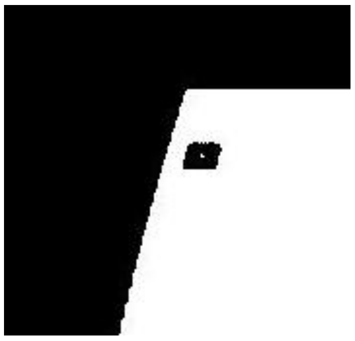

Fig. 5.12 Zoom of image Fig. 5.11 where a view of I1 is enlarged

As we have seen (see Fig. 5.12), the internal part of internal markers do not disappear at all with the algorithm chosen, but there are only few pixels forming it and it would be interesting to improve image so the internal part can be easily noticeable to allow the next steps determining the region as markers and avoiding that those internal parts are consider by next steps as isolated pixels or not desired regions. For this reason we have decided to add the first step of the image processing chain, pre-processing. This way we improve our digital image by enhancing details.

Pre-processing

As can be seen in pictures contained in Fig. 5.13 and Fig. 5.14 (I1), visually the difference between the two images (original and sharpened) is not noticeable but if we look the brightness values of the pixels we see that sharpen filter modifies these values although human eye is barely able to recognize changes.

Notice the differences shown in matrix values between Fig. 5.13 and Fig. 5.14.

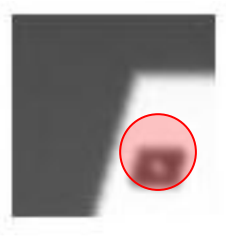

244	234	215	209	204	202	200	201	202	200	201	202	201	201	201	202	205
236	216	195	176	169	166	165	165	166	165	166	165	165	163	164	165	168
227	204	173	153	139	136	135	135	135	135	133	133	133	133	132	133	135
225	194	162	135	121	115	114	115	116	116	114	112	112	112	111	111	113
214	182	150	123	110	105	105	106	110	110	106	102	99	98	97	97	100
201	170	139	116	103	102	104	114	120	121	114	102	96	92	90	93	97
187	156	133	111	100	99	110	123	139	140	129	115	98	92	90	92	99
178	146	123	107	97	100	113	134	152	160	149	128	108	93	91	93	101
171	139	116	100	95	98	113	134	152	162	158	138	116	100	92	95	106
166	131	108	98	93	94	106	121	138	149	148	139	119	103	94	97	110
160	125	106	95	92	92	96	109	120	131	135	128	117	102	96	100	115
149	123	105	95	91	91	94	98	108	114	119	117	108	103	97	103	120
147	123	108	99	96	96	96	100	101	107	109	108	106	102	103	109	131
151	131	118	110	107	108	108	109	110	112	114	114	112	112	114	125	145
168	149	140	133	131	132	131	131	132	133	133	134	133	134	138	147	165
195	182	174	170	168	168	168	167	167	166	167	166	167	168	171	177	193

149	128	108	93	91
158	138	116	100	92
148	139	119	103	94
135	128	117	102	96
119	117	108	103	97
109	108	106	102	103

Fig. 5.13 Internal marker original image. Matrix of image value.

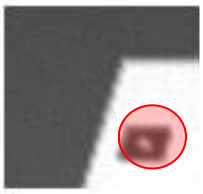

252	250	203	215	209	210	204	208	213	204	209	213	209	209	207	206	214
246	214	192	157	159	158	159	158	163	158	165	160	162	153	159	158	162
228	208	154	140	118	124	125	125	123	125	118	122	122	124	119	122	119
244	198	157	117	106	100	100	104	104	105	103	99	104	106	103	101	97
223	182	143	105	97	93	95	88	98	97	91	90	87	90	88	84	83
206	171	128	103	88	97	91	115	117	121	111	85	88	84	79	88	84
179	145	134	100	89	85	109	120	158	151	128	116	82	86	85	86	92
171	134	114	102	84	92	109	147	175	195	170	131	104	76	86	86	86
164	130	109	86	86	88	114	149	174	191	191	150	116	95	81	87	95
164	117	91	93	86	82	105	120	147	165	161	159	121	100	82	86	96
163	107	96	85	88	86	81	108	116	137	148	134	125	93	86	89	102
134	111	93	85	81	82	87	82	105	107	120	121	99	103	81	88	101
135	106	95	86	87	89	83	94	82	98	98	95	98	87	91	85	119
131	113	101	93	90	97	96	96	96	97	102	102	96	97	93	109	131
152	125	125	115	115	121	116	116	119	121	118	123	118	119	124	130	150
185	178	170	169	167	168	169	165	166	161	168	162	165	164	166	166	197

170	131	104	76	86
191	150	116	95	81
161	159	121	100	82
148	134	125	93	86
120	121	99	103	81
98	95	98	87	91

Fig. 5.14 Internal marker sharpened image. Matrix of image values

Comparing matrix values between original and sharpened image, we can see two kind of behaviour. (This behaviour is also valid in case of external markers. We have decided to show internal markers results because the size of markers is smaller.)

On one hand, some pixels have more or less the same value in sharpened image (for example, from 119 to 121 or from 116 to 116 that remain constant), that means that the values have been smoothed (low changes in image) to leave out noise, transforming them into a similar value or remaining the same. On the other hand, (for example, from 158 to 191 or from 93 to 76) pixel values become darker or brighter, respectively. In those cases sharpening filter detects abruptly changes in image. If in our two examples we consider 158 a bright pixel and 93 a dark one (that is what they are respect their transformed value although in the range from 0 to 255 of our image they will be considered the opposite) after sharpening we have changes from bright to darker or from dark to brighter, that means that our sharpen filter considers them as details and it enhanced them.

Fig. 5.15 Left: E1 of original image; Right: E1 of sharpened image

In Fig. *5.15*, the sharpen filter effect is visually more noticeable than in I1 case shown in Fig. 5.13 and Fig. 5.14. The external circle appears in sharpened image on the right clearer, the limits, where contrast is higher, appear better defined as in original image.

So as we can see including this step before the thresholding, noise will be reduced and details will be enhanced making more remarkable the differences between transitions and favouring the distinction of internal parts of our markers as for example the case shown in Fig. 5.12 above.

What we have until now is a binarization of a sharpened image. If we look back to Fig. 5.9 and Fig. 5.11 we see there are a lot of isolated pixels that do not belong to structure or markers but have appeared after binarizing as a kind of noise in the image. So before labelling the existent regions in the images it is necessary to clean images so the identification of desired regions is easier.

At this point we have to differentiate between internal and external case.

In the case of internal markers, the morphological operator applied into image to clean it is closing as described in Appendix B.

Results are shown in Fig. 5.16.

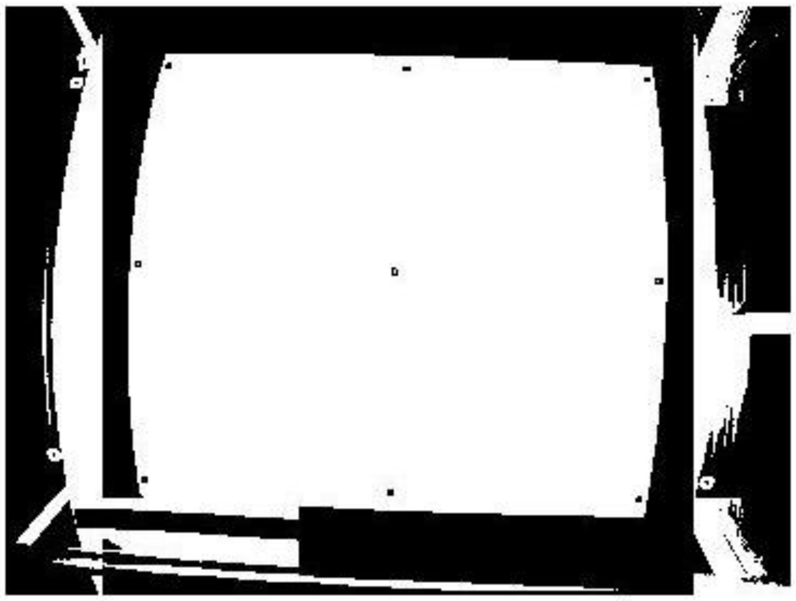

Fig. 5.16 Closing morphological operator applied to binarized image of internal markers

In the case of external markers, the morphological operator applied into image to clean it is opening as described in Appendix B.

Results are shown in Fig. 5.17.

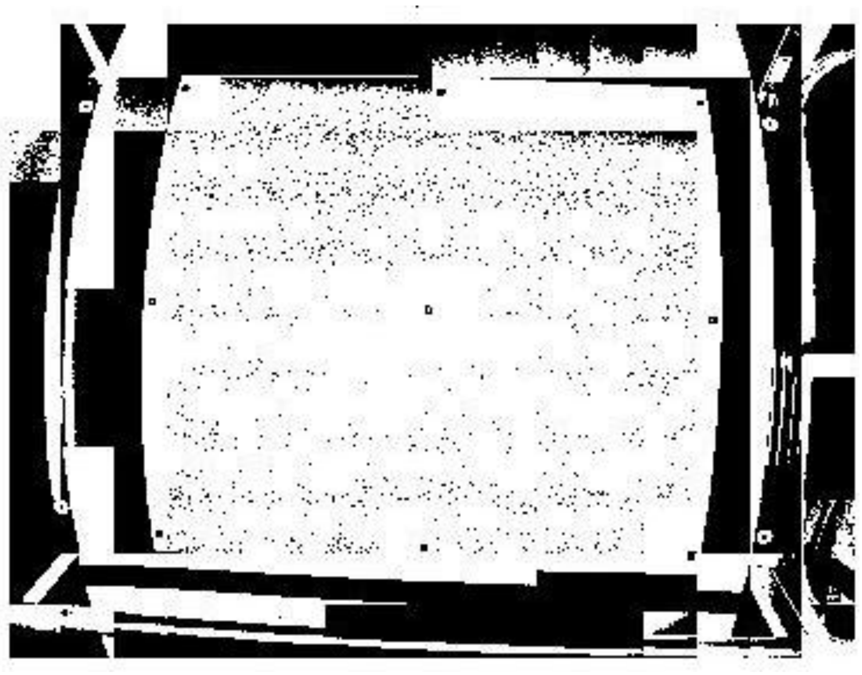

Fig. 5.17 Opening morphological operator applied to binarized image of external markers

If we compare Fig. 5.9 and Fig. 5.17 we see that black regions are accentuated, opposite to white ones. It is very useful in our purpose because we ensure that the internal part of the external marker do not disappear. This way, our markers maintain their appearance.

Otherwise, comparing Fig. 5.11 and Fig. 5.16 we see the opposite phenomenon and are white ones which we want to improve for not losing the internal part of internal markers.

Our images are prepared for labelling, well, a previous step is needed in case of internal markers (contrast transformation) as described in Section 3.1.

Labelling

As follows labelling described in Section 2.3 is done (see Fig. 5.18 and Fig. 5.19).

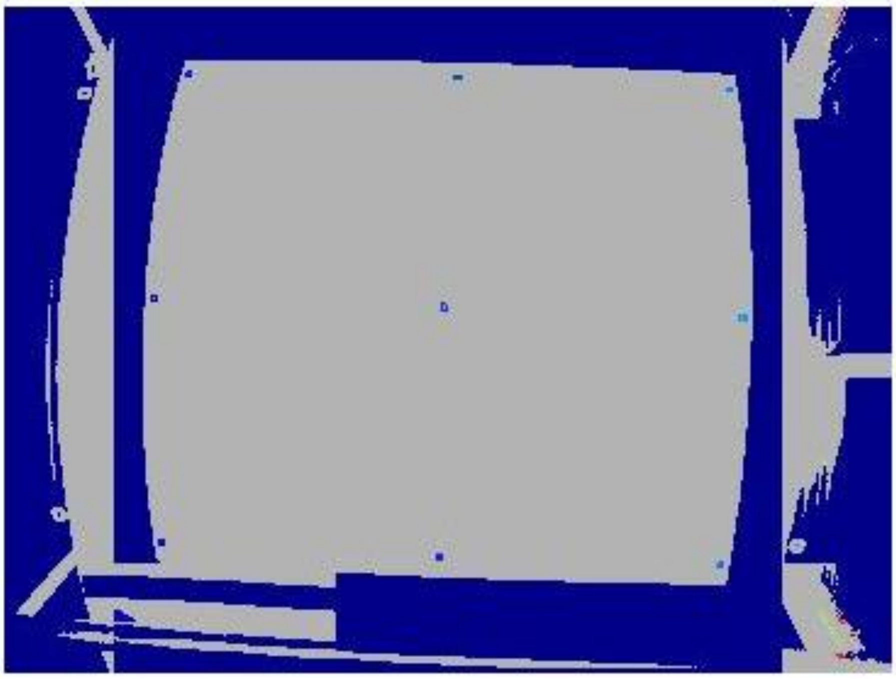

Fig. 5.18 Labelling after contrast transformation, case of internal markers

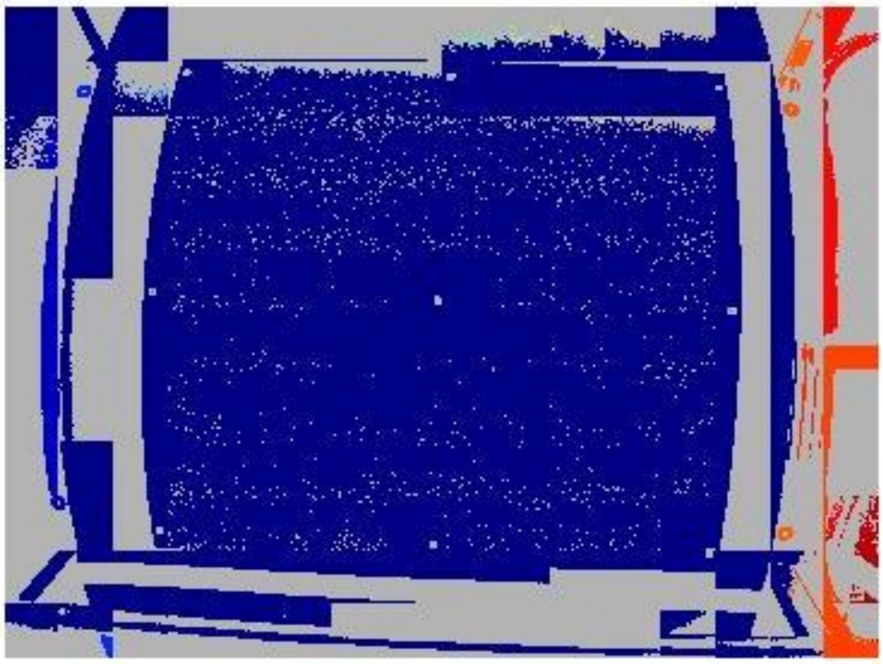

Fig. 5.19 Labelling image in case of external markers

Here, we show a coloured version of labelling to easily see the different regions, although the application internally differentiates them by a label number. The regions detected by our development are those coloured, the ones in gray are considered as background and for that reason they are discarded from now on, undesirable regions.

With these colours it is fast to see how all our markers are consider regions of interest and thanks to the criteria described in Section 2.3 we will be able to reject some of those undesirable labelled regions.

At this point we have to work separately internal and external markers. Some criteria as size of regions is common to both markers but there are some other ones only usable for internal markers. We are going to show the results separately depending on which kind of marker we are extracting.

Shape classification and Object Recognition: Internal markers

In the case of internal markers the strategy was to implement SIFT in our C++ project but we were not able to make it. So the results shown in this report correspond to the SIFT algorithm in Matlab [10] but applied to image obtained by C++ performance.

We have considered different situations and according to the results we have get to the final solution described in Section 3, where the range for size and the ratios of rectangularity are described.

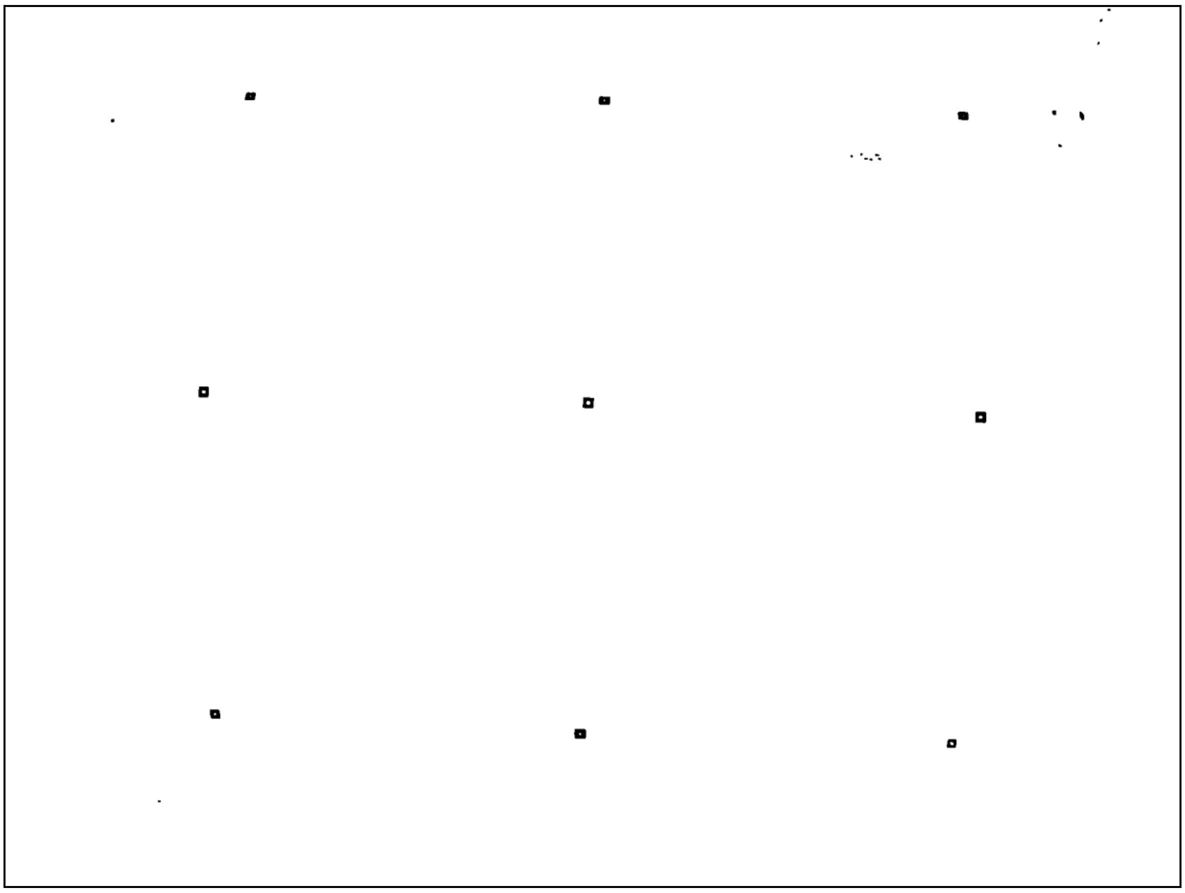

Fig. 5.20 Resulting image with upper size range

As a starting point, we have considered only the upper value for range in size (not lower) and we see in Fig. 5.20 as all markers are shown but there are also some other noisy regions we do not want. We have also runned the application in case of only having applied one or more of the ratios (results are explained widely below in different cases) and all resulting images where very similar to that one shown above, noisy. What we are going to show as follows is how affect the different criterion selected, and its combination, and how the results change at recognizing markers when we apply SIFT algorithm.

Case 1: We have applied an upper threshold value for size and Kurtosis ratio. The image we obtain is very close to Fig. 5.20. We see that SIFT does not detect neither the marker I1 nor I3 (see Fig. 5.21). But it is also relevant the fact that in the zone nearly I3 one of the noisy regions is detected as marker (See Fig. 5.22). The rest of markers are properly detected by SIFT.

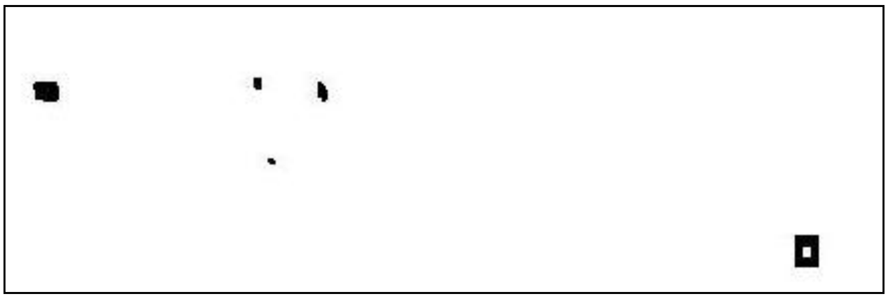

Fig. 5.21 Marker I3. SIFT does not detect marker or noise

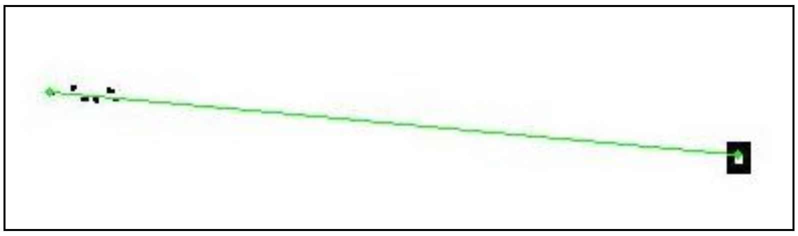

Fig. 5.22 Noise near I3 which is detected as a marker by SIFT

As noisy regions are smaller than our markers we thought that a good solution, although losing relevant information from our markers, was to apply dilation (morphological operator described in Appendix B) with an appropriate structurant element so it will erase in part or completely the noisy regions. The tests made were with a 2x2 and 3x3 structurant element. The problems still remained. So it is demonstrated that applying an upper range and only kurtosis parameter for rectangularity does not grant a good detection of all our markers.

Case 2: We have applied an upper threshold value for size and rectangularity ratio. We see that in I7 and I9, SIFT algorithm is able to distinguish noise from marker (See Fig. 5.23 and Fig. 5.24). It analyses both regions and finally extracts only I9.

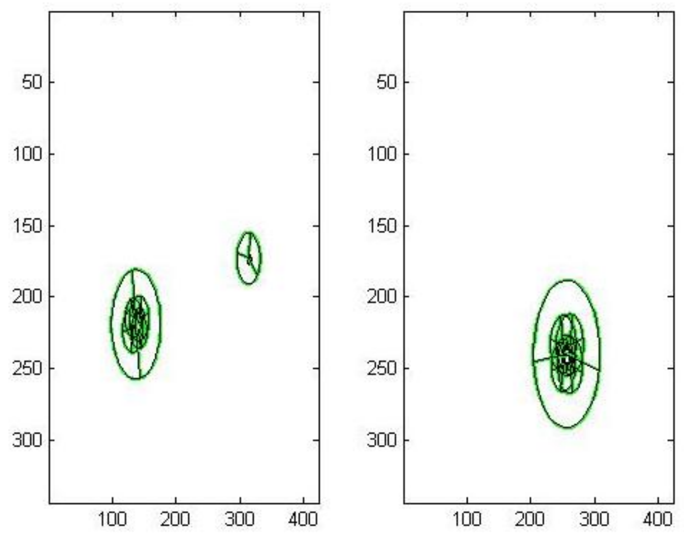

Fig. 5.23 SIFT frame of marker I9. On the left the study marker where noise and marker are analyse. On the right, the template marker

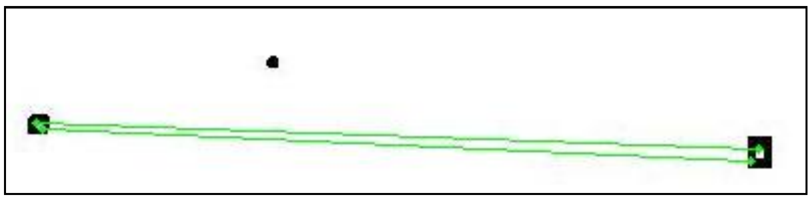

Fig. 5.24 SIFT detects marker as marker and reject noise (I9)

At extracting I1 we find the same situation as described in Fig. 5.22 where noise is detect as marker and the marker is rejected as region of interest.

We apply also dilation (3x3) in this case and we see the results obtained for I9 in Fig. 5.25.

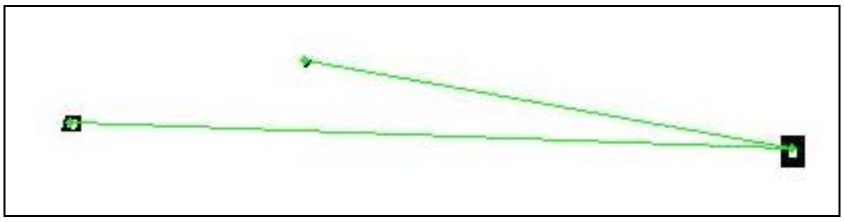

Fig. 5.25 SIFT detects marker and noise as marker I9

Now the marker is detected but also noise, two different keypoint in the image of study are considered by SIFT as one keypoint in the template. As a result rectangularity applied with an upper size range value, with or without dilation, does not ensure that a region in image is detected as a correct internal marker.

Case 3: We have applied an upper threshold value for size and both, rectangularity and Kurtosis, ratio.

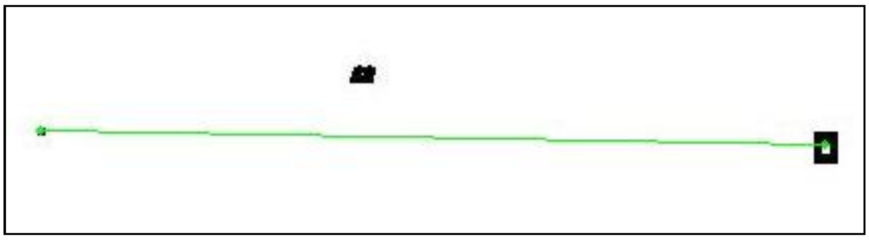

Fig. 5.26 SIFT detects noise as marker and discards marker I1

We see there is a wrong detection. I1 remains unrecognized and in its place noise is detected. We see also that I1 is greatly affected by affine features and that its hole in the middle is really small. We apply dilation 2x2 (See Fig. 5.27) and dilation 3x3 (Fig. 5.28) and we see what happens.

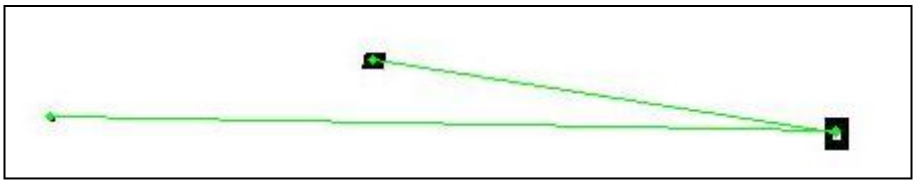

Fig. 5.27 Detector SIFT after applying dilation with a 2x2 structurant element. Noise and marker are detected.

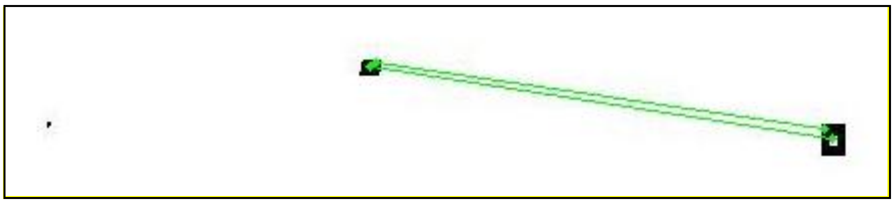

Fig. 5.28 Detector SIFT after applying dilation with a 3x3 structurant element. Marker is detected and noise is rejected

We see that applying an appropriate structurant element the results change. With this morphological operator we win some white pixels in the middle of the marker and this way, SIFT is able to match the keypoints of the study marker and the template. Dilation has a double function, as well as it transforms the inside of the marker to something more similar to the template it also reduces noise, making the undesirable area smaller and also more different. So keypoints from marker of study are another ones which not correspond to the ones in template.

From the results of 3 cases, we see that our conflictive regions are those small, which can become wrong detections. A good solution seems to select a range with an upper and lower size values and see if those undesirable noisy areas are reduced. If they are not erased we can use the combining of lower and upper size range and dilation.

Case 4: We have applied an upper and lower threshold value for size without ratios. As we have seen in all our cases, the more conflictive pixels are I1, I2 and I3. The reason is not only noise but also their projection on the cylindrical surface (big affine effect). If we apply both thresholding values we see that the problem of noise almost disappears and now the detection of the markers have more keypoints in common. See Fig. 5.29 where I7 is shown.

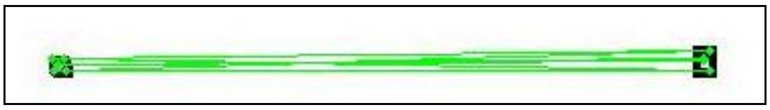

Fig. 5.29 SIFT detection of marker I7

However, the problem of no detection of I1, I2 and I3 still remains. So dilation will be the better solution.

As a summary, what we have decided is to use the combination of size and both rectangularity criteria. It has been proved that small regions are the most annoying and that the presence of a lower value of size range reduces highly these undesirable appearances. In our GUI there is an option called Optimization (described in Section 4.4), that can be applied after discarding regions with the methods described and which applies dilation to improve the inside part of the marker and this way make the SIFT algorithm extraction more robust.

Before ending this part, it is important to say that can appear problems with dilation if we are not careful. We can not chose any structurant element and not all sizes, because dilation is applied to whole image and we want to improve the internal part of conflictive markers but not modifying so much those rightly detected. If we do not take care of that we will alter the properties of our markers and then leading to wrong detections. See figures below to value the effect.

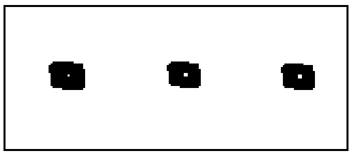

Fig. 5.30 From left to right: resulting marker, dilation 2x2 and dilation 3x3 of marker I3

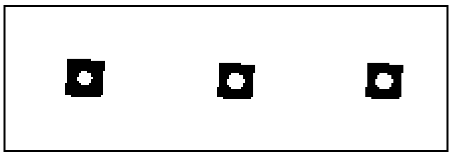

Fig. 5.31 From left to right: resulting marker, dilation 2x2 and dilation 3x3 of marker I5

If the structurant element is big enough the inside part of the marker can arrive to be part of the background, and the marker lose its features.

Shape classification and Object Recognition: External markers

In the case of external markers we are not interested in rectangularity ratios and the only problem we have is to choose an appropriate size range and contours will extract circular markers.

As follows we can see the results of applying an upper threshold of the image.

Fig. 5.32 Resulting image (before applying contours) with only upper size value

We can identify our markers and some other noisy regions. Internal markers do not appear because the labelling used in external markers considers internal markers as undesirable and they are rejected in the labelling step.

Fig. 5.33 Resulting image (after applying contours) with only upper size value where centre of ellipses are detected in red

Although those regions are not detected as circles (see Fig. 5.33 where only external markers are detected as ellipses, in red) for avoiding the possibility of wrong detections we are going to select a lower and upper size range as in the case of internal markers. Mostly noisy regions disappear. Detecting circles is not really the problem in this case as can be seen in Fig. 5.34 and Fig. 5.35 where the only noisy region remaining is not a circle. For that reason, it is not detected (in red).

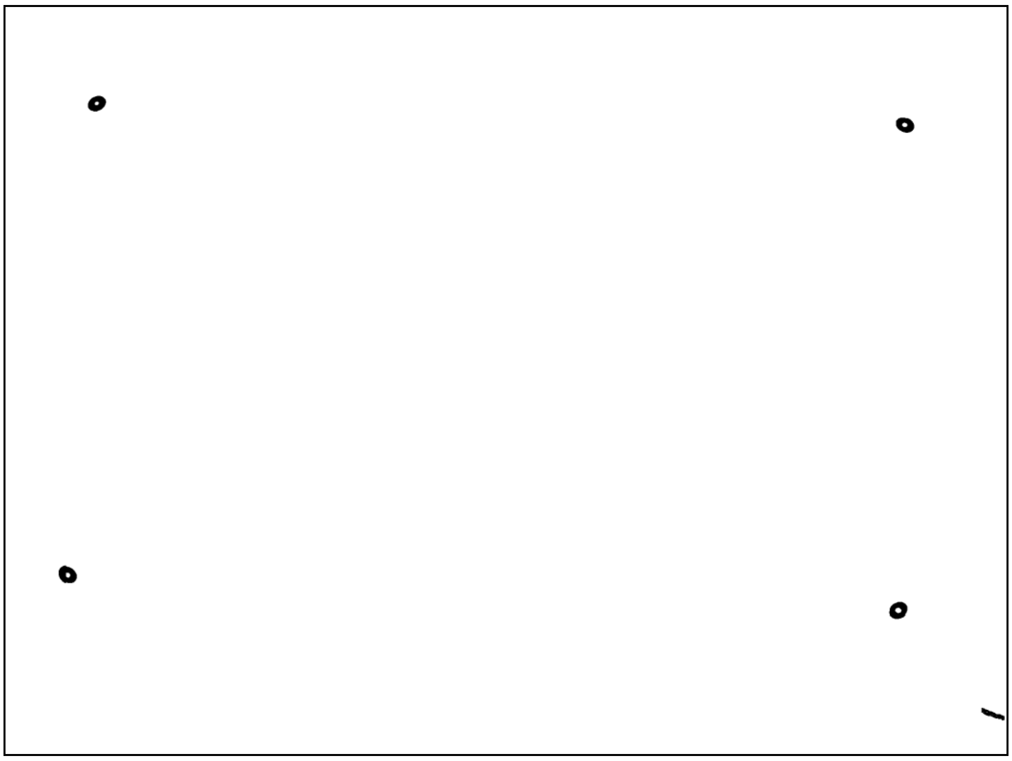

Fig. 5.34 Resulting image (before applying contours) with upper and lower size value

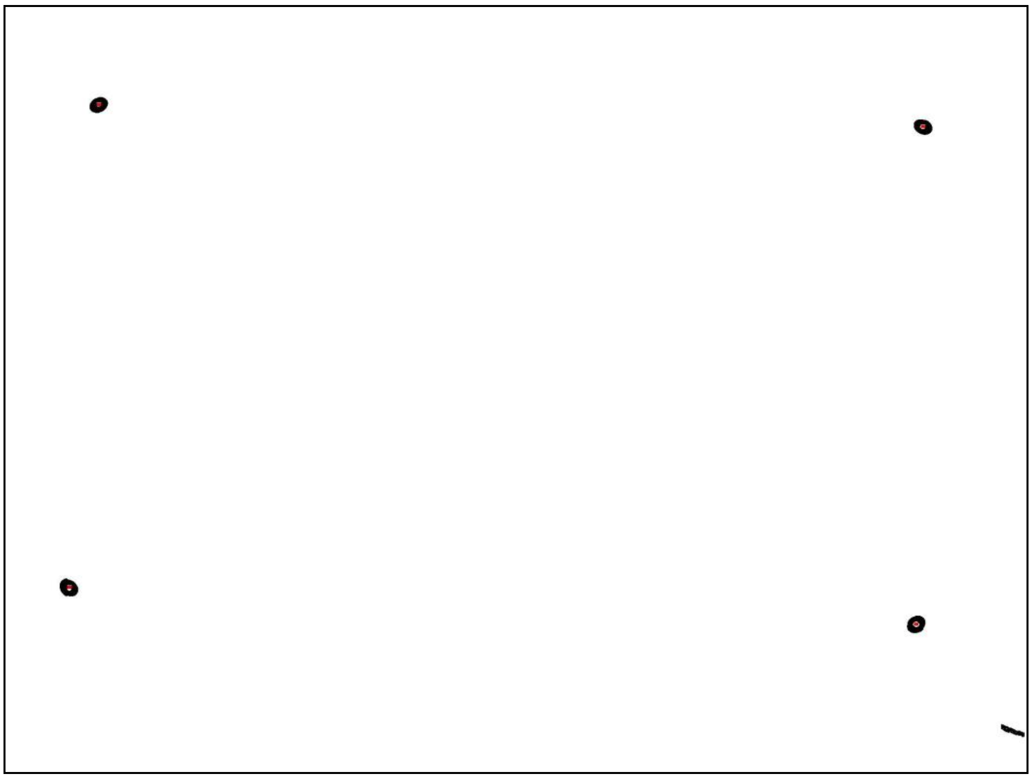

Fig. 5.35 Resulting image (after applying contours) with upper and lower size value where centres of ellipses are detected in red

With external markers the critical moment appears before this step, at thresholding. We find that some of the parts of the cylindrical structure are very similar to our external markers, in terms of brightness, and also very close. That makes that, if wrong parameters in Wall's algorithm block are chose, some undesirable regions and our markers become connected and we lose the properties of our external markers which will not be extracted. The effect can be seen in Fig. 5.37.

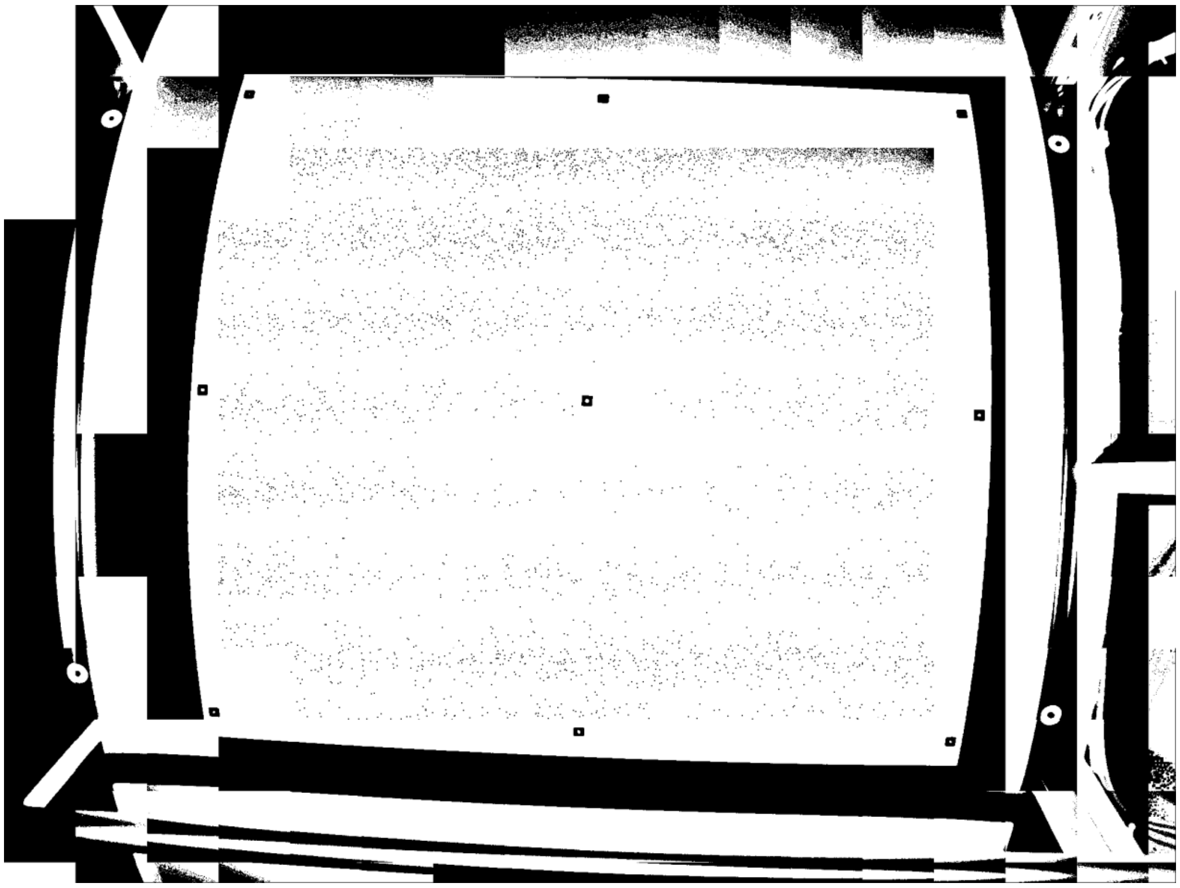

Fig. 5.36 Adequate size of Wall's algorithm for detecting external markers.

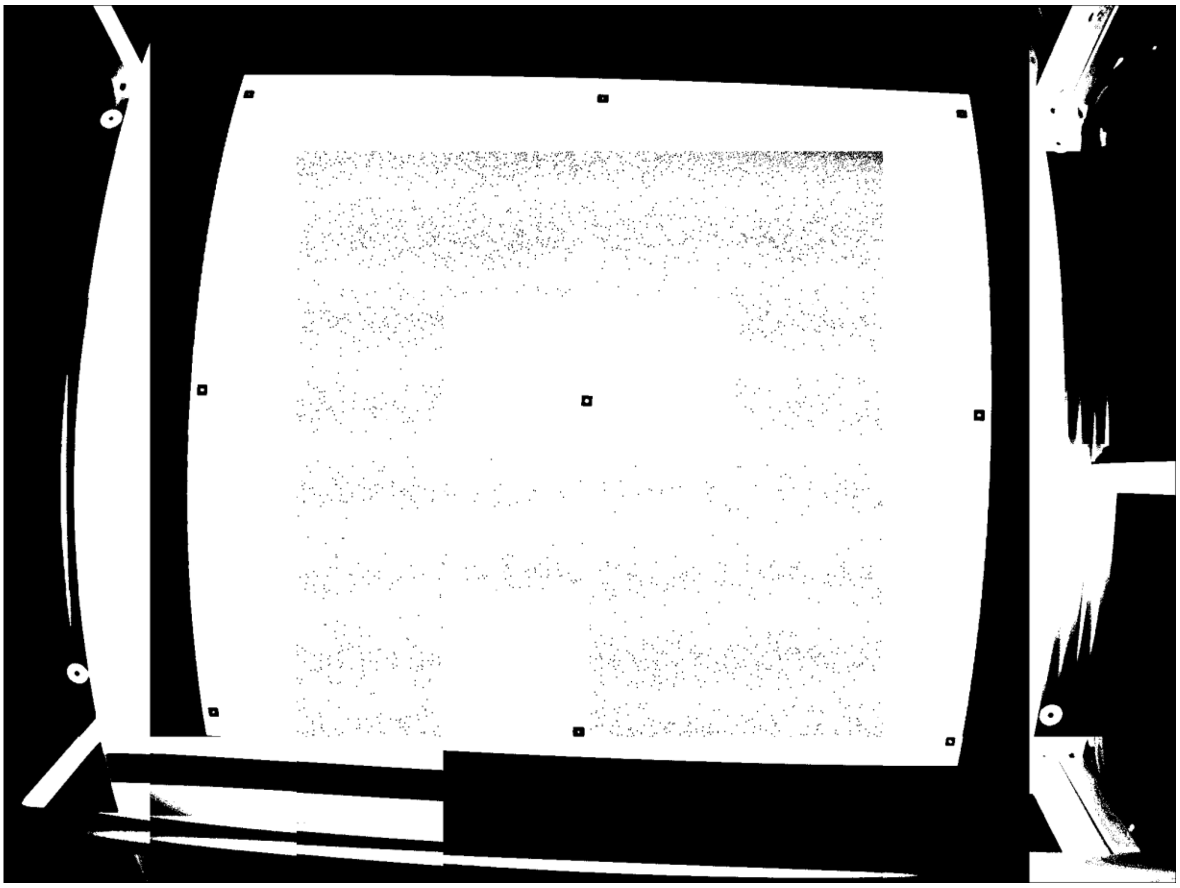

Fig. 5.37 Inadequate size of Wall's algorithm for detecting external markers (256x256)

If we take a look to Fig. 5.37 we see that E2 is not noticeable and E3 appears connected to the structure. After labelling both will disappear and the result will be a wrong detection as can be seen in Fig. 5.38.

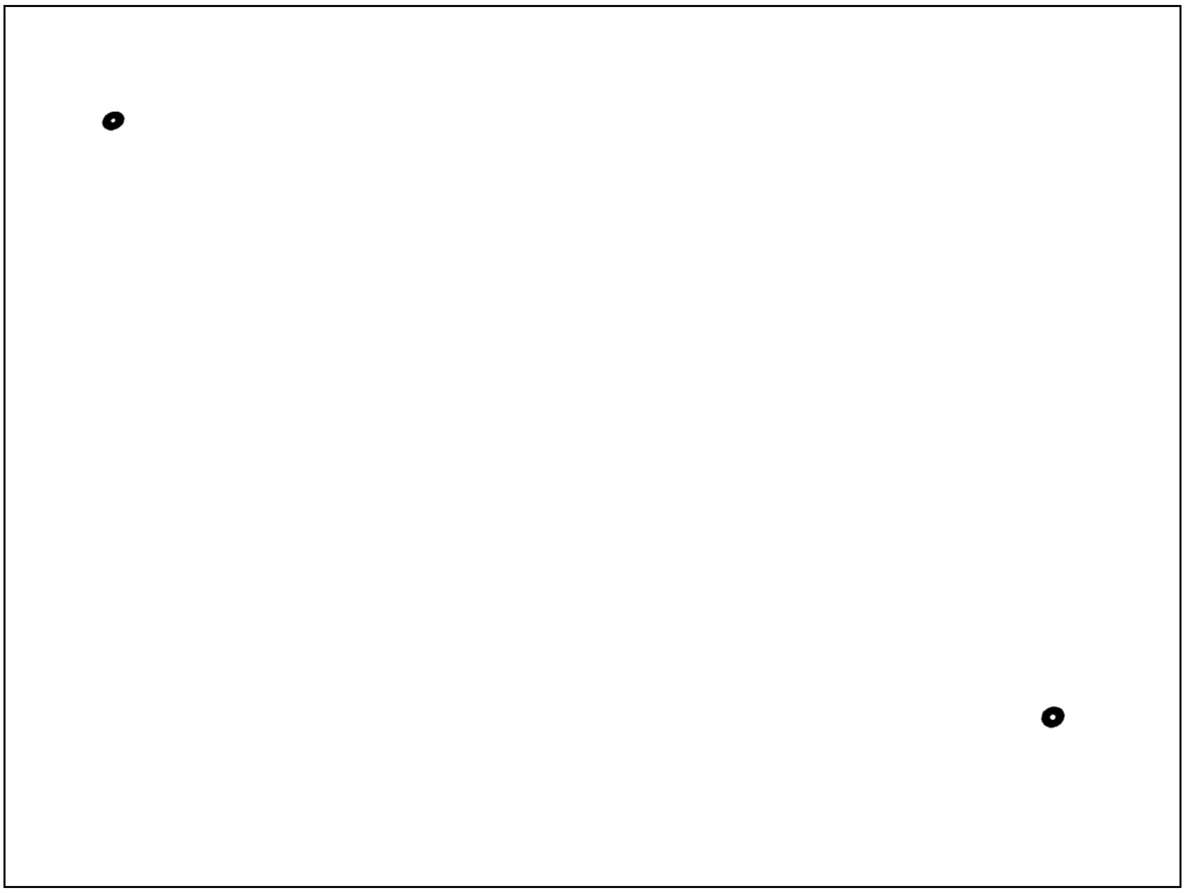

Fig. 5.38 Wrong detection of External Markers. E2 and E3 are not detected

It is relevant at this point to remember that the whole process have to be controlled by a person in order to obtain good results.

Rotation

As we have only one testimage we have done another test with the same image but rotated (testimage_rotate.bmp).

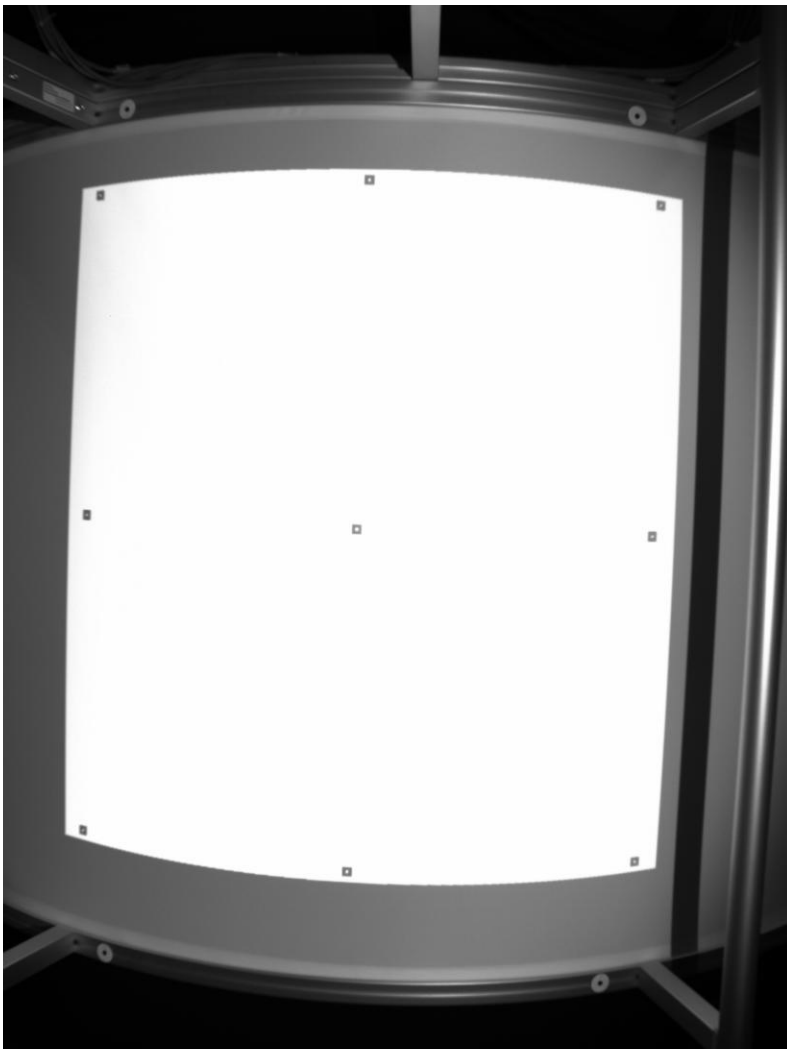

Fig. 5.39 testimage_rotate.bmp, a rotation 90 degrees to the left of testimage

For our application the image after rotating 90 degrees to the left becomes completely different. Some changes in the image are mentioned as follows:

- Image size: the new size of image is 1536x 2048, width and height change respect original testimage (2048x 1536)

- Light distribution: now the effect of light will affect to other markers, so the conflictive ones (those in the upper row) will change

- Size of Wall's algorithms: the same sizes of blocks will give different binary images and the regions determined will not be the same.

The features that will remain the same are those relative to our markers, rectangularity and ellipticity.

In the case of internal markers, if we maintain the size of Wall's blocks (256x256), the resulting binary image is Fig. 5.40 which can be compared with Fig. 5.11.

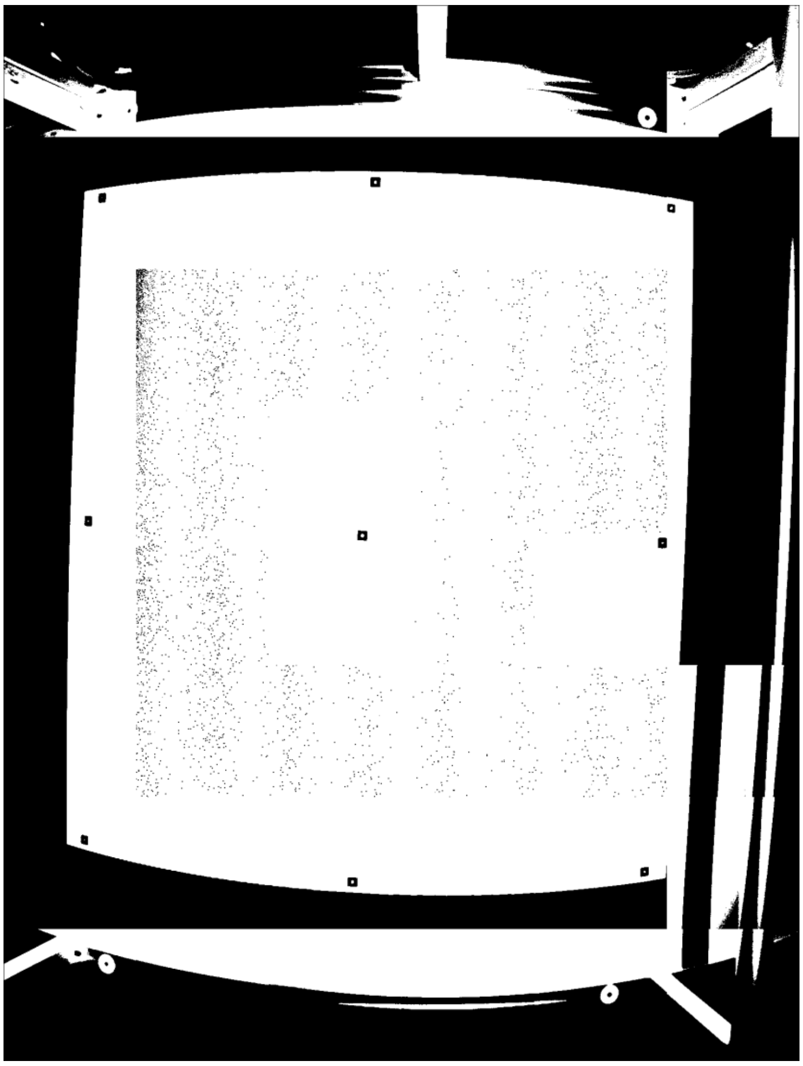

Fig. 5.40 Binarization of testimage_rotate.bmp with Wall's blocks size of 256x256

Mainly differences can be seen in noisy isolated pixels in the area enclosured by new I1, I2, I4 and I5, and in the upper-central part and down-left parts of the structure. Binarization respects internal markers and its internal hole so detection will follow properly.

In the case of external markers, the results of the binarization are shown in Fig. 5.41

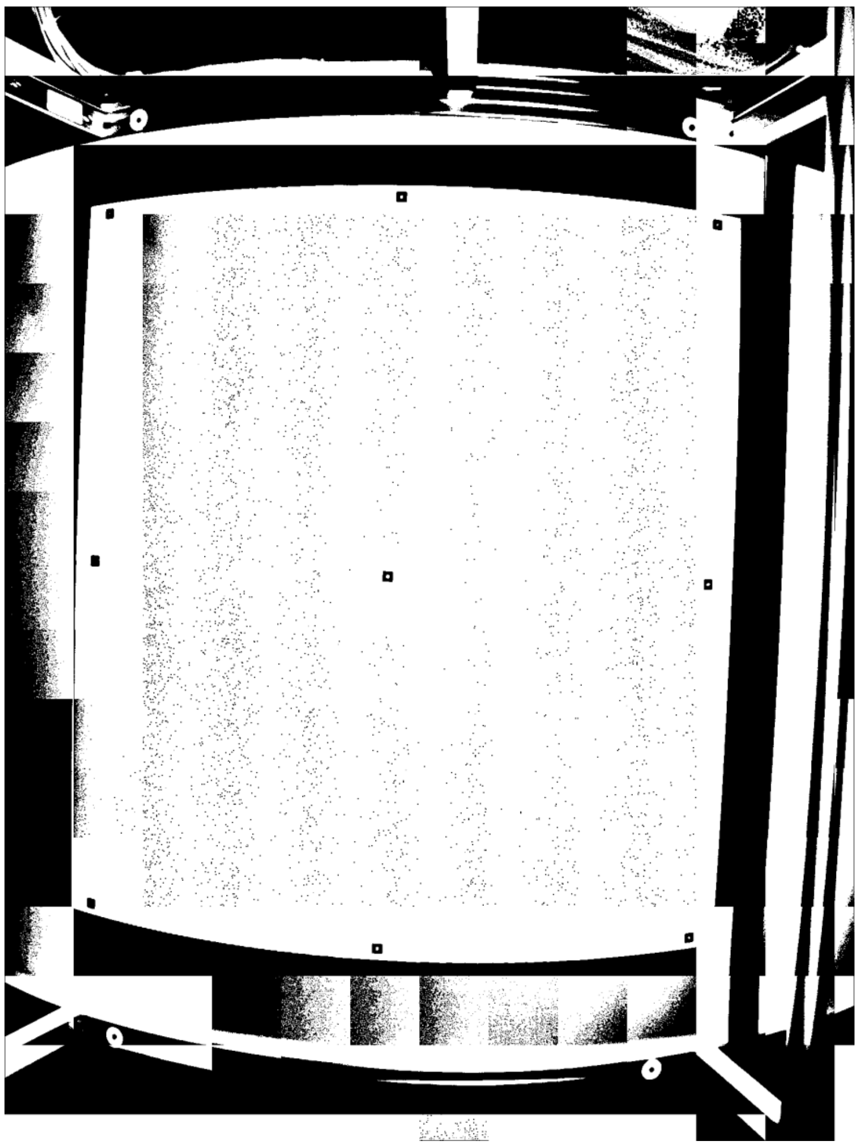

Fig. 5.41 Binarization of testimage_rotate.bmp with Wall's blocks size of 125x125

In this case we see that maintaining Wall's block size (125x125), our external markers E2, E3 and E4 are part of a big region which will be erased when we discard big regions as shown in Fig. 5.44 (left). Seeing the results of the binarization it has no sense to continue with detection of external markers and is at this point when the fact we have exposed many times in this report is relevant, it is the importance of the visual interaction between application and user to improve application for an optimal extraction of markers.

So user has to choose an adequate size of Wall's algorithm in order to extract all markers. In our case we have chose 110x340 to show how a good result should be (and also show that Wall's blocks do not have to be squares). (See Fig. 5.42)

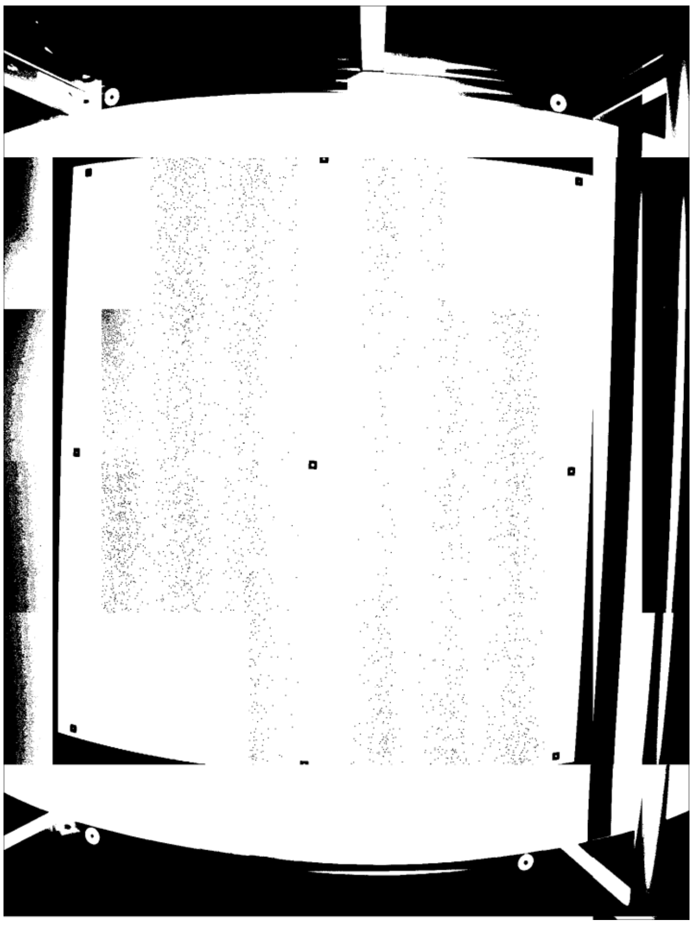

Fig. 5.42 Binarization of testimage_rotate.bmp with Wall's blocks size of 110x340

In the detection of internal markers we see that the results are as expected and the same as case of testimage.bmp, but we have observed that little changes in kurtosis parameter (`((kx<-1.07)&&(kx>-1.32))`) will lead to wrong detections (See Fig. 5.43).

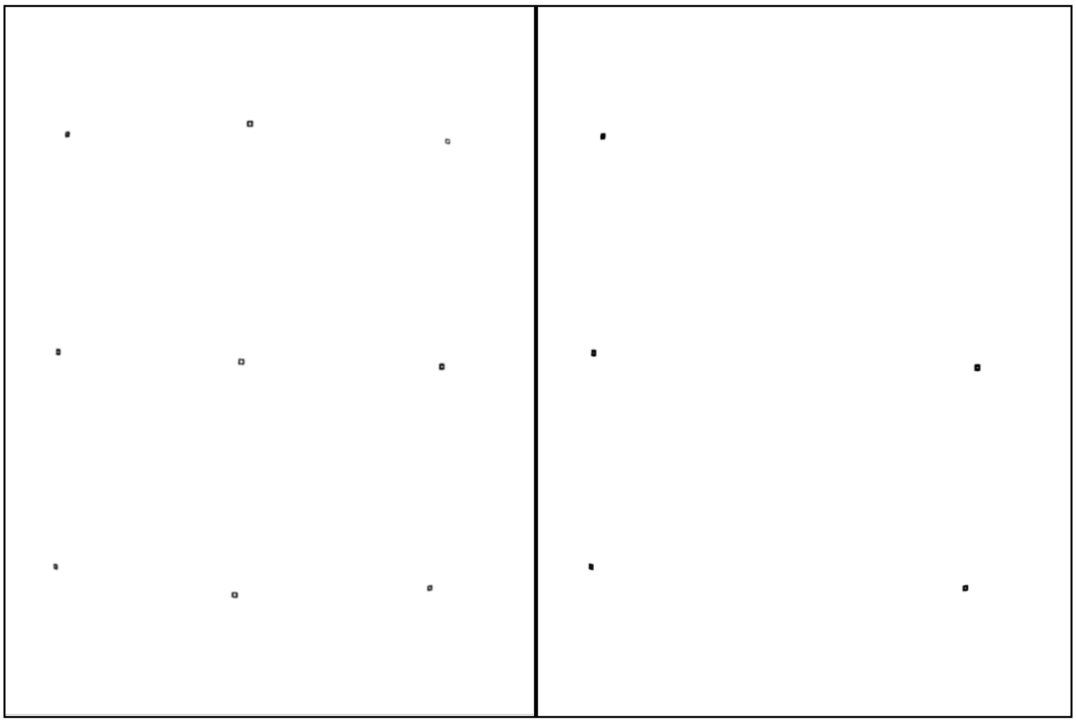

Fig. 5.43 Detection of internal markers. Left: all markers are detected; Right: I2, I3, I5 and I8 are not detected

Seeing this results it is obvious that the range chose for kurtosis parameter could be a problem. If we had more testimages we could surely determine if the range chose for kurtosis is available in all cases or perhaps a readjustment should be done in order to detect correctly all internal markers of different side projections.

In Fig. 5.44 wrong and the right detection of external markers are shown.

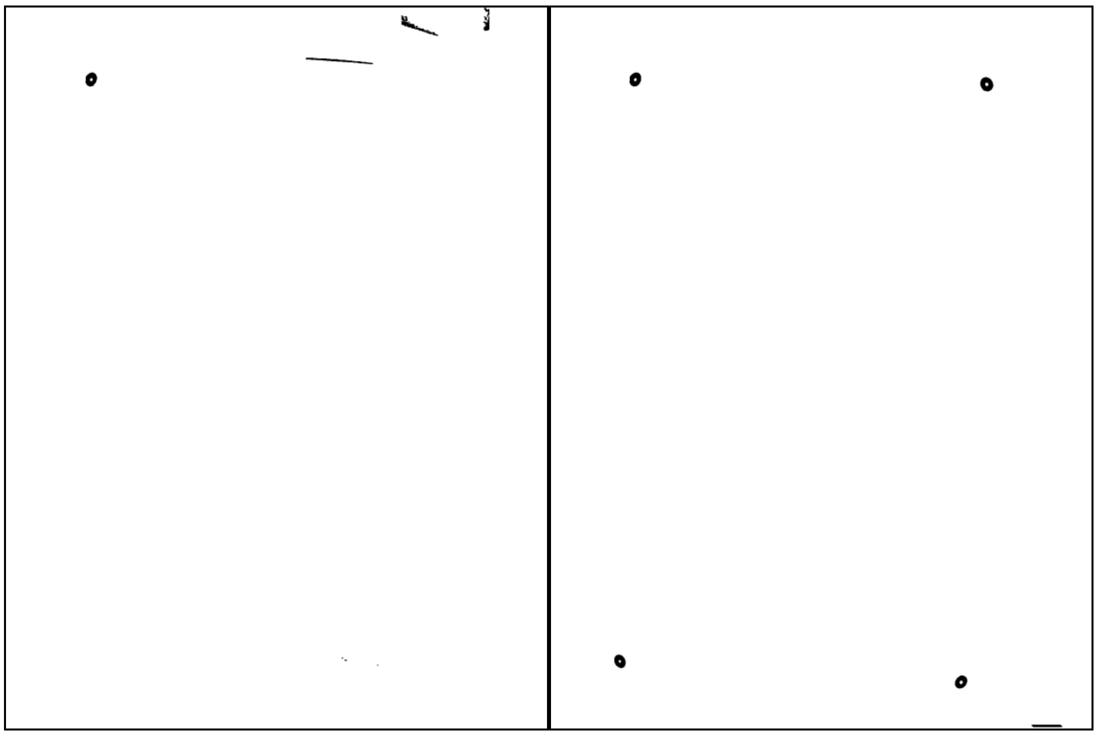

Fig. 5.44 Detection of external markers. Left: E2, E3 and E4 are not detected because in binarization they are connected to a big region; Right: right detection.

So altogether what we see from the results of running our application to testimage and rotate image is that the values and ratios selected are good at extracting markers in both cases internal and external. The first step of pre-processing is really important to ensure a better performance of next steps in the image processing chain. The use of different sizes for Wall's blocks is possible in local-thresholding but it is important the supervising of the binarized image obtained in order not to loose relevant information of desired objects which will cause non detections after labelling if a wrong size is chosen.

In case of internal markers the combination of 3 descriptors described performs a good extraction and SIFT algorithm gives robustness to the object recognition. In the case of external markers, the method based on contours obtains right detections of external markers.

We have seen that some little changes in ratios/parameters affect to the results obtained so the problem we find is the small amount of images of test that we have. More images should be taken in order to conform a larger database and this way ensure that the adjustment of the parameters and ratios respond properly to all cases.

6. Conclusions

Immersive environments were born to provide the user a panorama of 360 degrees with which he/she can interact. Immersion consists in giving the user the impression of being in a real world at any place at any time although he/she is in a virtual reality recreated by computer with the aim of giving this reality sensation. The immersive media techniques are a very ambitious line of study in nowadays image and video processing and it can be applied into many applications as live broadcasting of sport events, theatre, museums and music events and also immersive video gaming. In these scenarios it is very important the continuity of panorama recreation because human sight is very sensible to changes in illumination and transitions and, if continuity between images is not provide, user will not feel the total immersion. To obtain this continuity, different calibration systems are used.

In our case the scenario built in IGD Fraunhofer Institute, in the context of hArtes project, is a system based in an array of projectors and cameras where calibration is needed to provide immersion. So the objective is to correct those misalignments and overlappings in the junctions between projections so the changes are not noticeable for the person who is inside. The calibration has different steps and my contribution is the first step, which consists in the univocal recognition of internal (squares) and external (circles) markers from a projected image through image processing techniques. After this step a correction between real and ideal markers followed by a correction in the misalignments in junctions will be done.

My contribution to hArtes Project in IGD is the development and implementation of a GUI application in C++ programming language. The application searches, through image processing chain, the univocal recognizement of markers in a given image (desired markers left untouched and non desired ones are rejected) by developing a graphical interface between user and image obtained from projection onto cylindrical surface. The Win 32 console application developed has different buttons to select different options and a visor to see image results. As a starting point we have included a pre-processing step in which a greyscale transformation and a sharpen filter have been applied. After that, the processing chain has consisted in many steps. The first one is thresholding. A previous segmentation of image was needed (Wall's blocks algorithm) in order to avoid the effect of irregular illumination onto the projected image, after that a threshold value based in Ridley and Calvard's algorithm has been chosen and after all we have obtained a binary image. As a second step, we have labelled the regions in image and we have analyzed each region for determining if shape corresponds to our markers or not (through moments, rectangularity ratios and contours). As a final step the object recognition has been ensured thanks to application of SIFT as matching algorithm between our marker and the ideal one.

The results obtained show the importance of choosing a local threshold technique and an adequate size of Wall’s algorithm in order to perform a binarization which preserves our markers. It is at this point where it is also important the fact of the interaction between user and application, where thanks to the visor of the application user can determine if the parameters selected are valid in each case. After running the application we see that parameters and ratios chosen are adequate at recognizing markers in testimage given, although our images of testing are not enough (in amount) to ensure that the application will respond correctly to all of them, because we have also seen that little changes in parameters lead to wrong recognition. So as a further approach it will be interesting to build a larger data base in order to adjust parameters (if required) to ensure this extraction in all cases.

Finally, this project has been left at the disposal of IGD- Fraunhofer for hArtes project and/or further projects in which my contribution could be useful.

7. References

[1] RAFAEL C. GONZALEZ, RICHARD E. WOODS *Digital Image Processing*, Prentice Hall Second edition 2002

[2] MILAN SONKA, VACLAV HLAVAC, ROGER BOYLE *Image Processing Analysis and Machine Vision*, Pacific Grove, CA : PWS Pub. 1999

[3] KENNETH R. CASTLEMAN *Digital image processing*, Englewood Cliffs, N.J. Prentice-Hall, c1979

[4] DMITRIJ CSTVERIKOV *Basic Algorithms for Digital Image Analysis* Eötvös Loránd University Budapest http://visual.ipan.sztaki.hu/ELTEfoliak/

[5] BERNT SCHIELE *Slides in Computer Vision Subject* TU Darmstadt 2007

[6] MEHMET SEZGIN, BULENT SANKUR *Survey over image thresholding techniques and quantitative performance evaluation,* Journal of Electronic Imaging 13(1), 146–165 2004

[7] SHAPIRO, LINDA G. & STOCKMAN, GEORGE C. *Computer Vision,* Prentice Hall 2002

[8] *PIERRE D. WELLNER Adaptive Thresholding for the Digital Desk* Technical Report EPC-1993-110

[9] T. W. RIDLER, S. CALVARD, *Picture thresholding using an iterative selection method*, IEE Trans. System, Man and Cybernetics, SMC-8 (1978) 630-632

[10] ANDREA VEDALDI An implementation of SIFT detector and descriptor University of California at Los Angeles 2006)

[11] PAUL L. ROSIN *Measuring rectangularity* August 1999

[12] PAUL L. ROSIN *Measuring Shape: Ellipticity, Rectangularity and Triangularity* IEEE 2000 and Revision of July 2002

[13] TOUSSAINT 1983, PIRZADEH 1999 *Solving geometric problems with rotating Callipers*

[14] A.P. REEVES *The General Theory of Moments fro Shape Analysis and the Parallel Implementation of Moment Operations* TR-EE October 1981

[15] A. P. REEVES AND A. ROSTAMPOUR *Shape Analysis of Segmented Objects Using Moments* IEEE August 1981

[16] D. G. LOWE *Object recognition from Local Scale invariant features* International Conference on Computer *Vision,* Corfu, Greece (September 1999)

[17] D. G. LOWE, *Local feature view clustering for 3D object recognition* IEEE Conference on Computer Vision and Pattern Recognition*,* Kauai, Hawaii (December 2001)

[18] D. G. LOWE *Distinctive Image Features from scale-Invariant Keypoints* International Journal of Computer Vision, 60, 2 (*2004)*

[19] M. BROWN, D. G. LOWE *Invariant features from interest point groups* British Machine Vision Conference, BMVC 2002, Cardiff*,* Wales *(*September 2002*)*

[20] MUNDY, ZISSERMAN *Geometric Invariance in Computer Vision* Cambridge, MA, The MIT Press. (1992)and REISS 1993.

[21] MIKOLAJCZYK, SCHMID *A performance evaluation of Local Descriptors* 2005

[22] J. BEIS , D. G. LOWE *Shape indexing using approximate nearest-neighbour search in high dimensional spaces* Proceeding of IEEE Computer Society Conference on Computer Vision and Pattern recognition 1997

[23] HERBERT BAY, TINNE TUYTELAARS AND LUC VAN GOOL *SURF: Speeded Up Robust Features,* 9th European Conference on Computer Vision, 7-13 May 2006

[24] JOHANNES BANER, NIKO SÜNDERHAUF, PETER PROTZEL *Comparing several implementations of two recently published feature detectors 2007*

[25] HARRIS, STEPHENS *A combined corner and edge detector*, *Proc.* 4th Alvey Vision Conf., Manchester, 1988.

[26] M.KUDZINAVA, R. GARCIA, J.MARTI *Feature based matching of underwater images*

A. Ridley and Calvard's method

Using thresholding there is normally an error performing segmentation:

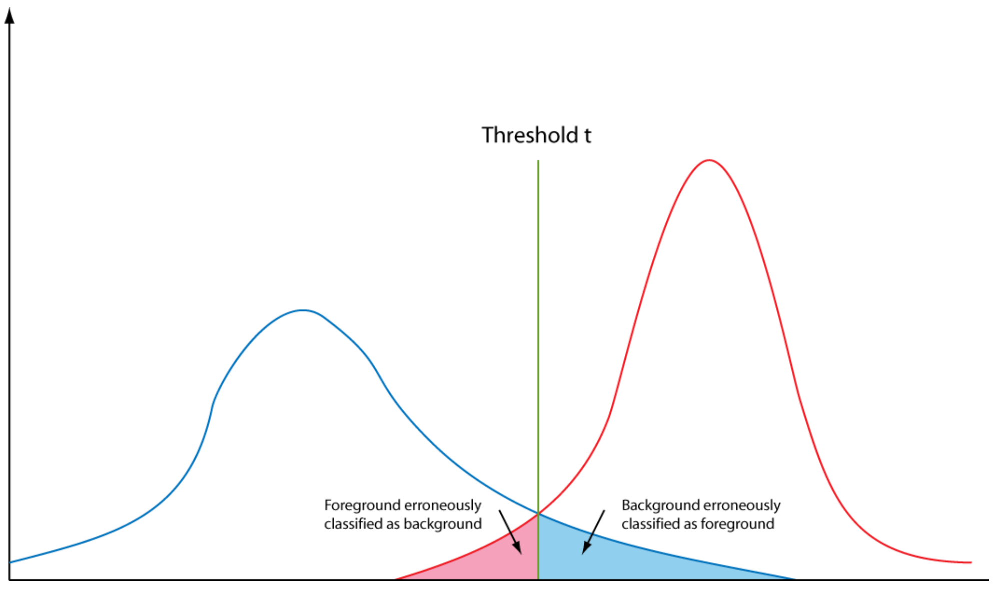

Fig. A.1 The queues of two different Gaussian distributions can lead to erroneous detections at thresholding (from Digital Image Analysis Lars Audal July 24th 2006)

We assume that the histogram is the sum of two distributions *b(z)* and *f(z)* where *b* and *f* are the normalized background and foreground distributions respectively and *z* is the gray level.

If *B* and *F* are prior probabilities for the background and foreground, altogether have to be 1 (*B*+*F*=*1*) and the histogram can be written as:

$$h(z) = B\, b(z) + F\, f(z)$$

Given a threshold *t* the probabilities of erroneously classifying a pixel is given by:

$$E_B(t) = \int_{-\infty}^{t} f(z)dz$$

$$E_F(t) = \int_{t}^{\infty} b(z)dz$$

So the total error will be:

$$E(t) = F\int_{-\infty}^{t} f(z)dz + B\int_{t}^{\infty} b(z)dz$$

Using Leibniz's rule for derivation of integrals and setting the derivative equal to zero the optimal value for t is found:

$$\frac{E(t)}{dt} = 0 \Rightarrow Ff(T) = Bb(T)$$

Assuming b(z) and f(z) are Gaussians distributions it is possible to solve the above equation explicitly. The equation becomes:

$$\frac{B}{\sqrt{2\pi\sigma_B^2}} e^{-\frac{(T-\mu_B)^2}{2\sigma_B^2}} = \frac{F}{\sqrt{2\pi\sigma_F^2}} e^{-\frac{(T-\mu_F)^2}{2\sigma_F^2}}$$

Some algebraic manipulations will transform this equation into a second order equation in T:

$$(\sigma_B^2 - \sigma_F^2)T^2 + 2(\mu_B\sigma_F^2 - \mu_F\sigma_B^2)T + \sigma_B^2{\mu_F}^2 - \sigma_F^2{\mu_B}^2 + 2\sigma_B^2{\mu_F}^2 ln\left(\frac{B\sigma_F}{F\sigma_B}\right) = 0$$

If the standard deviations of the two distributions are equal (σ_B=σ_F=σ) then the expression can be simplified:

$$2(\mu_B - \mu_F)T - (\mu_B + \mu_F)(\mu_B - \mu_F) + 2\sigma^2\left(\frac{B}{F}\right) = 0$$

That can be solved explicitly for T:

$$T = \frac{(\mu_B + \mu_F)}{2} + \frac{\sigma^2}{(\mu_B - \mu_F)} ln\left(\frac{F}{B}\right)$$

If the two distributions B and F are roughly equiprobable then $\ln(1) \rightarrow 0$ and:

$$T = \frac{(\mu_B + \mu_F)}{2}$$

This equation is the foundation of Ridley and Calvard's method. As μ_B and μ_F are unknown we must estimate them based on suggested thresholds.

B. Morphological operators

- **Structuring element**: consists of a pattern specified as the coordinates of a number of discrete points relative to some origin. Normally cartesian coordinates are used and so a convenient way of representing the element is as a small image on a rectangular grid. The origin does not have to be in the centre of the structuring element, but often it is.

- **Dilation**: For each background pixel we superimpose the structuring element on first pixel of image so that the origin of the structuring element coincides with the image pixel position. If at least one pixel in the structuring element coincides with a foreground pixel in the image underneath, then the input pixel is set to the foreground value. If all the corresponding pixels in the image are background, however, the pixel is left at the background value. We repeat the process through whole image.

- **Erosion**: The basic effect of the operator on a binary image is to erode away the boundaries of regions of foreground pixels (i.e. white pixels, typically). Thus areas of foreground pixels shrink in size, and holes within those areas become larger.

- **Opening**: The effect of the operator is to preserve foreground regions that have a similar shape to this structuring element, or that can completely contain the structuring element, while eliminating all other regions of foreground pixels.

- **Closing**: The effect of the operator is to preserve background regions that have a similar shape to this structuring element, or that can completely contain the structuring element, while eliminating all other regions of background pixels.

C. How are images formed?

In this appendix we include a short explanation about how objects of real world become digital images so we can work with them in the computer.

An image is a visual representation of a person, an object or an environment. It contains descriptive information about what it represents.

An image can be defined as a two-dimensional continuous function $f(x, y)$ where x and y are spatial (plane) coordinates and the amplitude of f at any pair of coordinates (x, y) is called intensity or gray-level of the image at that point.

When we project the real world onto a two-dimensional image plane, we uncover the two key questions of image formation:

- What determines where the image of one point will appear?
- What determines how bright the image of some surface will be?

To answer these questions it is necessary to consider two processes to convert the continuous sensed data (image) into digital form: sampling and quantization.

- Sampling (Spatial resolution): Is the process of digitalizing the image in spatial domain. The sampling process may be viewed as partitioning the x y plane into a grid, with the centre of each grid being a pixel. The digitizing of the x and y coordinate values is based on geometry of image formation which determines where in the image plane the projection of a point in the scene will be placed (see Appendix D for more information). Sampling determines spatial resolution, which is the smallest discernable detail in image. The more pixels in a fixed range, the higher resolution.

- Quantization (Gray-scale resolution): is the process of digitizing amplitude f values into discrete gray values. Physics of light determine the brightness of a point in the image plane as a function of illumination and surface properties. Radiometry theory demonstrates existent linear relationship between them. (See Appendix E). Quantization determines the gray-scale resolution which refers to smallest discernible change in gray-scale level. The more bits the higher the resolution.

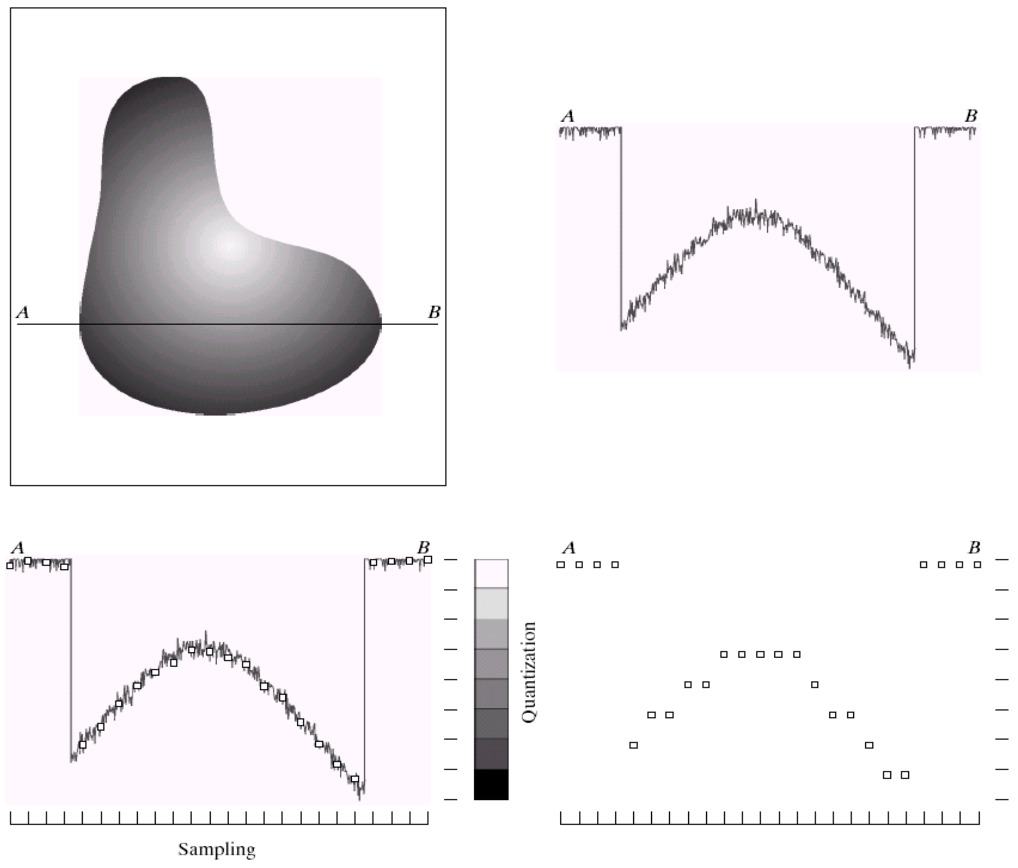

Fig. C.1 Upper left: continuous image; Upper right: A scan line from A to B in the continuous image; Down left: sampling and quantization; Down right: digital scan line (by Chapter 2 of [1])

Once we know where each pair of coordinates are projected and with which intensity, it is time to convert optical image into an electrical image thanks to camera electronics. This process is called sensing and it is widely explained in Appendix F. (The explanation of the process is only valid for cameras based on CMOS sensor as used in our project to capture the images. Some other cameras as based on CCD Sensor do not work the same way and they are not described in this report).

After sensing the objective of generating digital image from sensed data is completed.

$$f(x,y) \rightarrow \boxed{Sampling \,\&\, Quantization} \rightarrow f(i,j)$$

$$0 < f(x,y) < \infty \qquad\qquad MxN$$

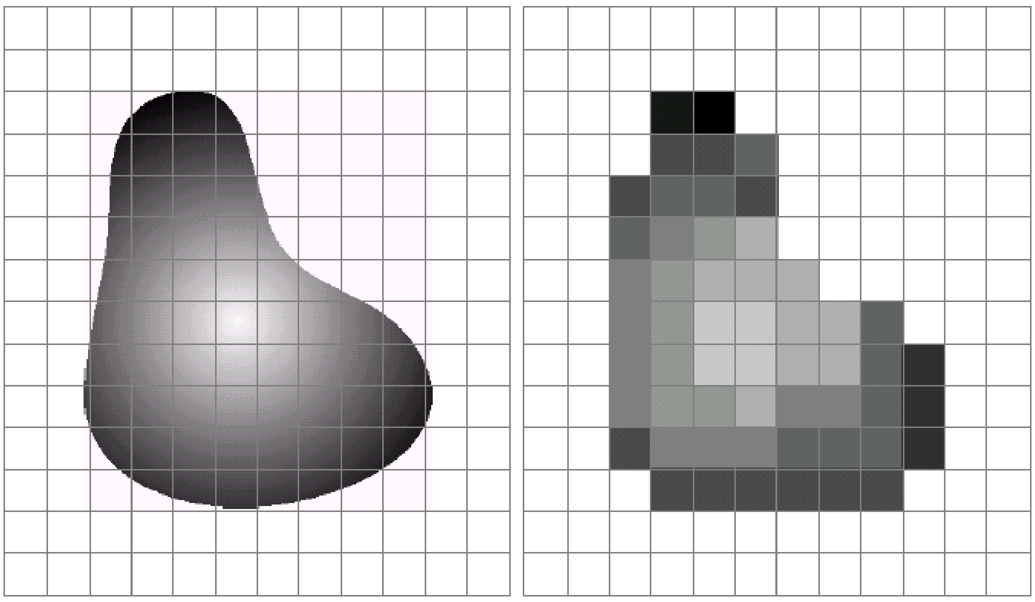

Fig. C.2 Left: This image illustrates a continuous image projected onto a sensor array. Right: result of image sampling and quantization (by Chapter 2 of [1])

The result of sampling and quantization is a matrix of real numbers. Fig. C.3 shows the coordinate conversion used throughout this book.

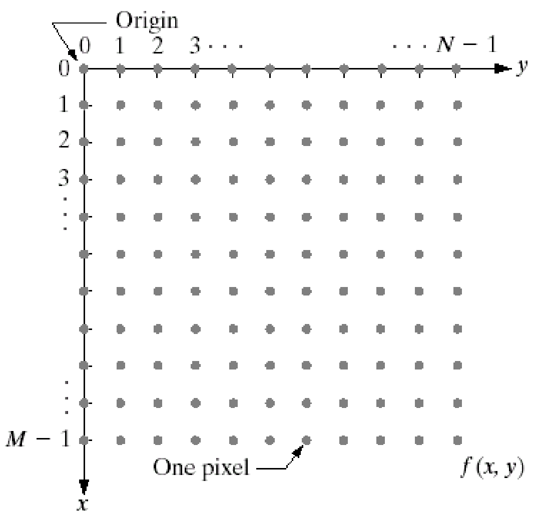

Fig. C.3 Coordinate system for the representation of digital images (by Chapter 2 of [1])

We obtain the digital image of the scene we want to analyse so we are prepared to start working on our project of detecting internal and external markers.

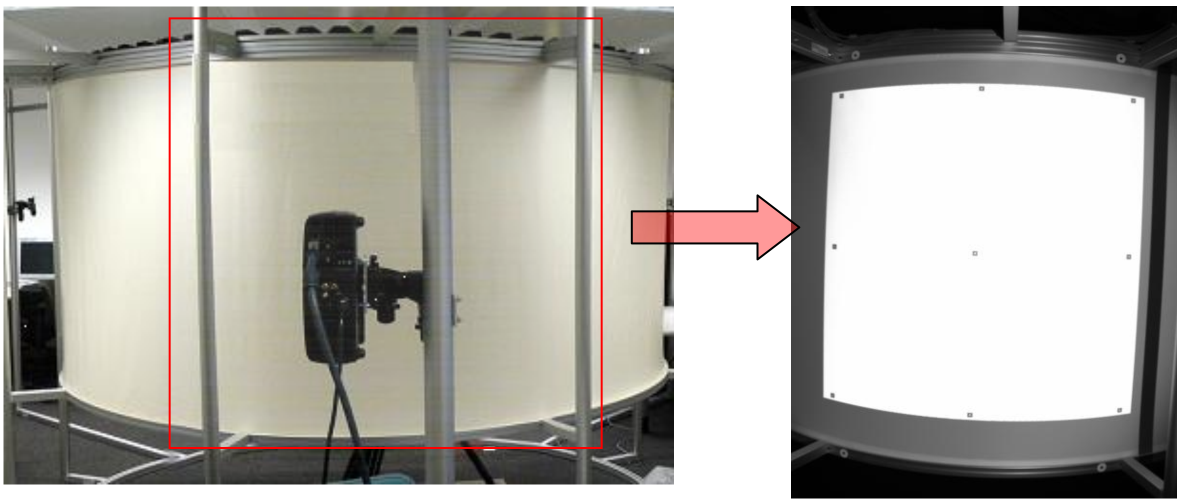

Fig. C.4 On the left we see the scenario of our project. On the right we see the image captured by the camera previously projected by projector onto region in red of the cylindrical surface

During image capture, transmission, or processing noise can occur and it may be dependent or independent of the image content. In all cases the image noise is a random and unwanted variation in brightness or colour information in an image. In Appendix G different kind of noises that can affect in our case are shown.

D. Geometry of image formation

The mathematical relationship between the coordinates of a 3D point and its projection onto the image plane can be modelled, as a first approximation, by a pinhole camera.

The ideal pinhole camera is described as a black box with a small hole. When rays coming from illuminated objects penetrate through the small hole you will see them inside the black box, over one of the walls, reduced in size and inverted due to the intersection of the rays of light that pass through.

The wall where the object projection is shown is known as the image plane and the small hole as the camera aperture.

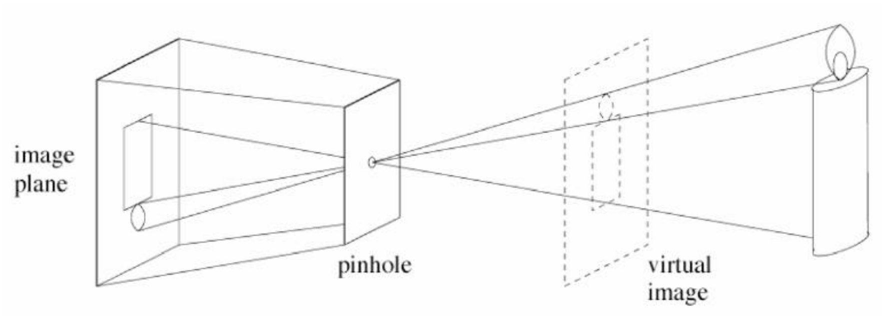

Fig. D. 1 Pinhole model (from slides TU-Darmstadt Bernt Schiele- Computer Vision SS2007)

In the ideal case (the simplest) no lenses are used to focus light, so it does not consider the effects of optical systems on an image.

We can introduce thin lenses in the pinhole system. The mission of lenses placed in the aperture is to focus the bundle of rays from each scene point onto the corresponding point in the image plane. This way we obtain the same projection as the pinhole but it also gathers a finite amount of light. The larger the lens the larger the solid angle it subtends when seen from the object.

It can also appear degradation which can be due to effects of diffraction because of the wave nature of light or due to lens aberration, imperfectly designed and manufactured optical systems.

If we use a wide pinhole, light from the source spreads across the image (i.e., not properly focussed) making it blurry.

If we narrow the pinhole, only a small amount of light is let in. That means that the image sharpness is limited by diffraction, when light passes through does not travel in a straight line and light is scattered in many directions (quantum effect).

In general the aim of using lens is to enlarge aperture size while keeping the image focussed.

Although it is not a perfect model it is a reasonable good description for computer vision and computer graphics and some of the effects can be compensated with an adequate coordinate transformation of the 3D projection on the image coordinates.

Coordinate transformation: homogeneous coordinates

For mapping three dimensional points to a two dimensional plane we consider two kind of 3D projection:

Orthographic projection

These projections are a set of transformations often used to show profile, detail or precise measurements of a real object. The camera direction (normal component of the viewing plane) is always parallel to one of the 3D axes. If we have a 3D point (a_x, a_y, a_z) and we want to project it to a 2D point (b_x, b_y) using projection parallel to the y axis (Profile view).

We can use the equations

$$b_x = s_x \cdot a_x + c_x$$

$$b_y = s_z \cdot a_z + c_z$$

where *s* is an arbitrary scale factor and *c* an arbitrary offset. Constants are optional and can be used to a better alignment of the viewpoint.

In this kind of projection, lengths of all points of the projected image have the same scale independent of whether they are near or far away to the viewer. As a result, lengths near to the viewer appear foreshortened. In order to solve this problem we can use Perspective Projection.

Perspective projection

It is more complex than orthographic. For the understanding of how this projection works we have to think about the 2D projection as a viewfinder, where the camera’s position, orientation and field of view control the behaviour of the projection transformation.

We consider:

$a_{x,y,z}$ – object coordinates (particular concrete point of the object)

$c_{x,y,z}$ – location of the camera

$\varphi_{x,y,z}$ – rotation of the camera

$e_{x,y,z}$ – viewer position in camera coordinates

$b_{x,y}$- 2D projection of $a_{x,y,z}$

Note: if $c_{x,y,z}$ =<0,0,0> and $\varphi_{x,y,z}$=<0,0,0>, the 3D vector <1,2,0> becomes <1,2> in the projected 2D vector.

We define a new point $d_{x,y,z}$ which is a translation of the point $a_{x,y,z}$ into the coordinate system defined by *c* (camera coordinates). This can be achieved by subtracting *c* from *a* and then applying a vector rotation matrix using – φ to the result. Assuming left-hand system of axes:

$$\begin{pmatrix} d_x \\ d_y \\ d_z \end{pmatrix} = \begin{pmatrix} 1 & 0 & 0 \\ 0 & \cos-\varphi_x & \sin-\varphi_x \\ 0 & -\sin-\varphi_x & \cos-\varphi_x \end{pmatrix} \cdot \begin{pmatrix} \cos-\varphi_y & 0 & -\sin-\varphi_y \\ 0 & 1 & 0 \\ \sin-\varphi_y & 0 & \cos-\varphi_y \end{pmatrix} \cdot \begin{pmatrix} -\cos-\varphi_z & \sin-\varphi_z & 0 \\ -\sin-\varphi_z & \cos-\varphi_z & 0 \\ 0 & 0 & 1 \end{pmatrix} \cdot \left[\begin{pmatrix} a_x \\ a_y \\ a_z \end{pmatrix} - \begin{pmatrix} c_x \\ c_y \\ c_z \end{pmatrix} \right]$$

If we used the projection plane as x/y, this transformed point $d_{x,y,z}$ can be projected onto the 2D plane using:

$$b_x = (e_x - d_x)\frac{e_z}{d_z} \qquad b_y = (e_y - d_y)\frac{e_z}{d_z}$$

or using homogeneous coordinates to unify the representation for points and lines by adding in one dimensionality:

$$\begin{pmatrix} f_x \\ f_y \\ f_z \\ f_w \end{pmatrix} = \begin{pmatrix} 1 & 0 & 0 & -e_x \\ 0 & 1 & 0 & -e_y \\ 0 & 0 & 1 & 0 \\ 0 & 0 & \frac{1}{e_z} & 0 \end{pmatrix} \cdot \begin{pmatrix} d_x \\ d_y \\ d_z \\ 1 \end{pmatrix}$$

with $b_x = \frac{f_x}{f_w}$ and $b_y = \frac{f_y}{f_w}$

Homogeneous coordinates make possible the calculations in projective spaces just as Cartesian coordinates do in Euclidean space.

Image formation (geometrical)

We have to be able to transform object coordinates, 3D information, onto pixel coordinates, 2D information, so we can work with information contained in the photo captured.

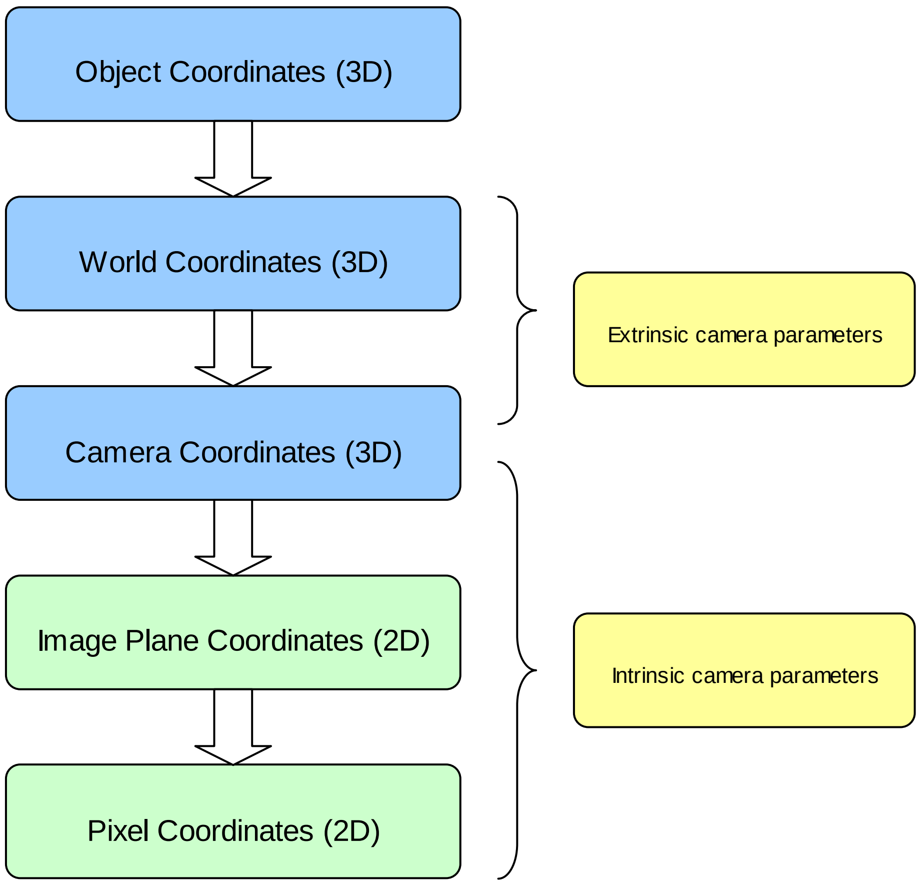

Considering a camera with a thin lens (pinhole camera), it performs a perspective projection and we can find a matrix which describes the mapping between 3D points of the world to 2D points on the image plane.

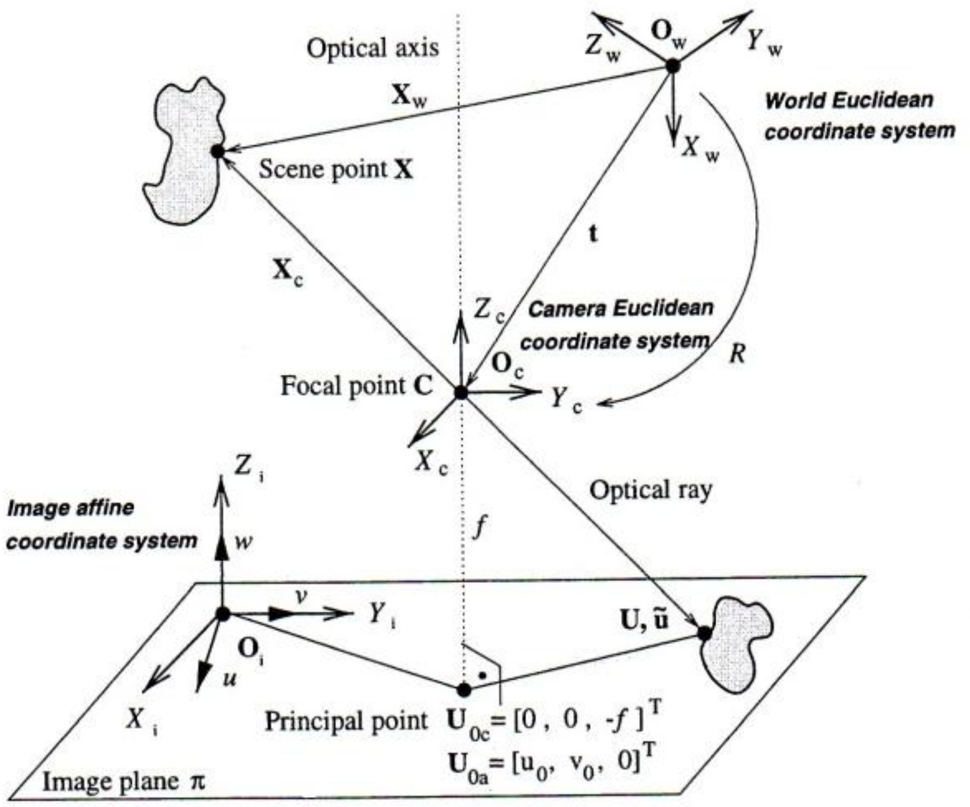
Optical axis
Z_w
O_w
Y_w
X_w
World Euclidean coordinate system
X_w
Scene point X
t
X_c
Z_c
Camera Euclidean coordinate system
O_c
R
Focal point C
Y_c
X_c
Optical ray
Z_i
Image affine coordinate system
w
f
v
Y_i
U, ũ
O_i
u
X_i
Principal point $U_{0c} = [0, 0, -f]^T$
$U_{0a} = [u_0, v_0, 0]^T$
Image plane π

Fig. D.2 Geometry of a linear perspective camera

We can see at the bottom of Fig. D.2, the image plane π where real world projects with a vertical perpendicular line called optical axis. Perpendicularly to this line the lens is positioned at the focal point C (optical centre) with a focal length f.

The projection is performed by an optical ray reflected from a scene point X (point of the object or surface). This ray passes through the optical centre C and hits the image plane π at the point U.

We need to define four coordinate systems in order to understand the mathematics.

Coordinate system	**Notation**	**Origin**	**Points expressed in coordinate system**
World Euclidean	W	O_w	X, U
Camera Euclidean	C	O_c=C	Z
Image Euclidean	I	O_i	X, Y
Image affine	A	O_i	Coordinates u,v,w

Coordinates *w* and *v* have the same orientation as Z_i and Y_i but this is not the case with *u* and X_i. The reason why is that pixels need not to be perpendicular and axes can be scaled differently. The affine coordinate system is induced by the arrangement of the retina.

U_0 is the intersection of the optical axis with the image plane π and this point U_o in affine coordinate system is expressed as $U_{0a}=[u_0,v_0,0]^T$.

A representation of a point in the world coordinate system, for example X, is a vector 3x1. To express this point in the camera Euclidean coordinate system (X_c) we have to align the coordinate systems by translating and rotating the world point.

Rotation (R) consists in three elementary rotations pan, tilt and roll, axes x, y and z respectively. Translation (t) vector gives three elements of the translation. So there are six degrees of freedom called extrinsic parameters.

$$X_c = \begin{pmatrix} x_c \\ y_c \\ z_c \end{pmatrix} = R(X_w - t)$$

This point is projected onto the image plane π (through the thin lens we suppose ideal), we call it U_c.

The projected point U_c can be derived from the similar triangles of the image:

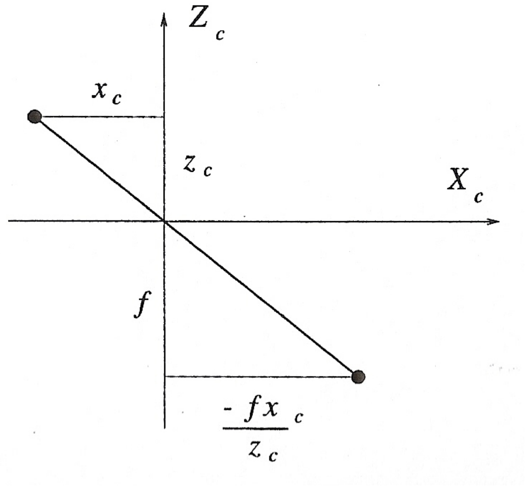

Fig. D.3 Similar triangles

and we obtain

$$U_c = \begin{pmatrix} \frac{-fx_c}{z_c} \\ \frac{-fy_c}{z_c} \\ -f \end{pmatrix}$$

It remains to derive where the projected point is positioned in the image affine coordinates system, i.e., to determine the coordinates which the real camera actually delivers.

The origin of the image in image affine coordinate system is at the top left corner and represents a shear and rescaling of the image Euclidean coordinate system.

U_c can be represented in the 2D image plane π by homogeneous coordinates as ũ =$[U,V,W]^T$ and in 2D Euclidean as u =$[u,v]^T$=$[U/W,V/W]^T$.

Homogeneous coordinates allow us to express affine transformation as a multiplication by a 3x3 matrix with a, b and c unknown, which describe the shear together with scaling along the axes:

$$\tilde{u} = \begin{pmatrix} U \\ V \\ W \end{pmatrix} = \begin{pmatrix} a & b & -u_0 \\ 0 & c & -v_0 \\ 0 & 0 & 1 \end{pmatrix} \cdot \begin{pmatrix} \frac{-fx_c}{z_c} \\ \frac{-fy_c}{z_c} \\ 1 \end{pmatrix} = \begin{bmatrix} -fa & -fb & -u_0 \\ 0 & -fc & -v_0 \\ 0 & 0 & 1 \end{bmatrix} \cdot \begin{pmatrix} \frac{x_c}{z_c} \\ \frac{y_c}{z_c} \\ 1 \end{pmatrix}$$

We can multiply both sides of the equation by per z_c and this way we can remove it and rewrite the expression depending on K, the camera calibration matrix:

$$z_c\,\tilde{u} = \begin{bmatrix} -fa & -fb & -u_0 \\ 0 & -fc & -v_0 \\ 0 & 0 & 1 \end{bmatrix} \cdot R(X_w - t) = KR(X_w - t)$$

As we can see the matrix is upper-triangular and these coefficients are called intrinsic parameters of the camera and describe the specific camera independent on its position and orientation in space.

If we express the scene point X in homogeneous coordinates $X'_w = [X_w, 1]T$, we can write the perspective projection using a single 3x4 matrix. The leftmost 3x3 submatrix describes rotation and the rightmost column a translation.

$$\tilde{u} = \begin{pmatrix} U \\ V \\ W \end{pmatrix} = \; KR \,|\, -KRt \;\cdot \begin{pmatrix} X_w \\ 1 \end{pmatrix} = M \begin{pmatrix} X_w \\ 1 \end{pmatrix} = MX_w'$$

where X' is the 3D scene point in homogeneous coordinates and M is called the Projective Matrix or camera matrix.

Thanks to the introduction of projective space and homogeneous coordinates we obtain a linear equation to express the transformation from the 3D world to 2D.

E. Physics of light: Radiometry

The physics of light determines the brightness of a point in the image plane as a function of illumination and surface properties.

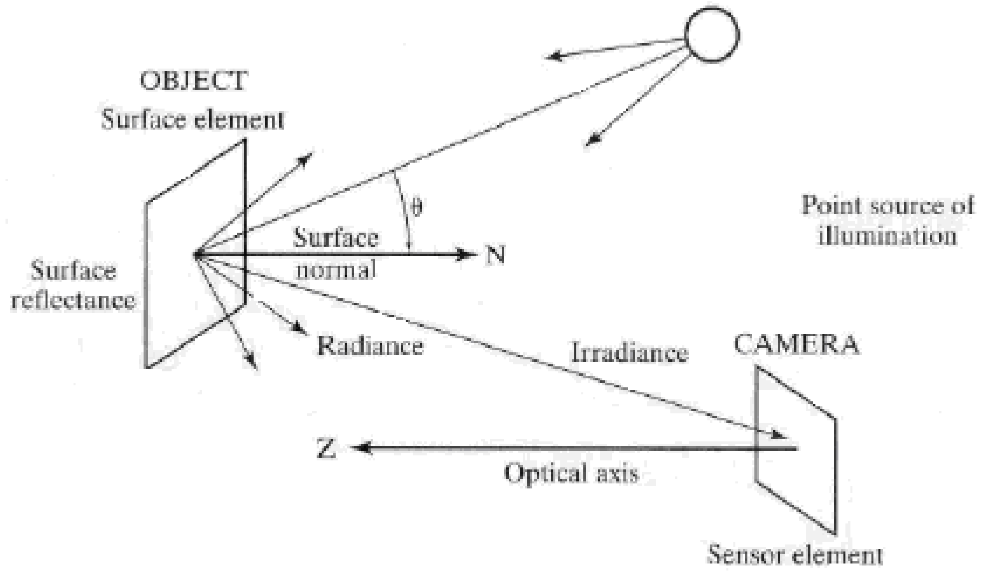

Fig. E.1 How rays of light project onto surface element and they onto camera sensor

- The scene is illuminated by a single source
- The scene reflects radiation towards the camera
- The camera senses it via chemicals on film (sensing).

With the knowledge of radiometrics concepts (Appendix H) we can differentiate between two concepts of brightness:

Scene Radiance: it is related to the energy flux emitted from a surface. This emission depends on how the objects are illuminated and how they reflect light. Scene Radiance can be measured by the Radiance (L).

Image Irradiance: it which is related to energy flux incident on the image plane and can be measured by the Irradiance (E). This term depends on how much light arrives to the surface of the object coming from the scene point X.

The measurement of the brightness in the image also depends on the spectral sensitivity of the sensor.

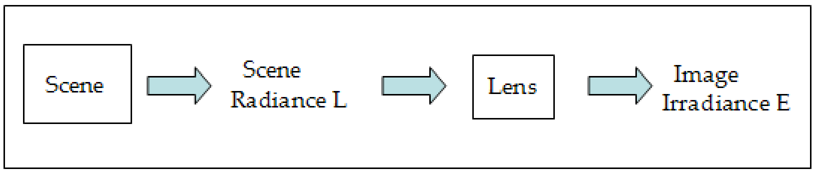

Fig. E.2 Scheme from scene radiance to image irradiance

What is really important of all this concepts is that we are working with a linear mapping because there is a lineal dependency between Radiance and Irradiance.

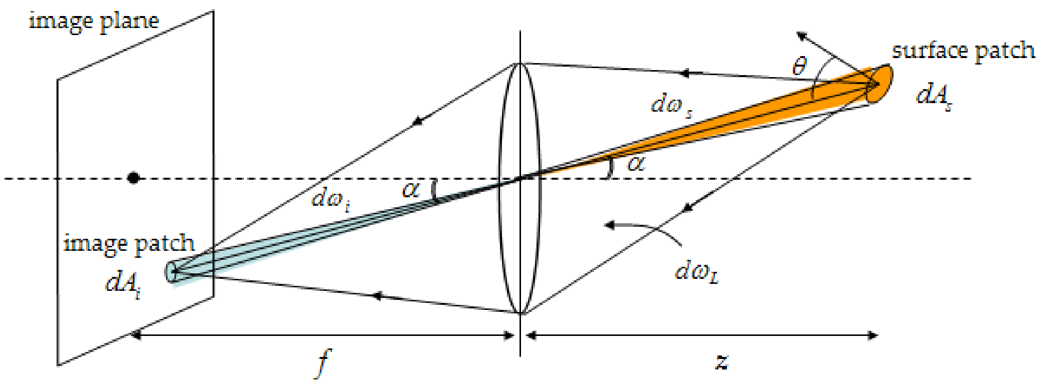

Fig. E.3 Relationship between angles and areas of the surface and the image plane

From the image we can see that solid angles (orange and blue) are the same $dw_i = dw_s$ and we can find a relationship between areas $\frac{dA_s}{dA_i}$. So the solid angle subtended by the lens is:

$$d\omega_L = \frac{\pi d^2}{4} \frac{\cos\alpha}{\left(\frac{z}{\cos\alpha}\right)^2}$$

The flux received by lens from dA_S is the same as the flux projected onto the image dA_i:

$$L(dA_s \cos\vartheta) \cdot dw_L = E \cdot dA_i$$

If we combine both equations we obtain:

$$E = L\frac{\pi}{4}\left(\frac{d}{f}\right)^2 \cos\alpha^{\,4}$$

which demonstrates the relationship between Image Irradiance and Scene Radiance.

The constant of proportionality depends on the optical system and with a small field of view the effects of the 4th power cosine are small.

We must have an aperture of finite size (different from zero) because we need to gather a finite amount of light in the image plane but with small pinhole. That is because of the wave nature of light which has higher diffraction at the edge of the pinhole and the light is spread over the image. As we make the pinhole smaller the larger fraction of incoming light is deflected far from the direction of the incoming ray.

F. Sensing

The objective we pursue is to convert the optical image into an electrical image (from optical signal through photoreceptors and photodetectors to electrical signal):

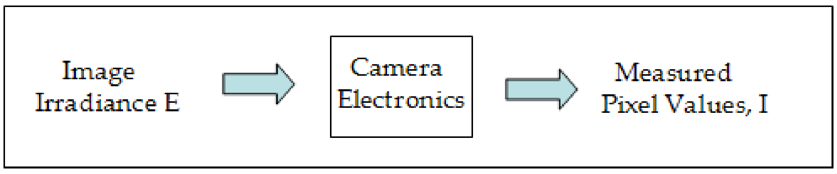

Fig. F.1 Scheme from image irradiance to pixel values

A non-linear mapping is made by the camera electronics to reach the objective. These electronics can consist of different photodetectors (sensors) as photodiodes (PIN, APD,…), photoresistances and phototransistors. In our case we have used a camera consisting in a CMOS Sensor known as active pixel sensor (APS).

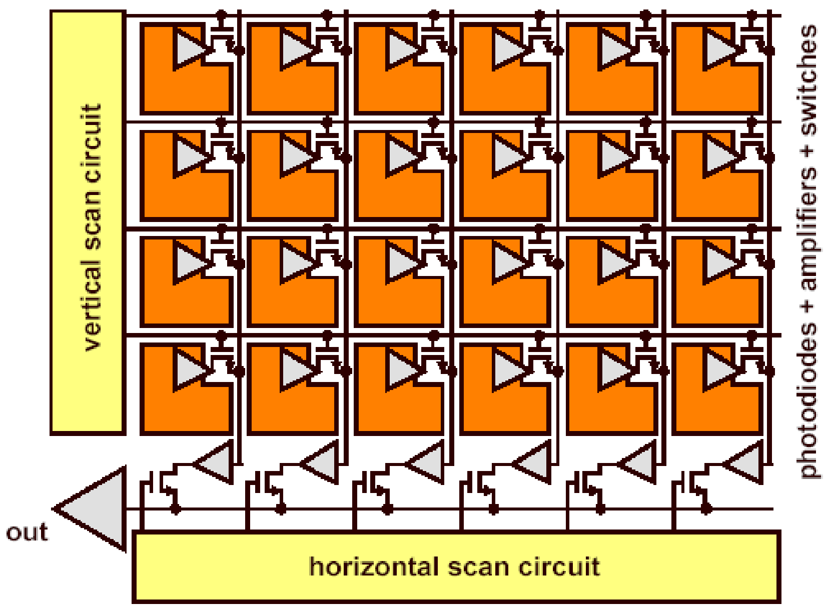

Fig. F.2 CMOS sensor: APS (from Albert Theuwissen- Chief Technology Officer DALSA Corp)

An APS is an image sensor consisting in an integrated circuit containing an array of pixel sensors where each pixel gets its individual amplifier. This small amplifier boosts the photodiode signal fed to the column line and solves the noise problem of the large column lines. All amplifiers are analogue in nature, i.e., no two amplifiers are perfectly matched as far as gain and off-set are concerned. Therefore the introduction of an amplifier within every pixel increases the non-uniformity between the various pixels of the array. This effect shows up as fixed-pattern noise. This is a disadvantage of CMOS image sensor relative to other ones like CCD used in higher quality photographic works.

Every pixel consists of a photodetector, a transfer gate (TX), a reset gate (RST), a selection gate (RS: row selection), source-follower readout transistor (M_{SF}) and a selection transistor (M_{SEL}).

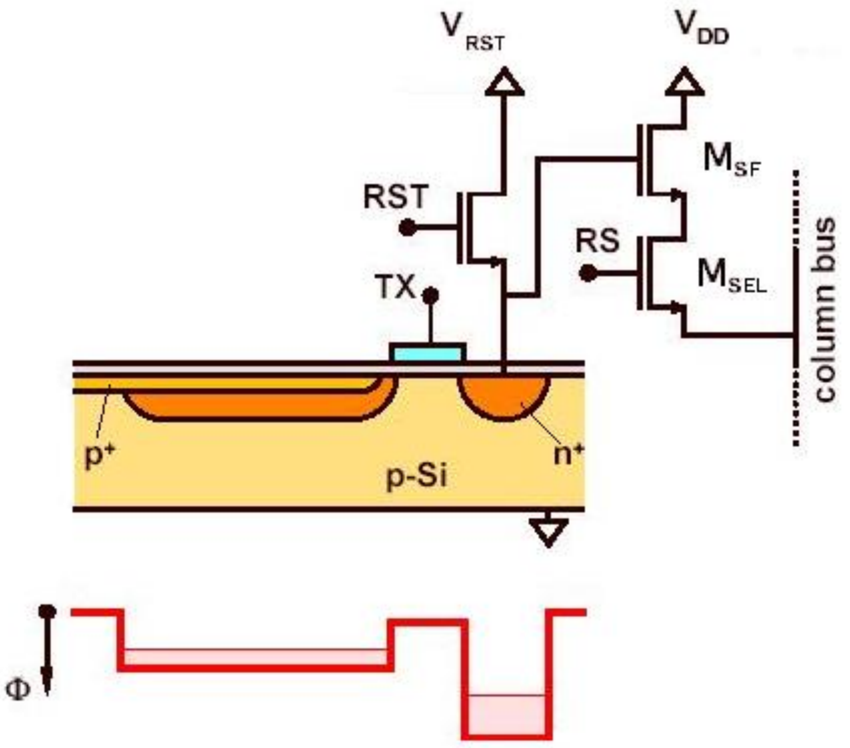

Fig.F.3 Pixel sensor and its transistors (from Albert Theuwissen- Chief Technology Officer DALSA Corp)

The photodetector is usually a photodiode. In this case the photodiode does not have any electrical connection to force the collected charge out of the photodiode. To initiate the charge transport from the photodiode towards the floating diffusion (n+) the transfer gate (TX) is pulsed.

When light comes it causes an accumulation or integration of charge on the ‘parasitic’ capacitance of the photodiode, creating a voltage change related to the incident light.

- Transistor M_{rst} acts as a switch to reset the device. When this transistor is turned on the photodiode is effectively connected to the power supply V_{RST}. This way it clears all integrated charge. As the reset transistor is n+ type the pixel operates in soft reset.

- Transistor M_{sf} acts as a buffer. It is an amplifier which allows the pixel voltage to be observed without removing the accumulated charge. Its power supply V_{DD} is typically tied to the power supply of the reset transistor.

- Transistor M_{sel} is a switch that allows that read-out electronics read a single row of the pixel array.

An advantage of using electronics is that allows us to read directly the signal of each pixel and this way we can avoid the effect of blooming. Blooming makes that light intensity received by a pixel affects the adjacent pixels. The disadvantage is that in light receptors (photodiodes) there is a lot of electronics (elements placed on the sensor surface) which are not sensitive to light, and that means that thee is a factor, fill factor, which determines the percentage of the pixel area that is exposed to light during exposure and although ideally this would be 100%, in practice this value may be reduced to approx. 30-50% depending on the sensor technology. A solution is the use of micro lenses which increase the fill factor up to 70% and collect the light that falls onto the photocell increasing the useable sensor area.

Digital image sensors can only detect light intensity but not colour information. To produce colour sensors a colour filter is applied on each photocell (pixel). The colour filter distribution corresponds to the colour sensitivity of the human eye and is called Bayer filter pattern and consists of two out of every four pixels have a green filter, one pixel has a red filter and one has a blue filter.

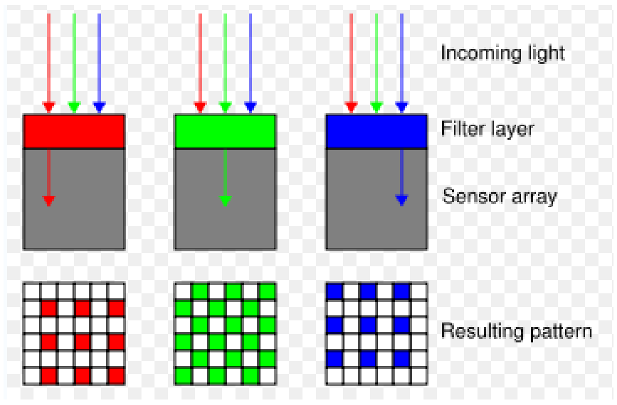

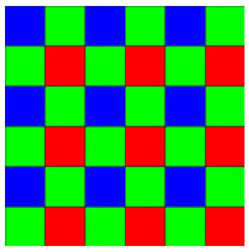

Fig. F.4 Bayer filter and resulting pattern

The camera used, uEye camera, transmit the image data in Bayer format. This format can be converted to Y8, RGB or YUV format on the PC at runtime.

G. Noise

Shot noise:

- **Photon shot noise**: due to statistical quantum fluctuations because of the variation in the number of photons sensed at a given exposure level. Shot noise follows a Poisson distribution (similar to Gaussian) and has a root mean square value proportional to the square root of the image intensity and the noises at different pixels are independent from each other.

- **Dark-current shot noise**: noise coming from the dark leakage current in the image sensor. The higher the temperature of a pixel in the image sensor is, the higher is the dark current. If the exposure is long enough so the hot pixel charge exceeds the linear charge capacity it will appear impulsive noise.

Impulsive noise or salt-and-pepper noise: the image appears to be corrupted by isolated noisy pixels whose brightness differs significantly from that of the neighbourhood (dark pixels in bright regions and bright pixels in dark regions).

Amplifier noise: it can be described as an additive and Gaussian noise which is independent at each pixel and independent of the signal intensity, caused by thermal noise and including that noise coming from the reset noise of capacitors (kTC noise). In colour cameras, as blue channel is more amplified, there is more noise in blue channel.

Quantization noise: occurs when the levels of quantization are insufficient. It has an approximately uniform distribution and can be signal dependent, though it will be signal independent if other noise sources are big enough to cause dithering. Dithering is a technique to create illusion of colour depth in images with a limited colour palette (colour quantization). When there are not enough colours available in the palette a diffusion between coloured pixels of the palette is made. The human eye perceives this diffusion as a mixture of the colours within it.

H. Radiometrics concepts

Solid Angle: is the angle in three-dimensional space that an object subtends at a point

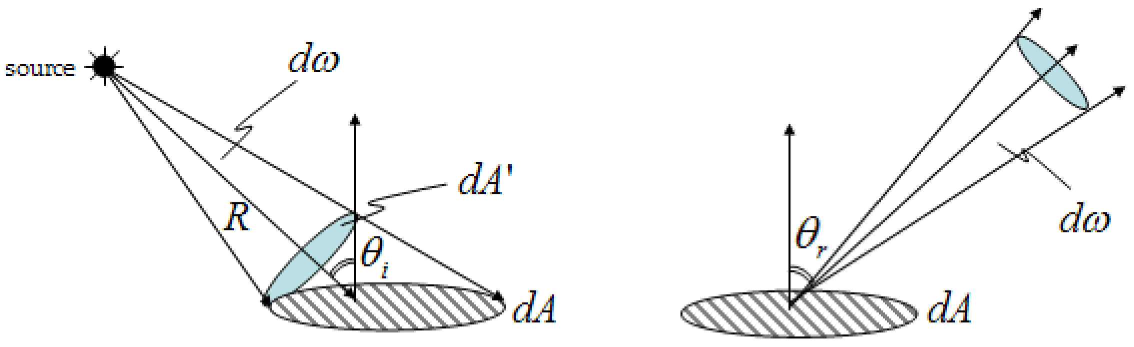

Fig. H.1 Solid angle

$d\omega$: solid angle subtended by dA

dA': foreshortened area

dA: surface area

$$d\omega = \frac{dA'}{R_2} = \frac{dA\cos\vartheta_i}{R_2} \qquad \text{(steradian)}$$

Radiant Intensity of Source: flux per unit of solid angle from a point source into a particular direction.

$$J = \frac{d\phi}{d\omega} \qquad \text{(W/steradian)}$$

$d\phi$: light flux (power) emitted

Surface irradiance (Image Irradiance): the rate at which the radiant flux is delivered to a surface (amount of light incident at the image of the surface point). It does not depend on where the light is coming from.

$$E = \frac{d\phi}{dA} \quad (\mathrm{W/m^2})$$

Surface radiance (Scene radiance): is the flux per projected unit area and per unit solid angle radiated, transmitted or reflected by a surface (amount of light incident at the image of the surface point).

$$L = \frac{d2\phi}{(dA\cos\vartheta r)d\omega} \qquad \text{(W/m}^2\text{/steradian)}$$

- Depends on direction ϑr: angle between the normal surface and the specified direction
- Surface can radiate into whole hemisphere
- L depends on reflectance properties of surface

I. Report of SIFT algorithm in Matlab

```
Computing frames and descriptors.

SIFT: computing scale space...(10.584 s gss; 0.682 s dogss) done

SIFT scale space parameters [PropertyName in brackets]

  sigman [SigmaN]        : 0.500000

  sigma0 [Sigma0]        : 2.015874

       O [NumOctaves]    : 6

       S [NumLevels]     : 3

    omin [FirstOctave]   : -1

    smin                 : -1

    smax                 : 3

SIFT detector parameters

  thersh [Threshold]     : 6.666667e-003

       r [EdgeThreshold] : 10.000

SIFT descriptor parameters

  magnif [Magnif]        : 3.000

     NBP [NumSpatialBins]: 4

     NBO [NumOrientBins] : 8

SIFT: processing octave -1

SIFT: 3 initial points (0.359 s)

SIFT: 3 away from boundary

SIFT: 2 refined (0.027 s)
```

```
SIFT: computing descriptors...done (1.714 s)

SIFT: processing octave 0

SIFT: 4 initial points (0.120 s)

SIFT: 4 away from boundary

SIFT: 4 refined (0.000 s)

SIFT: computing descriptors...done (0.539 s)

SIFT: processing octave 1

SIFT: 1 initial points (0.019 s)

SIFT: 1 away from boundary

SIFT: 1 refined (0.000 s)

SIFT: computing descriptors...done (0.126 s)

SIFT: processing octave 2

SIFT: 0 initial points (0.005 s)

SIFT: 0 away from boundary

SIFT: 0 refined (0.000 s)

SIFT: computing descriptors...done (0.047 s)

SIFT: processing octave 3

SIFT: 0 initial points (0.002 s)

SIFT: 0 away from boundary

SIFT: 0 refined (0.000 s)

SIFT: computing descriptors...done (0.007 s)

SIFT: processing octave 4

SIFT: 0 initial points (0.001 s)
```

```
SIFT: 0 away from boundary

SIFT: 0 refined (0.000 s)

SIFT: computing descriptors...done (0.002 s)

SIFT: computing scale space...(12.359 s gss; 0.646 s dogss) done

SIFT scale space parameters [PropertyName in brackets]

  sigman [SigmaN]        : 0.500000

  sigma0 [Sigma0]        : 2.015874

       O [NumOctaves]    : 6

       S [NumLevels]     : 3

    omin [FirstOctave]   : -1

    smin                 : -1

    smax                 : 3

SIFT detector parameters

  thersh [Threshold]     : 6.666667e-003

       r [EdgeThreshold] : 10.000

SIFT descriptor parameters

  magnif [Magnif]        : 3.000

     NBP [NumSpatialBins]: 4

     NBO [NumOrientBins] : 8

SIFT: processing octave -1

SIFT: 0 initial points (0.343 s)

SIFT: 0 away from boundary

SIFT: 0 refined (0.000 s)
```

```
SIFT: computing descriptors...done (1.759 s)

SIFT: processing octave 0

SIFT: 7 initial points (0.076 s)

SIFT: 7 away from boundary

SIFT: 5 refined (0.000 s)

SIFT: computing descriptors...done (0.673 s)

SIFT: processing octave 1

SIFT: 0 initial points (0.032 s)

SIFT: 0 away from boundary

SIFT: 0 refined (0.000 s)

SIFT: computing descriptors...done (0.151 s)

SIFT: processing octave 2

SIFT: 1 initial points (0.003 s)

SIFT: 1 away from boundary

SIFT: 1 refined (0.000 s)

SIFT: computing descriptors...done (0.032 s)

SIFT: processing octave 3

SIFT: 0 initial points (0.001 s)

SIFT: 0 away from boundary

SIFT: 0 refined (0.000 s)

SIFT: computing descriptors...done (0.005 s)

SIFT: processing octave 4

SIFT: 0 initial points (0.001 s)
```

```
SIFT: 0 away from boundary

SIFT: 0 refined (0.000 s)

SIFT: computing descriptors...done (0.002 s)

Computing matches.

Matched in 0.034 s
```